A Theoretical Study of Raman Optical Activity

Brian Peter Clark

Doctor of Philosophy

University of Glasgow

Chemistry Department

October 1981

TABLE OF CONTENTS

	Page
Acknowledgements	1
Summary	2
List of Tables	4
List of Figures	5
Chapter 1. Introduction	6
References	8
Chapter 2. The Basic Equations of Raman Optical Activity	9
References	15
Chapter 3. The Simple Two-Group Model for Rayleigh and Raman Optical Activity	16
3.1. Introduction	16
3.2. The Rayleigh Theory	16
3.3. The Raman Theory	19
3.4. The Raman Optical Activity of the Bending Vibrations of the Simple Two-Group Structure . . .	24
3.5. Discussion	28
References	30
Chapter 4. A General Two-Group Model of Rayleigh and Raman Optical Activity	31
4.1. Introduction	31
4.2. The Rayleigh Theory	31
4.3. The Raman Theory	32
4.3.1. The Inertial Term	32
4.3.2. Initial Formulation of the General Theory .	33
4.3.3. The Bond Polarizability Theory Proper . .	35
4.3.4. The Final Form of the General Bond Polarizability Theory of Raman Optical Activity . . .	39
4.4. Discussions	42

TABLE OF CONTENTS (continued)

Page

References 48

Chapter 5. The Atom-Dipole Interaction Model of Rayleigh and Raman Optical Activity . . . 49

References 56

Chapter 6. A General Two-Group Model Calculation on (+)-R-Bromochlorofluoromethane . . 57

6.1. Introduction 57

6.2. The Normal Coordinate Analysis . . . 57

6.3. The Raman Optical Activity Calculation . . 60

6.3.1. The Bond Polarizability Data . . . 60

6.3.2. The Calculated Circular Intensity Differences of (+)-R-Bromochlorofluoromethane . . . 62

References 66

Chapter 7. A General Two-Group Model Calculation on (+)-(3R)-Methylcyclohexanone . . . 67

7.1. Introduction 67

7.2. The Normal Coordinate Analysis . . . 67

7.2.1. Molecular Geometry 67

7.2.2. Internal Coordinates 69

7.2.3. The Molecular Force Field 69

7.2.4. Results of the Normal Coordinate Analysis . 69

7.3. The Rayleigh and Raman Optical Activity Calculation 76

7.3.1. The Bond Polarizability Data . . . 76

7.3.2. The Calculated Circular Intensity Differences of (+)-(3R)-Methylcyclohexanone . . . 79

References 88

Chapter 8. Raman Optical Activity Spectra of Related Molecules 89

Raman Optical Activity of Menthol and Related Molecules 90

TABLE OF CONTENTS (continued)

	Page
Raman Optical Activity of Pinenes, Carenes, and Related Molecules	97
References	102
Appendix	103
References	106

ACKNOWLEDGEMENTS

I express my sincerest thanks to Dr. Laurence D. Barron. His boundless enthusiasm, energy and patience together with an insight for the subject made him the perfect supervisor.

I also thank Dr. Laurence A. Nafie who very kindly sent me a normal coordinate analysis computer package and advised me on how to set it up.

I thank Dr. Christopher Morrow who carried out the molecular mechanics calculation in Chapter 7.

Finally, I am grateful to João Ramos who helped with the diagrams.

SUMMARY

The principal task of this thesis was to develop theoretical expressions which would enable the Rayleigh and Raman optical activity of any chiral molecule to be calculated. This was carried out by generalising an existing theoretical construct- the so-called simple two-group model. The generalised two-group model is based on a bond polarizability scheme: with the appropriate bond polarizability data together with a reliable normal coordinate analysis of a chiral molecule its Rayleigh and Raman optical activity can be calculated.

The theory was first applied to a small chiral molecule, (+)-R-bromochlorofluoromethane. This substance has not been resolved in sufficient quantity for its Raman optical activity to be measured but the results were compared with those calculated by the atom-dipole interaction model of Rayleigh and Raman optical activity, the major alternative to the generalised two-group model. The comparison yielded no correlation. A short exposition of this atom-dipole interaction model is given, considering it in relation to the generalised two-group model.

The second molecule to be subjected to a calculation was (+)-(3R)-methylcyclohexanone. Apart from limited success with carbon-hydrogen bending vibrations, the agreement between observed and calculated results was disappointing, mainly due to the poor quality of the force field for the normal coordinate analysis. When an accurate force field becomes available it will be a simple matter to repeat the calculation.

Finally, in a different vein from the preceding part of the thesis, the Raman optical activity spectra of several series of related

molecules were studied - menthols, pinenes and carenes. Several stereochemical correlations were pointed out involving, in particular, bands characteristic of the isopropyl and gem-dimethyl groups, methyl torsions and out-of-plane olefinic hydrogen deformations.

LIST OF TABLES

Page

6.1. Internal Coordinate Definitions for Bromochlorofluoromethane 58

6.2. The Observed and Calculated Normal Modes of Bromochlorofluoromethane 59

6.3. Bond Polarizability Data for Bromochlorofluoromethane 61

6.4. The Calculated Polarized and Depolarized Circular Intensity Differentials of (+)-R-Bromochlorofluoromethane 63

6.5. Comparison of the Circular Intensity Differences of (+)-R-Bromochlorofluoromethane Calculated by the General Two-Group (GTG) Model and the Atom-Dipole Interaction (ADI) Model 64

7.1. The Principal Cartesian Coordinates of (+)-(3R)-Methylcyclohexanone 68

7.2. Values of the Force Constants for 3-Methylcyclohexanone 70

7.3. Calculated Vibrational Frequencies and Potential Energy Distribution of 3-Methylcyclohexanone . 72

7.4. The Measured Raman and Infrared Spectra of 3-Methylcyclohexanone 74

7.5. Comparison of Observed (Raman) and Calculated Vibrational Frequencies of 3-Methylcyclohexanone . . 77

7.6. Bond Polarizability Data for 3-Methylcyclohexanone 78

7.7. The Calculated Polarized and Depolarized Circular Intensity Differences of (+)-(3R)-Methylcyclohexanone 80

7.8. Observed Depolarized Circular Intensity Differences of (+)-(3R)-Methylcyclohexanone 83

7.9. Comparison of Observed and Calculated Depolarized Circular Intensity Differences (400-1700 cm^{-1}) of (+)-(3R)-Methylcyclohexanone 85

LIST OF FIGURES

	Page
2.1. The Experimental Arrangement for the Observation of Raman Optical Activity	9
3.1. The Simple Two-Group Model	16
3.2. Simple Two-Group Geometry with Group Symmetry Axes in Parallel Planes	19
3.3. General Geometry for Simple Two-Group Model . .	24
4.1. Two Series of Related Compounds Suitable for Bond Polarizability Study Mentioned in Text . .	43
4.2. (S)- α-Phenylethylisocyanate	47
6.1. The Internal Coordinates of Bromochlorofluoromethane	57
7.1. The Depolarized Circular Intensity Sum and Difference Spectra of Neat (+)-(3R)-Methylcyclohexanone .	67
7.2. The Equatorial Conformation of (+)-(3R)-Methylcyclohexanone	67
7.3. The Atom Numbering System for 3-Methylcyclohexanone	67
7.4. The Internal Coordinates of 3-Methylcyclohexanone .	69
7.5. The Bond Numbering System for 3-Methylcyclohexanone	76

CHAPTER 1

INTRODUCTION

Vibrational optical activity is a powerful new technique for studying the stereochemistry of optically active substances. At present, research into the subject involves two complementary techniques, namely, infrared circular dichroism and vibrational Raman optical activity. This work deals with this latter effect. Several excellent reviews of both techniques have been written recently covering the theoretical and experimental development of both branches of vibrational optical activity.[1-9] Possibly the most exciting development at the present moment is the advent of extremely sophisticated instrumentation - Fourier transform infrared spectrometers[10] and multi-channel laser Raman photon counting systems.[11-13] These will enable more subtle effects to be detected, providing more detailed and reliable data to inspire new theoretical advances and allow existing theories to be stringently tested.

Briefly, infrared circular dichroism is an extension of ordinary visible circular dichroism into the infrared region of the electromagnetic spectrum. A small difference in the extinction coefficients using right and left circularly polarized radiation is measured for the vibrational transitions of a chiral molecule. Raman optical activity, on the other hand, is a scattering phenomenon. The chiral molecule now exhibits a difference in the intensity of scattered Raman (and Rayleigh) radiation using left and right circularly polarized visible light.

This thesis presents a generalisation of the "two-group" model of Barron and Buckingham (see Chapters 3 and 4) enabling Rayleigh

and Raman optical activity spectra to be calculated for any chiral molecule. This theory, based on a bond polarizability model, is used to calculate the Rayleigh and Raman optical activity of selected molecules (Chapters 6 and 7).

A comparison of the generalised two-group model is given with the "atom-dipole interaction" model - the other major method for calculating Rayleigh and Raman optical activity (Chapter 5).

In Chapter 8 some speculations are made as to the origins of several features in the Raman optical activity spectra of a series of related organic molecules. While most of the molecules studied are too large and complicated for an application of the theory developed in this thesis, useful stereochemical information may be obtained by examining spectral features that obviously have the same origins in a number of structurally related chiral molecules.

REFERENCES

1. L.D. Barron and A.D. Buckingham, Ann. Rev. Phys. Chem., 26, 381 (1975).

2. L.D. Barron, in Molecular Spectroscopy, Vol. 4, ed. by R.F. Barrow, D.A. Long and J. Sheriden, The Chemical Society, London (1976).

3. L.D. Barron, in Advances in Infrared and Raman Spectroscopy, Vol. 4, ed. by R.J.H. Clark and R.E. Hester, Heyden, London (1978).

4. L.D. Barron, in Optical Activity and Chiral Discrimination, ed. by S.F. Mason, Reidel, Dordrecht (1979).

5. L.D. Barron, Accts. Chem. Res., 13, 90 (1980).

6. L.A. Nafie and M. Diem, Accts. Chem. Res., 12, 296 (1979).

7. L.A. Nafie, in "Vibrational Spectra and Structure", to be published.

8. P.J. Stephens and R. Clark, in Optical Activity and Chiral Discrimination, ed. by S.F. Mason, Reidel, Dordrecht (1979).

9. S.F. Mason, in Advances in Infrared and Raman Spectroscopy, Vol. 8, ed. by R.J.H. Clark and R.E. Hester, to be published.

10. L.A. Nafie, M. Diem and D.W. Vidrine, J. Amer. Chem. Soc., 101, 496 (1979).

11. H. Boucher, T.R. Brocki, M. Moskovits and B. Bosnich, J. Amer. Chem. Soc., 99, 6870 (1977).

12. T.R. Brocki, M. Moskovits and B. Bosnich, J. Amer. Chem. Soc., in the press.

13. W. Hug and H. Surbeck, Chem. Phys. Lett., 60, 186 (1979).

CHAPTER 2

THE BASIC EQUATIONS OF RAYLEIGH AND RAMAN OPTICAL ACTIVITY

Formulae for the electric and magnetic moments induced in a molecule by the action of the electromagnetic field of a light wave may be deduced using time-dependent perturbation theory.[1] Most of the effects of interest to a chemist are adequately dealt with by considering the perturbation as the purely classical coupling energy of the molecule's electric and magnetic multipole moments with those of the light wave. This procedure yields expressions for the induced moments in terms of various property tensors of the molecule, from which the intensity of the radiation scattered by the molecule may be obtained. The most familiar of these property tensors is the electric dipole-electric dipole polarizability tensor. For a chiral molecule one may then obtain formulae for the difference in scattered intensity using left and right circularly polarized light as a function of the property tensors.[2] The relevant equations are given below. First, let us define the experimental set-up, (Figure 2.1). The most convenient method of measuring differential scattering is to observe the scattered radiation at 90° to the direction of the incident light. All the expressions in this work will be for 90° scattering.

If circularly polarized light propagates in the positive direction of the z-axis and the scattered radiation is analysed by a detector along the y-axis we have several experimental quantities that can be measured:

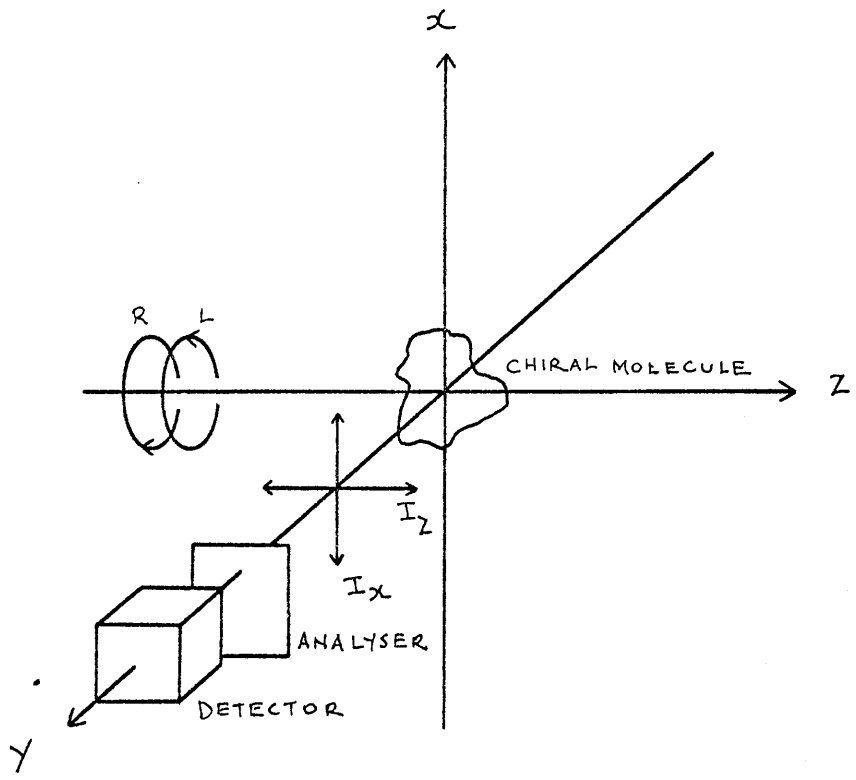

Figure 2.1. The Experimental Arrangement for the Observation of Raman Optical Activity.

R = Right circularly polarized light
L = Left circularly polarized light

1) with no analyser present, the total intensity of scattered radiation;

2) with an analyser admitting only light polarized in the xy-plane, the polarized scattering intensity, I_x;

3) with an analyser admitting only light polarized in the yz-plane, the depolarized scattering intensity, I_z.

The expressions for I_x and I_z involve different combinations of the property tensors so that additional information is gained by making intensity measurements with an analyser present. We will always quote results for both polarized and depolarized scattering. If required, unpolarized intensities may be simply obtained by summing the depolarized and polarized contributions.

A convenient quantity which has been used to describe Rayleigh and Raman optical activity is the circular intensity difference,[3] Δ, defined as

$$\Delta_\alpha = (I_\alpha^R - I_\alpha^L)/(I_\alpha^R + I_\alpha^L) \qquad \alpha = x, z \qquad (2.1)$$

where I_α^R and I_α^L are the scattered intensities with α-polarization in right and left circularly polarized light, respectively.

An alternative quantity has been proposed recently,[4] the chirality number, q, which is defined using differential scattering cross-sections. The advantage of the chirality number is that it refers to an enantiomerically pure sample. However, in order to be consistent with the substantial amount of theoretical work carried out in the field, we retain the use of the circular intensity difference. No confusion is likely to arise from doing this. For enantiomerically pure substances the two quantities are related by

$$q = -2\Delta \qquad (2.2)$$

Before going any further, it should be mentioned that cartesian tensor notation is used here. Greek subscripts denote vector or tensor components and can be equal to x, y, or z. A repeated Greek suffix implies a summation over the three cartesian components. The Kronecker delta, $\delta_{\alpha\beta}$, and the unit alternating tensor, $\varepsilon_{\alpha\beta\gamma}$, have their usual meanings.[5]

The perturbation theory calculations outlined above give us, for Rayleigh scattering from an isotropic fluid[2] (in SI units)

$$\Delta_x = \frac{2(7\alpha_{\alpha\beta}G'_{\alpha\beta} + \alpha_{\alpha\alpha}G'_{\beta\beta} + \frac{1}{3}\omega\alpha_{\alpha\beta}\varepsilon_{\alpha\gamma\delta}A_{\gamma\delta\beta})}{c(7\alpha_{\lambda\mu}\alpha_{\lambda\mu} + \alpha_{\lambda\lambda}\alpha_{\mu\mu})} \tag{2.3a}$$

$$\Delta_z = \frac{4(3\alpha_{\alpha\beta}G'_{\alpha\beta} - \alpha_{\alpha\alpha}G'_{\beta\beta} - \frac{1}{3}\omega\alpha_{\alpha\beta}\varepsilon_{\alpha\gamma\delta}A_{\gamma\delta\beta})}{2c(3\alpha_{\lambda\mu}\alpha_{\lambda\mu} - \alpha_{\lambda\lambda}\alpha_{\mu\mu})} \tag{2.3b}$$

where $\underset{\sim}{\alpha}$ is the electric dipole-electric dipole polarizability tensor, $\underset{\sim}{G'}$ is the electric dipole-magnetic dipole optical activity tensor, $\underset{\sim}{A}$ is the electric dipole-electric quadrupole optical activity tensor, ω is the angular frequency of the incident radiation, and c is the speed of light. The explicit forms of the tensors are[1]

$$\alpha_{\alpha\beta} = \tfrac{2}{\hbar}\sum_{j\neq n}\omega_{jn}(\omega_{jn}^2-\omega^2)^{-1}\mathrm{Re}(\langle n|\mu_\alpha|j\rangle\langle j|\mu_\beta|n\rangle) = \alpha_{\beta\alpha} \tag{2.4a}$$

$$G'_{\alpha\beta} = -\tfrac{2}{\hbar}\sum_{j\neq n}\omega(\omega_{jn}^2-\omega^2)^{-1}\mathrm{Im}(\langle n|\mu_\alpha|j\rangle\langle j|m_\beta|n\rangle) \tag{2.4b}$$

$$A_{\alpha\beta\gamma} = \tfrac{2}{\hbar}\sum_{j\neq n}\omega_{jn}(\omega_{jn}^2-\omega^2)^{-1}\mathrm{Re}(\langle n|\mu_\alpha|j\rangle\langle j|\Theta_{\beta\gamma}|n\rangle) \tag{2.4c}$$

where Re and Im denote real and imaginary parts, respectively, and $\omega_{jn} = \omega_j - \omega_n$ is the angular frequency of the transition from state n to state j. The summations are over all the excited states of the molecule. The operators $\underset{\sim}{\mu}$, $\underset{\sim}{m}$ and $\underset{\sim}{\Theta}$ are the electric dipole, magnetic dipole and electric quadrupole moments, respectively, and are defined as

$$\mu_\alpha = \sum_i e_i r_{i\alpha} \tag{2.5a}$$

$$m_\alpha = \sum_i (e_i/2m_i) \varepsilon_{\alpha\beta\gamma} r_{i\beta} p_{i\gamma} \tag{2.5b}$$

$$\Theta_{\alpha\beta} = \tfrac{1}{2} \sum_i e_i (3 r_{i\alpha} r_{i\beta} - r_i^2 \delta_{\alpha\beta}) \tag{2.5c}$$

where the sums are over all particles, i, of the molecule each having position vector $\underset{\sim}{r}_i$, charge e_i, mass m_i and linear momentum $\underset{\sim}{p}_i$.

The same expressions (2.3a&b) apply to Raman scattering if the tensor products are replaced by the appropriate tensor transition moment products.[6] For example, instead of $\alpha_{\alpha\beta} G'_{\alpha\beta}$ we would have $\langle 0|\alpha_{\alpha\beta}(Q_\rho)|1_\rho\rangle\langle 1_\rho|G'_{\alpha\beta}(Q_\rho)|0\rangle$, where $|0\rangle$ is the ground vibrational state and $|1_\rho\rangle$ is the vibrational state in which all the normal modes are in the ground state except normal mode Q_ρ which is in its first excited state. The tensors are now operators connecting vibrational states and are dependent on the normal coordinate.

If we had accurate wavefunctions for all the eigenstates of a chiral molecule we could calculate $\underset{\sim}{\alpha}$, $\underset{\sim}{G'}$ and $\underset{\sim}{A}$ directly as functions of Q and so obtain values for the Rayleigh and Raman circular intensity differences. Unfortunately, for molecules large enough to be chiral, accurate wavefunctions, in general, are a long way off. Hence, the task for anyone wishing to calculate

circular intensity differences is to find an empirical, or at least semi-empirical, model with which to obtain reliable estimates of the tensor quantities involved.

Since the quest is for a theory based on some empirical method, the exact quantum-mechanical forms of the property tensors, as given in (2.4a,b,&c), are of limited use at the moment. One very important aspect of the tensors, though, is their symmetry properties, and these can be deduced from (2.4a,b,&c)[7]. The polarizability tensor, $\alpha_{\alpha\beta}$, transforms as the product of two dipole moments, $\mu_\alpha \mu_\beta$. Since the dipole moment is a polar vector (it changes sign under inversion), we can see that the sign of the product of two dipole moments, and hence $\alpha_{\alpha\beta}$, will be unchanged under inversion and is therefore a second rank polar tensor. The optical activity tensor, $G'_{\alpha\beta}$, on the other hand, transforms as the product of an electric dipole moment and a magnetic dipole moment, $\mu_\alpha m_\beta$. Since m_β does not change sign under inversion (an axial vector), $\mu_\alpha m_\beta$, and hence $G'_{\alpha\beta}$, changes sign under inversion and is therefore a second rank axial tensor. Although $A_{\alpha\beta\gamma}$ does not transform like $G'_{\alpha\beta}$, the product $\varepsilon_{\alpha\gamma\delta} A_{\gamma\delta\beta}$, the form in which the tensor always appears in the formulae for the circular intensity difference, does transform as a second rank axial tensor.

Rayleigh optical activity is dependent on products like $\alpha_{xy} G'_{xy}$, $\alpha_{zx} G'_{zx}$, where the same components of $\underset{\sim}{\alpha}$ and $\underset{\sim}{G'}$ are involved. The symmetry requirements for $\alpha_{\alpha\beta} G'_{\alpha\beta}$ to be non-vanishing is that the totally symmetric representation of a molecule's point group contains identical components of $\underset{\sim}{\alpha}$ and $\underset{\sim}{G'}$. The only

occasion this is possible is when the molecule belongs to a chiral point group (which contains only proper rotation elements) where polar and axial tensors are not differentiated.

Similarly, for Raman optical activity, which is dependent on products like $\langle 0 | \alpha_{xy}(Q_\rho) | 1_\rho \rangle \langle 1_\rho | G'_{xy}(Q_\rho) | 0 \rangle$, the same components of $\underset{\sim}{\alpha}(Q_\rho)$ and $\underset{\sim}{G}'(Q_\rho)$ must transform identically to the normal coordinate Q_ρ; and again this is only possible in the chiral point groups.

REFERENCES

1. A.D. Buckingham, Adv. Chem. Phys., 12, 107 (1967).

2. P.W. Atkins and L.D. Barron, Mol. Phys., 16, 453 (1969).

3. L.D. Barron and A.D. Buckingham, Mol. Phys., 20, 1111 (1971).

4. W. Hug and H. Surbeck, Chem. Phys. Lett., 60, 186 (1979).

5. H. Jeffreys, Cartesian Tensors, Cambridge University Press, 1931.

6. G. Placzek, in Handbuch der Radiologie, Vol. 6, Part 2, ed. by E. Marx, Akademische Verlagsgesellschaft, Berlin, 1934.

7. L.D. Barron, in Advances in Infrared and Raman Spectroscopy, Vol. 4, ed. by R.J.H. Clark and R.E. Hester, Heyden, London, 1978.

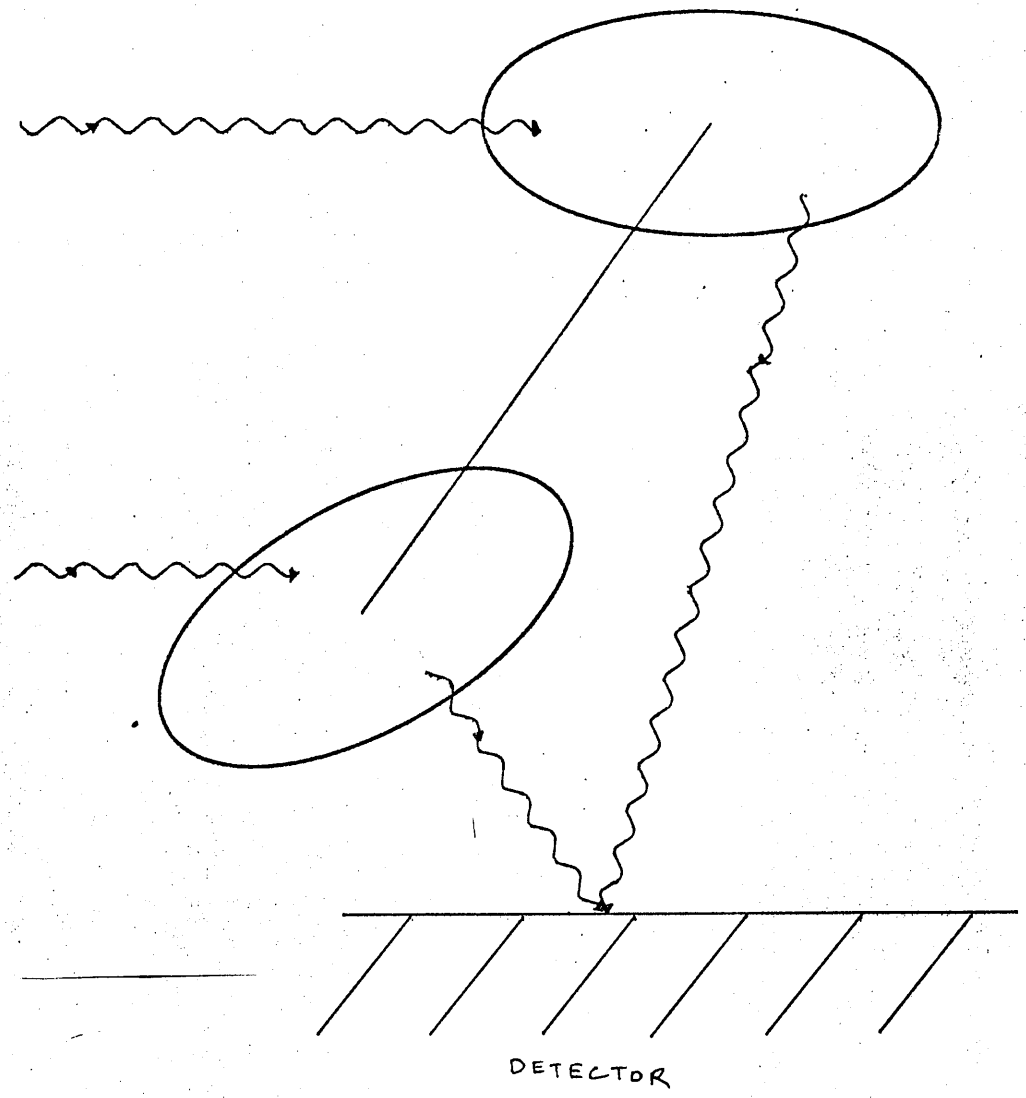

Figure 3.1. - The Simple Two-Group Model : Differential Scattering is Generated through Interference between Waves Independently Scattered from the Two Groups.

in the molecular property tensors

$$\alpha_{\alpha\beta} \longrightarrow \alpha_{\alpha\beta} \tag{3.2a}$$

$$G'_{\alpha\beta} \longrightarrow G'_{\alpha\beta} + \tfrac{1}{2}\omega\,\varepsilon_{\beta\gamma\delta}R_{\gamma}\alpha_{\alpha\delta} \tag{3.2b}$$

$$A_{\alpha\beta\gamma} \longrightarrow A_{\alpha\beta\gamma} - \tfrac{3}{2}R_{\beta}\alpha_{\alpha\gamma} - \tfrac{3}{2}R_{\gamma}\alpha_{\alpha\beta} + R_{\delta}\alpha_{\alpha\delta}\delta_{\beta\gamma} \tag{3.2c}$$

If we take two neutral achiral groups chirally disposed to each other, as in Figure 3.1, assuming no electron exchange between them, then we may write the molecular property tensors as sums of group property tensors referred to local origins including, where necessary, their origin-dependent parts. Choosing the molecular origin to be at the local origin of group 1 we have

$$\alpha_{\alpha\beta} = \alpha_{1\alpha\beta} + \alpha_{2\alpha\beta} \tag{3.3a}$$

$$G'_{\alpha\beta} = G'_{1\alpha\beta} + G'_{2\alpha\beta} - \tfrac{1}{2}\omega R_{21\gamma}\alpha_{2\alpha\delta} \tag{3.3b}$$

$$A_{\alpha\beta\gamma} = A_{1\alpha\beta\gamma} + A_{2\alpha\beta\gamma} + \tfrac{3}{2}R_{21\beta}\alpha_{2\alpha\gamma} + \tfrac{3}{2}R_{21\gamma}\alpha_{2\alpha\beta} - R_{21\delta}\alpha_{2\alpha\delta}\delta_{\beta\gamma} \tag{3.3c}$$

where $\alpha_{i\alpha\beta}, G'_{i\alpha\beta}$ and $A_{i\alpha\beta\gamma}(i = 1,2)$ are the property tensors of group i referred to a local origin on group i and $\underset{\sim}{R}_{21} = \underset{\sim}{R}_2 - \underset{\sim}{R}_1$ is the vector from the origin on group 1 to that on group 2.

In writing (3.3a-c) we have assumed there is no static or dynamic coupling between the groups.

Using (3.3a-c) we can write down the relevant tensor products required in the expressions for the Rayleigh circular intensity difference (2.3a&b). These are

$$\alpha_{\alpha\beta}G'_{\alpha\beta} = -\tfrac{1}{2}\omega\varepsilon_{\beta\gamma\delta}R_{21\gamma}\alpha_{1\alpha\beta}\alpha_{2\delta\alpha} + \alpha_{1\alpha\beta}G'_{2\alpha\beta} + \alpha_{2\alpha\beta}G'_{1\alpha\beta} \tag{3.4a}$$

$$\tfrac{1}{3}\omega\alpha_{\alpha\beta}\varepsilon_{\alpha\gamma\delta}A_{\gamma\delta\beta} = -\tfrac{1}{2}\omega\varepsilon_{\beta\gamma\delta}R_{21\gamma}\alpha_{1\alpha\beta}\alpha_{2\delta\alpha} + \tfrac{1}{3}\omega\alpha_{1\alpha\beta}\varepsilon_{\alpha\gamma\delta}A_{2\gamma\delta\beta} + \tfrac{1}{3}\omega\alpha_{2\alpha\beta}\varepsilon_{\alpha\gamma\delta}A_{1\gamma\delta\beta} \tag{3.4b}$$

$$\alpha_{\alpha\alpha} G'_{\beta\beta} = 0 \qquad (3.4c)$$

$$\alpha_{\alpha\beta}\alpha_{\alpha\beta} = \alpha_{1\alpha\beta}\alpha_{1\alpha\beta} + \alpha_{2\alpha\beta}\alpha_{2\alpha\beta} + 2\alpha_{1\alpha\beta}\alpha_{2\alpha\beta} \qquad (3.4d)$$

$$\alpha_{\alpha\alpha}\alpha_{\beta\beta} = \alpha_{1\alpha\alpha}\alpha_{1\beta\beta} + \alpha_{2\alpha\alpha}\alpha_{2\beta\beta} + 2\alpha_{1\alpha\alpha}\alpha_{2\beta\beta} \qquad (3.4e)$$

In order to make the expressions involving the optical activity tensors manageable we must impose some symmetry restrictions on the groups. We have already stipulated that the groups are achiral. If, on top of this, they have threefold or higher rotation axes (here taken to be the 3 axis) the second rank axial tensors $G'_{\alpha\beta}$ and $\varepsilon_{\alpha\gamma\delta}A_{\gamma\delta\beta}$ have components that are either zero or anti-symmetric. Since the ordinary polarizability is always symmetric, all the optical activity-polarizability tensor products involving intrinsic group optical activity tensors are zero. This fact is used throughout this work. Similarly, optical activity-polarizability transition tensor products are zero in the Raman case. Since, at present, we always consider these pseudo-cylindrical groups, which in the general theory become bonds, we can construct a theory which requires a knowledge of the form and behaviour of solely the group polarizability tensors.

If the principal axes 1, 2 and 3 of pseudocylindrical group i are associated with unit vectors $\underset{\sim}{s}_i$, $\underset{\sim}{t}_i$ and $\underset{\sim}{u}_i$, its polarizability tensor may be written

$$\alpha_{i\alpha\beta} = \alpha_i(1-\kappa_i)\delta_{\alpha\beta} + 3\alpha_i\kappa_i v_{i\alpha}v_{i\beta} \qquad (3.5)$$

where

$$\kappa = (\alpha_{33} - \alpha_{11})/3\alpha \qquad (3.6a)$$

$$\alpha = \tfrac{1}{3}(\alpha_{11} + \alpha_{22} + \alpha_{33}) \qquad (3.6b)$$

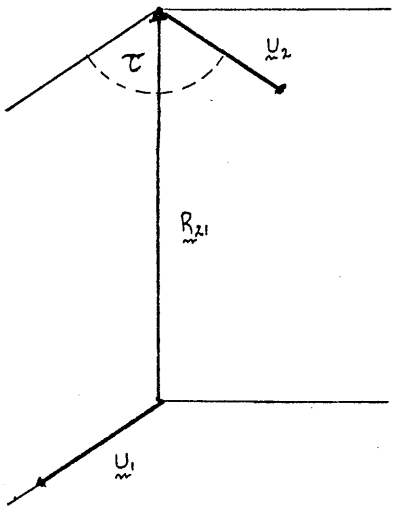

Figure 3.2. Simple Two-Group Geometry with Group Symmetry Axes in Parallel Planes.

Raman case if the ordinary tensors are replaced by transition tensor integrals, for example, $\alpha_{\alpha\beta} \rightarrow \langle f|\alpha_{\alpha\beta}|i\rangle$ where i and f label initial and final vibrational states, respectively. We now present the procedure leading to simple two-group Raman circular intensity differences.[1,3]

Assuming identical groups, if each group i is associated with a totally symmetric internal coordinate S_i (see Appendix) which preserves the pseudocylindrical symmetry of the group we can formulate idealized normal modes which arise from the symmetric and antisymmetric combinations of the internal coordinates. (If the groups are simply bonds, the S_i would be bond stretch coordinates.) Call these normal modes Q_+ and Q_-, respectively. We have the following relations

$$Q_+ = \frac{1}{\sqrt{2}}(S_1 + S_2) \tag{3.10a}$$

$$Q_- = \frac{1}{\sqrt{2}}(S_1 - S_2) \tag{3.10b}$$

$$S_1 = \frac{1}{\sqrt{2}}(Q_+ + Q_-) \tag{3.10c}$$

$$S_2 = \frac{1}{\sqrt{2}}(Q_+ - Q_-) \tag{3.10d}$$

The required transition tensor integral products are

$$\langle 0|\alpha_{\alpha\beta}|1_\pm\rangle\langle 1_\pm|G'_{\alpha\beta}|0\rangle = \tfrac{1}{3}\omega\langle 0|\alpha_{\alpha\beta}|1_\pm\rangle\langle 1_\pm|\varepsilon_{\alpha\gamma\delta}A_{\gamma\delta\beta}|0\rangle = \mp\tfrac{1}{2}\omega\varepsilon_{\beta\gamma\delta}R_{21\gamma}\langle 0|\alpha_{1\alpha\beta}|1_\pm\rangle\langle 1_\pm|\alpha_{2\delta\alpha}|0\rangle \tag{3.11a}$$

$$\langle 0|\alpha_{\alpha\alpha}|1_\pm\rangle\langle 1_\pm|G'_{\beta\beta}|0\rangle = 0 \tag{3.11b}$$

$$\langle 0|\alpha_{\alpha\beta}|1_\pm\rangle\langle 1_\pm|\alpha_{\alpha\beta}|0\rangle = \langle 0|\alpha_{1\alpha\beta}|1_\pm\rangle\langle 1_\pm|\alpha_{1\alpha\beta}|0\rangle + \langle 0|\alpha_{2\alpha\beta}|1_\pm\rangle\langle 1_\pm|\alpha_{2\alpha\beta}|0\rangle + 2\langle 0|\alpha_{1\alpha\beta}|1_\pm\rangle\langle 1_\pm|\alpha_{2\alpha\beta}|0\rangle \tag{3.11c}$$

$$\langle 0|\alpha_{\alpha\alpha}|1_\pm\rangle\langle 1_\pm|\alpha_{\beta\beta}|0\rangle = \langle 0|\alpha_{1\alpha\alpha}|1_\pm\rangle\langle 1_\pm|\alpha_{2\beta\beta}|0\rangle + \langle 0|\alpha_{2\alpha\alpha}|1_\pm\rangle\langle 1_\pm|\alpha_{2\beta\beta}|0\rangle + 2\langle 0|\alpha_{1\alpha\alpha}|1_\pm\rangle\langle 1_\pm|\alpha_{2\beta\beta}|0\rangle \tag{3.11d}$$

where $|0\rangle$ is the ground vibrational state and $|1_+\rangle$ and $|1_-\rangle$ are the first excited states of the symmetric and antisymmetric normal modes, respectively. Again, we have taken the groups to have threefold symmetry axes which enables us to omit the intrinsic optical activity tensors. Note also that the optical activity-polarizability tensor transition moment involving the origin-dependent part of $\underset{\sim}{A}$ is identical to that involving the origin-dependent part of $\underset{\sim}{G'}$.

We may treat the polarizability as a function of the normal coordinates and write it in a power series -

$$\alpha_{\alpha\beta}(Q_\pm) = (\alpha_{\alpha\beta})_0 + \left(\frac{\partial\alpha_{\alpha\beta}}{\partial Q_\pm}\right)_0 Q_\pm + \cdots \tag{3.12}$$

where a zero subscript denotes a quantity evaluated at $Q_\pm = 0$. Using the fact that only terms linear in the normal coordinate give a non-zero matrix element for fundamental transitions,[4] the calculation now devolves upon the calculation of $(\partial\alpha_{\alpha\beta}/\partial Q_\pm)_0 = \sum_i (\partial\alpha_{i\alpha\beta}/\partial Q_\pm)_0$.

We have that

$$\left(\frac{\partial\alpha_{i\alpha\beta}}{\partial Q_\pm}\right)_0 = \sum_j \left(\frac{\partial\alpha_{i\alpha\beta}}{\partial S_j}\right)_0 \left(\frac{\partial S_j}{\partial Q_\pm}\right)_0 \qquad i = 1,2 \tag{3.13}$$

Employing (3.10c&d) this gives

$$\left(\frac{\partial \alpha_{1\alpha\beta}}{\partial Q_\pm}\right)_0 = \frac{1}{\sqrt{2}}\left(\frac{\partial \alpha_{1\alpha\beta}}{\partial S_1}\right)_0 \tag{3.14a}$$

$$\left(\frac{\partial \alpha_{2\alpha\beta}}{\partial Q_\pm}\right)_0 = \pm\frac{1}{\sqrt{2}}\left(\frac{\partial \alpha_{2\alpha\beta}}{\partial S_2}\right)_0 \tag{3.14b}$$

The relevant equations, (3.11), become

$$\mp\tfrac{1}{2}\omega\,\varepsilon_{\beta\gamma\delta}R_{21\gamma}\langle 0|\alpha_{1\alpha\beta}|1_\pm\rangle\langle 1_\pm|\alpha_{2\delta\alpha}|0\rangle = \mp\tfrac{1}{4}\omega\,|\langle 0|Q_\pm|1_\pm\rangle|^2\,\varepsilon_{\beta\gamma\delta}R_{21\gamma}\left(\frac{\partial\alpha_{1\alpha\beta}}{\partial S_1}\right)_0\left(\frac{\partial\alpha_{2\delta\alpha}}{\partial S_2}\right)_0 \tag{3.15a}$$

$$\langle 0|\alpha_{\alpha\beta}|1_\pm\rangle\langle 1_\pm|\alpha_{\alpha\beta}|0\rangle = \tfrac{1}{2}|\langle 0|Q_\pm|1_\pm\rangle|^2\left[\left(\frac{\partial\alpha_{1\alpha\beta}}{\partial S_1}\right)_0\left(\frac{\partial\alpha_{1\alpha\beta}}{\partial S_1}\right)_0 + \left(\frac{\partial\alpha_{2\alpha\beta}}{\partial S_2}\right)_0\left(\frac{\partial\alpha_{2\alpha\beta}}{\partial S_2}\right)_0 \pm 2\left(\frac{\partial\alpha_{1\alpha\beta}}{\partial S_1}\right)_0\left(\frac{\partial\alpha_{2\alpha\beta}}{\partial S_2}\right)_0\right] \tag{3.15b}$$

$$\langle 0|\alpha_{\alpha\alpha}|1_\pm\rangle\langle 1_\pm|\alpha_{\beta\beta}|0\rangle = \tfrac{1}{2}|\langle 0|Q_\pm|1_\pm\rangle|^2\left[\left(\frac{\partial\alpha_{1\alpha\alpha}}{\partial S_1}\right)_0\left(\frac{\partial\alpha_{1\beta\beta}}{\partial S_1}\right)_0 + \left(\frac{\partial\alpha_{2\alpha\alpha}}{\partial S_2}\right)_0\left(\frac{\partial\alpha_{2\beta\beta}}{\partial S_2}\right)_0 \pm 2\left(\frac{\partial\alpha_{1\alpha\alpha}}{\partial S_1}\right)_0\left(\frac{\partial\alpha_{2\beta\beta}}{\partial S_2}\right)_0\right] \tag{3.15c}$$

Remembering that we are dealing with vibrations which do not change the orientations of the groups, using (3.5), the local group derivatives are

$$\left(\frac{\partial\alpha_{i\alpha\beta}}{\partial S_i}\right)_0 = \frac{d}{dS_i}\left[\alpha_i(1-\kappa_i)S_{\alpha\beta} + 3\alpha_i\kappa_i U_{i\alpha}U_{i\beta}\right]_0$$

$$= \left[\frac{\partial \alpha_i (1-\kappa_i)}{\partial S_i}\right]_0 \delta_{\alpha\beta} + 3\left(\frac{\partial \alpha_i \kappa_i}{\partial S_i}\right)_0 U_{i\alpha} U_{i\beta} \qquad (3.16)$$

$\nu = 1, 2$

Substituting (3.16) in (3.15a-c), seeing that the transition integral factors cancel, the following circular intensity difference expressions are obtained for the molecular geometry in Figure 3.2[3]

$$\Delta_x^+ = \frac{24\pi R_{21}\left(\frac{\partial \alpha_i \kappa_i}{\partial S_i}\right)_0^2 \sin 2\tau}{\lambda\left[40\left(\frac{\partial \alpha_i}{\partial S_i}\right)_0^2 + 7\left(\frac{\partial \alpha_i \kappa_i}{\partial S_i}\right)_0^2 (5+3\cos 2\tau)\right]} \qquad (3.17a)$$

$$\Delta_x^- = -\frac{8\pi R_{21} \sin 2\tau}{7\lambda(1-\cos 2\tau)} \qquad (3.17b)$$

$$\Delta_z^+ = \frac{2\pi R_{21} \sin 2\tau}{\lambda(5+3\cos 2\tau)} \qquad (3.17c)$$

$$\Delta_z^- = -\frac{2\pi R_{21} \sin 2\tau}{3\lambda(1-\cos 2\tau)} \qquad (3.17d)$$

We should point out that in this analysis it is assumed that the two formally degenerate normal modes are split sufficiently for the Raman optical activity to appear (otherwise it would cancel out), yet not so much as to significantly change the make-up of the normal modes. For a real molecule this splitting might result from vibrational coupling to other internal coordinates.

This analysis has been extended to the case where the two groups do not lie in parallel planes[3,5] (although the C_2 symmetry

still exists). Reference 5 also derives expressions for the important case of both symmetric and non-symmetric vibrations of groups with C_{2v} symmetry. For these groups the intrinsic $\underset{\sim}{G'}$ tensors must be brought in.

Analytic forms for the circular intensity differences associated with the torsional vibration of the two-group structure have also been derived.[6,3] They are (for geometry in Figure 3.2)

$$\Delta_x = -\frac{8\pi R_{21} \sin 2\tau}{7\lambda(1-\cos 2\tau)} \tag{3.18a}$$

$$\Delta_z = -\frac{2\pi R_{21} \sin 2\tau}{3\lambda(1-\cos 2\tau)} \tag{3.18b}$$

3.4 The Raman Optical Activity of the Bending Vibrations of Simple Two-Group Structure

To complete the set of simple vibrational motions of the two-group structure we now derive expressions for the in-phase and out-of-phase combinations of the angle-bending internal coordinates associated with the two angles ϕ_1 and ϕ_2 (see Figure 3.3). The normal modes are

$$Q_+ = \frac{1}{\sqrt{2}}(\Delta\phi_1 + \Delta\phi_2) \tag{3.19a}$$

$$Q_- = \frac{1}{\sqrt{2}}(\Delta\phi_1 - \Delta\phi_2) \tag{3.19b}$$

If $\underset{\sim}{I}$, $\underset{\sim}{J}$, $\underset{\sim}{K}$ are unit vectors along the positive directions of the x-, y- and z-axes, respectively (shown in Figure 3.3),

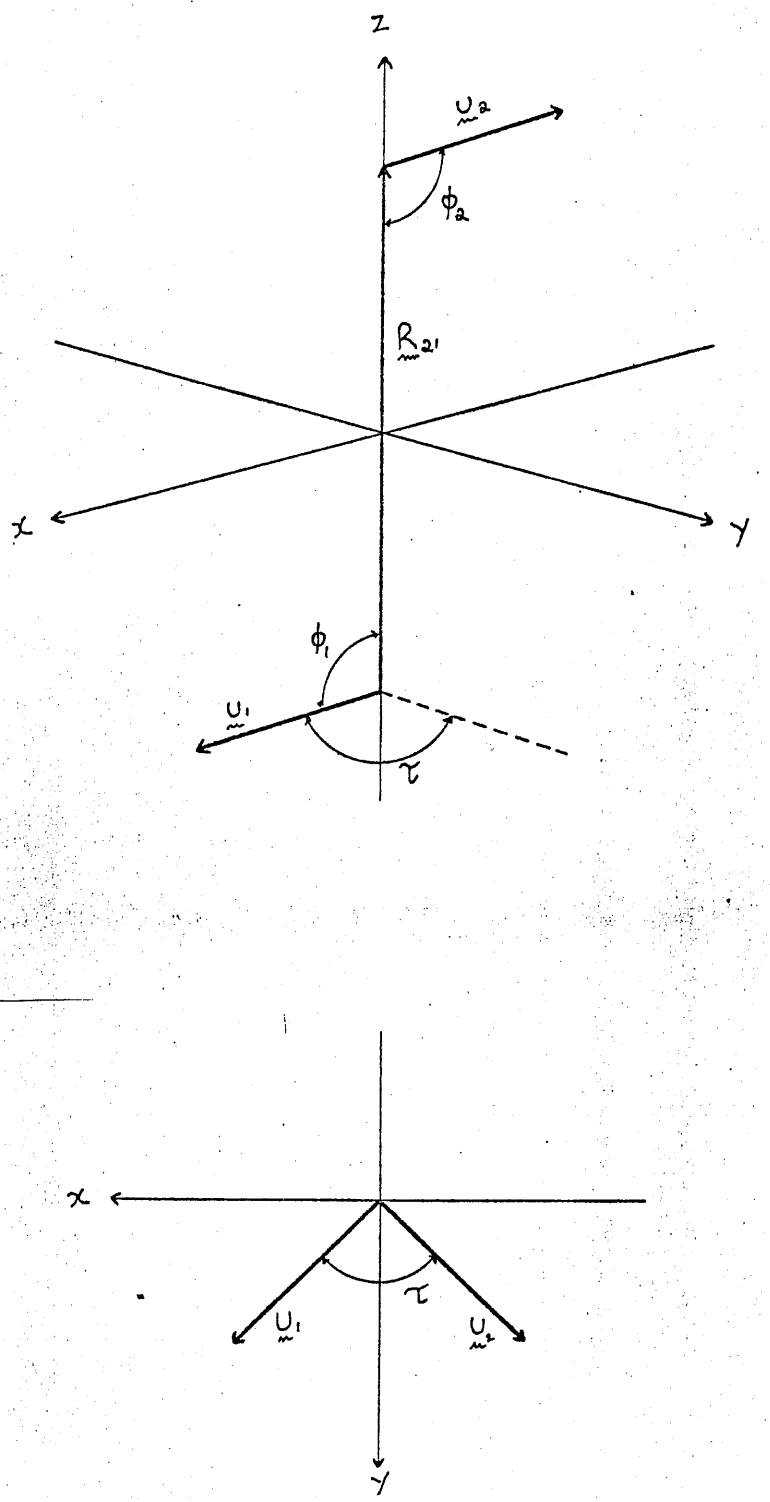

Figure 3.3. General Geometry for Simple Two-Group Model.

we have that

$$U_{1\alpha} = I_\alpha \sin\phi_1 \sin\tfrac{1}{2}\tau + J_\alpha \sin\phi_1 \cos\tfrac{1}{2}\tau + K_\alpha \cos\phi_1 \quad (3.20a)$$

$$U_{2\alpha} = -I_\alpha \sin\phi_2 \sin\tfrac{1}{2}\tau + J_\alpha \sin\phi_2 \cos\tfrac{1}{2}\tau - K_\alpha \cos\phi_2 \quad (3.20b)$$

giving

$$\begin{aligned} U_{1\alpha}U_{1\beta} = {} & I_\alpha I_\beta \sin^2\phi_1 \sin^2\tfrac{1}{2}\tau + \tfrac{1}{2}(I_\alpha J_\beta + J_\alpha I_\beta) \times \\ & \sin^2\phi_1 \sin\tau + \tfrac{1}{2}(I_\alpha K_\beta + K_\alpha I_\beta) \sin 2\phi_1 \sin\tfrac{1}{2}\tau \\ & + \tfrac{1}{2}(J_\alpha K_\beta + K_\alpha J_\beta) \sin 2\phi_1 \cos\tfrac{1}{2}\tau + J_\alpha J_\beta \times \\ & \sin^2\phi_1 \cos^2\tfrac{1}{2}\tau + K_\alpha K_\beta \cos^2\phi_1 \end{aligned} \quad (3.21a)$$

$$\begin{aligned} U_{2\alpha}U_{2\beta} = {} & I_\alpha I_\beta \sin^2\phi_2 \sin^2\tfrac{1}{2}\tau - \tfrac{1}{2}(I_\alpha J_\beta + J_\alpha I_\beta) \times \\ & \sin^2\phi_2 \sin\tau + \tfrac{1}{2}(I_\alpha K_\beta + K_\alpha I_\beta) \sin 2\phi_2 \sin\tfrac{1}{2}\tau \\ & - \tfrac{1}{2}(J_\alpha K_\beta + K_\alpha J_\beta) \sin 2\phi_2 \cos\tfrac{1}{2}\tau + J_\alpha J_\beta \times \\ & \sin^2\phi_2 \cos^2\tfrac{1}{2}\tau + K_\alpha K_\beta \cos^2\phi_2 \end{aligned} \quad (3.21b)$$

This gives us the form of the group polarizabilities using (3.5). Although we ultimately consider only the case where $\phi_1 = \phi_2$ we derive the equations in a general manner. If the equations were to be used with $\phi_1 \neq \phi_2$ the normal modes would not just be simple symmetric and antisymmetric combinations of the internal coordinates and suitable adjustments would have to be made to (3.19).

In a completely analogous fashion to the preceding section the group polarizability derivatives required are $(\partial\alpha_{\alpha\beta}/\partial\Delta\phi_i)_0$,

$(\partial\alpha_{i\alpha\alpha}/\partial\Delta\phi_i)$, $i=1,2$. These are obtained by first letting $\phi_i \to \phi_i + \Delta\phi_i$ in the group polarizability expressions and then differentiating with respect to $\Delta\phi_i$. Assuming that α_i and k_i are constant during the angle bending, this results in

$$\left(\frac{\partial\alpha_{1\alpha\beta}}{\partial\Delta\phi_1}\right)_0 = 3\alpha_1 k_1 \left[I_\alpha I_\beta \sin 2\phi_1 \sin^2 \tfrac{1}{2}\tau \right.$$

$$+ \tfrac{1}{2}(I_\alpha J_\beta + J_\alpha I_\beta)\sin 2\phi_1 \sin\tau + (I_\alpha k_\beta + k_\alpha I_\beta) \times$$

$$\cos 2\phi_1 \sin\tfrac{1}{2}\tau + (J_\alpha k_\beta + k_\alpha J_\beta)\cos 2\phi_1 \cos\tfrac{1}{2}\tau$$

$$\left. + J_\alpha J_\beta \sin 2\phi_1 \cos^2\tfrac{1}{2}\tau - k_\alpha k_\beta \sin 2\phi_1 \right] \quad (3.22a)$$

$$\left(\frac{\partial\alpha_{2\alpha\beta}}{\partial\Delta\phi_2}\right)_0 = 3\alpha_2 k_2 \left[I_\alpha I_\beta \sin 2\phi_2 \sin^2 \tfrac{1}{2}\tau \right.$$

$$- \tfrac{1}{2}(I_\alpha J_\beta + J_\alpha I_\beta)\sin 2\phi_2 \sin\tau + (I_\alpha k_\beta + k_\alpha I_\beta) \times$$

$$\cos 2\phi_2 \sin\tfrac{1}{2}\tau - (J_\alpha k_\beta + k_\alpha J_\beta)\cos 2\phi_2 \cos\tfrac{1}{2}\tau$$

$$\left. + J_\alpha J_\beta \sin 2\phi_2 \cos^2\tfrac{1}{2}\tau - k_\alpha k_\beta \sin 2\phi_2 \right] \quad (3.22b)$$

$$\left(\frac{\partial\alpha_{1\alpha\alpha}}{\partial\Delta\phi_1}\right)_0 = \left(\frac{\partial\alpha_{2\alpha\alpha}}{\partial\Delta\phi_2}\right)_0 = 0 \quad (3.22c)$$

The relevant tensor products are then (see last section)

$$\langle 0|\alpha_{\alpha\beta}|1_\pm\rangle\langle 1_\pm|G'_{\alpha\beta}|0\rangle = \tfrac{1}{2}\omega\langle 0|\alpha_{\alpha\beta}|1_\pm\rangle\langle 1_\pm|\varepsilon_{\alpha\gamma\delta}A_{\gamma\delta\beta}|0\rangle$$

$$= \mp\tfrac{1}{2}\omega\,\varepsilon_{\beta\gamma\delta}R_{21\gamma}\langle 0|\alpha_{1\alpha\beta}|1_\pm\rangle\langle 1_\pm|\alpha_{2\delta\alpha}|0\rangle$$

$$= \mp|\langle 0|Q_\pm|1_\pm\rangle|^2 \tfrac{9}{4}\omega R_{21}\alpha_1 k_1 \alpha_2 k_2 \times$$

$$\left(-\tfrac{1}{2}\sin 2\phi_1 \sin 2\phi_2 \sin 2\tau + \cos 2\phi_1 \cos 2\phi_2 \sin\tau\right) \quad (3.23a)$$

$$\langle o|\alpha_{\alpha\alpha}|1_\pm\rangle\langle 1_\pm|G'_{\beta\beta}|o\rangle = 0 \qquad (3.23b)$$

$$\langle o|\alpha_{\alpha\beta}|1_\pm\rangle\langle 1_\pm|\alpha_{\alpha\beta}|o\rangle = \langle o|\alpha_{1\alpha\beta}|1_\pm\rangle\langle 1_\pm|\alpha_{1\alpha\beta}|o\rangle$$
$$+ \langle o|\alpha_{2\alpha\beta}|1_\pm\rangle\langle 1_\pm|\alpha_{2\alpha\beta}|o\rangle + 2\langle o|\alpha_{1\alpha\beta}|1_\pm\rangle\langle 1_\pm|\alpha_{2\alpha\beta}|o\rangle$$
$$= 9|\langle o|Q_\pm|1_\pm\rangle|^2\{\alpha_1^2\kappa_1^2 + \alpha_2^2\kappa_2^2 \pm$$
$$\alpha_1\kappa_1\alpha_2\kappa_2[\sin 2\phi_1 \sin 2\phi_2(1+\cos^2\tau)$$
$$- 2\cos 2\phi_1 \cos 2\phi_2 \cos\tau]\} \qquad (3.23c)$$

$$\langle o|\alpha_{\alpha\alpha}|1_\pm\rangle\langle 1_\pm|\alpha_{\beta\beta}|o\rangle = 0 \qquad (3.23d)$$

Finally, letting $\phi_1 = \phi_2 = \phi$, $\alpha_1 = \alpha_2$ and $\kappa_1 = \kappa_2$ we have for the polarized and depolarized Raman circular differences (from 3.23a-d and 2.3a&b)

$$\Delta_x^\pm = \frac{16\langle o|\alpha_{\alpha\beta}|1_\pm\rangle\langle 1_\pm|G'_{\alpha\beta}|o\rangle}{7c\langle o|\alpha_{\lambda\mu}|1_\pm\rangle\langle 1_\pm|\alpha_{\lambda\mu}|o\rangle} \qquad (3.24a)$$

$$\Delta_z^\pm = \frac{4\langle o|\alpha_{\alpha\beta}|1_\pm\rangle\langle 1_\pm|G'_{\alpha\beta}|o\rangle}{3c\langle o|\alpha_{\lambda\mu}|1_\pm\rangle\langle 1_\pm|\alpha_{\lambda\mu}|o\rangle} \qquad (3.24b)$$

giving

$$\Delta_x^\pm = \frac{\mp 8\pi R_{21}(-\frac{1}{2}\sin^2 2\phi \sin 2\tau + \cos^2 2\phi \sin\tau)}{7\lambda[2 \pm \sin^2 2\phi(1+\cos^2\tau) \mp 2\cos^2 2\phi\cos\tau]} \qquad (3.25a)$$

$$\Delta_z^\pm = \frac{\mp 2\pi R_{21}(-\frac{1}{2}\sin^2 2\phi \sin 2\tau + \cos^2 2\phi \sin\tau)}{3\lambda[2 \pm \sin^2 2\phi(1+\cos^2\tau) \mp 2\cos^2 2\phi\cos\tau]} \qquad (3.25b)$$

3.5 Discussion

We now forward some general points about the simple two-group model.

An important result to have come from the simple two-group equations is that the model produces circular intensity differences that are of the correct order of magnitude, that is, about 10^{-3} - 10^{-4}. This may be seen by inserting realistic values for the parameters in the circular intensity difference equations. For example, putting $R_{21} = 0.15$ nm, $\tau = \frac{\pi}{6}$ and $\lambda = 500$ nm into (3.17c) we get that $\Delta_2^+ = 2.51 \times 10^{-4}$.

The most appealing feature of the simple two-group model is that in certain cases, as illustrated above, no polarizability derivative data are required. Indeed, in the theory of section 3.3, applicable to bond-stretch vibrations, only Δ_α^+ requires such knowledge. A useful piece of information can also be gained by looking at the numerators of Δ_2^+ and Δ_2^- : their magnitudes are equal, so that, if this mechanism is operative, there should be a conservative couplet produced in the unnormalized $(I^R - I^L)$ circular intensity difference spectrum. For the angle bending case we see that in the polarized and depolarized equations no polarizability data are required and the expressions reduce to purely geometrical considerations. Note here that conservative couplets are predicted for the unnormalized $(I^R - I^L)$ polarized and depolarized Raman optical activity spectra.

There are, however, some difficulties to be overcome before one may use the simple two-group model with any confidence and which account for the paucity of useful applications of the

theory. Firstly one must identify a pair of internal coordinates which produce symmetric and antisymmetric combinations. Then one has to pick out the appropriate bands in the Raman spectrum. There is no simple rule with which to predict the frequency ordering of the two bands although Raman polarization measurements may help here. Finally, one must convince oneself that the chosen internal coordinates are the major contributors to the Raman optical activity of the normal modes. There is no reason to suppose that, in general, the internal coordinates that make the major contribution to a normal mode make the major contribution to its Raman optical activity. Having taken the above factors into consideration, and with a knowledge of the molecular conformation, one may then put the simple two-group model to use.

In conclusion, the main importance of the simple two-group model so far has been conceptual - it has enabled workers to obtain a feeling for the mechanism whereby Raman optical activity is generated. As we show in the next chapter, it has also provided the basis of a more complete, general theory for the circular intensity difference.

REFERENCES

1. L.D. Barron and A.D. Buckingham, J. Amer. Chem. Soc., 96, 4769 (1974).

2. A.D. Buckingham and H.C. Longuet-Higgins, Mol. Phys., 14, 63 (1968).

3. L.D. Barron, in Optical Activity and Chiral Discrimination, Chapter 9, ed. by S.F. Mason, Reidel, 1979.

4. E.B. Wilson, J.C. Decius and P.C. Cross, Molecular Vibrations, McGraw-Hill, New York, 1955.

5. A.J. Stone, Mol. Phys., 29, 1461 (1975) ; 33, 293 (1977).

6. L.D. Barron, in Advances in Infrared and Raman Spectroscopy, Chapter 4, Vol. 4, ed. by R.J.H. Clark and R.E. Hester, Heyden, London, 1978.

CHAPTER 4

A GENERAL TWO-GROUP MODEL OF RAYLEIGH AND RAMAN OPTICAL ACTIVITY

4.1 Introduction

We now turn to the task of finding the relevant equations to calculate the Rayleigh optical activity, and the Raman optical activity in all the normal modes, of a completely general chiral molecule. In doing so it was found that, for the Raman effect, slightly more was required than simply summing all the two-group interactions possible using the equations of Chapter 3. A new term is required which has been called the "inertial" contribution to Raman optical activity.[1] Its presence is necessary to ensure a complete and origin-independent description of the effect.

In this chapter we present first the general Rayleigh expressions. Then we give the theory of the bond polarizability model followed by a derivation of the general Raman optical activity expressions and an overall critique of the theory.

4.2 The Rayleigh Theory

The Rayleigh theory is quite straightforward. No complications appear and the final expressions are simply summations over all terms in the molecule given by (3.8):

$$\alpha_{\alpha\beta} G'_{\alpha\beta} = \tfrac{1}{3}\omega \alpha_{\alpha\beta} \varepsilon_{\alpha\delta\kappa} A_{\delta\kappa\beta}$$

$$= -\tfrac{9}{2}\omega \varepsilon_{\beta\gamma\delta} \sum_{\substack{i,j \\ i<j}} R_{ij}\alpha_i\kappa_i \alpha_j\kappa_j U_{i\alpha} U_{i\beta} U_{j\delta} U_{j\alpha} \qquad (4.1a)$$

$$\alpha_{\alpha\beta}\alpha_{\alpha\beta} = \sum_{i,j} \left[3\alpha_i\alpha_j + 3\alpha_i\kappa_i\alpha_j\kappa_j (3U_{i\alpha}U_{i\beta}U_{j\alpha}U_{j\beta} - 1) \right] \qquad (4.1b)$$

$$\alpha_{\alpha\alpha}\alpha_{\beta\beta} = 9\left(\sum_i \alpha_i\right)^2 \qquad (4.1c)$$

The Rayleigh circular intensity differentials are easily obtained by substituting (4.1a-c) into (2.3).

4.3 The Raman Theory

4.3.1 The Inertial Term

In the simple two-group model the formulae for the transition moment product $\langle 0|\alpha_{\alpha\beta}|1_\pm\rangle\langle 1_\pm|G'_{\alpha\beta}|0\rangle$ was taken to be $\mp\frac{1}{2}\omega\varepsilon_{\beta\gamma\delta}R_{21\gamma}\langle 0|\alpha_{1\alpha\beta}|1_\pm\rangle\langle 1_\pm|\alpha_{2\delta\alpha}|0\rangle$ where the intrinsic $\underset{\sim}{G'}$ terms have been omitted, (3.11a). This implies that the vector $\underset{\sim}{R}_{21}$ does not change with the vibration. However, for the vibration of a real molecule this will not, in general, be the case and the variations of the inter-group vectors will have to be accounted for. In effect, this means that the quantity $\underset{\sim}{R}_{21}$ must be brought inside the transition moment integral thus

$$\mp\tfrac{1}{4}\omega\,\varepsilon_{\beta\gamma\delta}R_{21\gamma}\langle 0|\alpha_{1\alpha\beta}|1_\pm\rangle\langle 1_\pm|\alpha_{2\delta\alpha}|0\rangle$$
$$\longrightarrow \mp\tfrac{1}{4}\omega\,\varepsilon_{\beta\gamma\delta}\langle 0|\alpha_{1\alpha\beta}|1_\pm\rangle\langle 1_\pm|R_{21\gamma}\alpha_{2\delta\alpha}|0\rangle \qquad (4.2)$$

The quantity $R_{21\gamma}\alpha_{2\delta\alpha}$ is eventually expressed in a power series in the normal coordinate resulting in a new term dependent on $(\partial R_{21\gamma}/\partial Q)_0(\alpha_{2\alpha\beta})_0$. The quantity resulting from this term has been called the inertial contribution to Raman optical activity.[1]

4.3.2 Initial Formulation of the General Theory

Omitting intrinsic optical activity tensors, the Raman optical activity of the fundamental ($1_\rho \leftarrow 0$) transition of normal mode Q_ρ depends on

$$\begin{aligned}
&\langle 0|\alpha_{\alpha\beta}|1_\rho\rangle\langle 1_\rho|G'_{\nu\beta}|0\rangle \\
&= \tfrac{1}{3}\omega\langle 0|\alpha_{\nu\beta}|1_\rho\rangle\langle 1_\rho|\varepsilon_{\alpha\gamma\delta}A_{\gamma\delta\beta}|0\rangle \\
&= -\tfrac{1}{2}\omega\langle 0|\sum_i \alpha_{i\alpha\beta}|1_\rho\rangle\langle 1_\rho|\sum_j \varepsilon_{\beta\gamma\delta}R_{j\gamma}\alpha_{j\delta\alpha}|0\rangle
\end{aligned} \tag{4.3}$$

where the summations are over the bonds in the molecule. $\underset{\sim}{R}_j$ is the vector from an arbitrary molecular origin to the local origin of bond j. We now express the quantities in the transition integrals as a power series in Q_ρ (as in 3.12). Technically, this series should be over all the normal modes of the molecule, but if Q_ρ is the only normal mode that is being excited, then it is only the terms involving Q_ρ that can produce non-zero results. We then have

$$\alpha_{i\alpha\beta} = (\alpha_{i\alpha\beta})_0 + \left(\frac{\partial\alpha_{i\alpha\beta}}{\partial Q_\rho}\right)_0 Q_\rho + \tfrac{1}{2}\left(\frac{\partial^2\alpha_{i\alpha\beta}}{\partial Q_\rho^2}\right)_0 Q_\rho^2 + \cdots \tag{4.4a}$$

$$R_{j\gamma}\alpha_{j\delta\alpha} = (R_{j\gamma}\alpha_{j\delta\alpha})_0 + (R_{j\gamma})_0\left(\frac{\partial\alpha_{j\delta\alpha}}{\partial Q_\rho}\right)_0 Q_\rho + \left(\frac{\partial R_{j\gamma}}{\partial Q_\rho}\right)_0 (\alpha_{j\delta\alpha})_0 Q_\rho + \cdots \tag{4.4b}$$

Only terms linear in Q_ρ can effect a fundamental transition. Thus, rearranging and using the following matrix elements [2]

$$\langle 0|Q_\rho|1_\rho\rangle = \langle 1_\rho|Q_\rho|0\rangle = \left(\frac{\hbar}{2\omega_\rho}\right)^{\frac{1}{2}} \tag{4.5}$$

we can write (4.3) as

$$\langle 0|\alpha_{\alpha\beta}|1_\rho\rangle\langle 1_\rho|G'_{\alpha\beta}|0\rangle$$
$$= -\frac{\hbar\omega}{4\omega_\rho}\varepsilon_{\beta\gamma\delta}\left[\sum_{i<j}(R_{ji\gamma})_0\left(\frac{\partial\alpha_{i\alpha\beta}}{\partial Q_\rho}\right)_0\left(\frac{\partial\alpha_{j\delta\alpha}}{\partial Q_\rho}\right)_0\right.$$
$$\left. + \sum_i\left(\frac{\partial\alpha_{i\alpha\beta}}{\partial Q_\rho}\right)_0\sum_j(\alpha_{j\delta\alpha})_0\left(\frac{\partial R_{j\gamma}}{\partial Q_\rho}\right)_0\right] \tag{4.6}$$

If required, this equation may be taken one step further by using the relation between the normal coordinates and the internal coordinates[2], S_q, which comprise it:

$$S_q = \sum_\rho^{3N-6} L_{q\rho}Q_\rho \tag{4.7}$$

where 3N - 6 is the number of normal modes of the chiral molecule containing N atoms. The coefficients $L_{q\rho}$ of the matrix $\underline{L}$ are obtained from a normal coordinate analysis of the molecule (see Appendix).

Equation (4.6) now becomes

$$\langle 0|\alpha_{\alpha\beta}|1_\rho\rangle\langle 1_\rho|G'_{\alpha\beta}|0\rangle$$
$$= -\frac{\hbar\omega}{4\omega_\rho}\varepsilon_{\beta\gamma\delta}\left\{\sum_{i<j}(R_{ji\gamma})_0\left[\sum_q\left(\frac{\partial\alpha_{i\alpha\beta}}{\partial S_q}\right)_0 L_{q\rho}\right]\times\right.$$
$$\left[\sum_r\left(\frac{\partial\alpha_{j\delta\alpha}}{\partial S_r}\right)_0 L_{r\rho}\right] + \left[\sum_i\sum_q\left(\frac{\partial\alpha_{i\alpha\beta}}{\partial S_q}\right)_0 L_{q\rho}\right]\times$$
$$\left.\left[\sum_j(\alpha_{j\delta\alpha})_0\sum_r\left(\frac{\partial R_{jr}}{\partial S_r}\right)_0 L_{r\rho}\right]\right\} \tag{4.8}$$

In a similar fashion, the polarizability products required are

$$\langle o|\alpha_{\nu\beta}|1_p\rangle\langle 1_p|\alpha_{\alpha\beta}|o\rangle$$
$$= \frac{\hbar}{2\omega_p}\sum_i\left(\frac{\partial\alpha_{i\nu\beta}}{\partial Q_p}\right)_o\sum_j\left(\frac{\partial\alpha_{j\alpha\beta}}{\partial Q_p}\right)_o$$
$$= \frac{\hbar}{2\omega_p}\left[\sum_i\sum_q\left(\frac{\partial\alpha_{i\nu\beta}}{\partial S_q}\right)_o L_{qp}\right]\left[\sum_j\sum_r\left(\frac{\partial\alpha_{j\nu\beta}}{\partial S_r}\right)_o L_{rp}\right] \qquad (4.9a)$$

$$\langle o|\alpha_{\alpha\alpha}|1_p\rangle\langle 1_p|\alpha_{\beta\beta}|o\rangle$$
$$= \frac{\hbar}{2\omega_p}\sum_i\left(\frac{\partial\alpha_{i\nu\nu}}{\partial Q_p}\right)_o\sum_j\left(\frac{\partial\alpha_{j\beta\beta}}{\partial Q_p}\right)_o$$
$$= \frac{\hbar}{2\omega_p}\left[\sum_i\sum_q\left(\frac{\partial\alpha_{i\nu\nu}}{\partial S_q}\right)_o L_{qp}\right]\left[\sum_j\sum_r\left(\frac{\partial\alpha_{j\beta\beta}}{\partial S_r}\right)_o L_{rp}\right] \qquad (4.9b)$$

4.3.3 The Bond Polarizability Theory Proper

In this section we derive the final form of the various vector and polarizability derivatives which were given in the last section. This part of the work is all conventional[3], but it will be given again in a notation which suits our calculation.

The polarizability of a pseudocylindrical bond, i , is given by (3.7)

$$\alpha_{i\alpha\beta} = \alpha_{i\perp}\delta_{\nu\beta} + \Delta_i U_{i\alpha} U_{i\beta} \qquad (4.10)$$

where we have replaced $\alpha_{i\parallel} - \alpha_{i\perp}$ by Δ_i . The derivative with respect to the normal coordinate Q_p is

$$\left(\frac{\partial\alpha_{i\alpha\beta}}{\partial Q_p}\right)_o = \left(\frac{\partial\alpha_{i\perp}}{\partial Q_p}\right)_o\delta_{\alpha\beta} + \left(\frac{\partial\Delta_i}{\partial Q_p}\right)_o(U_{i\nu}U_{i\beta})_o$$
$$+ \Delta_i\left[\frac{\partial(U_{i\nu}U_{i\beta})}{\partial Q_p}\right]_o$$

$$= \sum_q \left\{ \left(\frac{\partial \alpha_{i\perp}}{\partial S_q} \right)_0 \delta_{\alpha\beta} + \left(\frac{\partial \Delta_i}{\partial S_q} \right)_0 (U_{i\alpha} U_{i\beta})_0 \right.$$

$$\left. + \Delta_i \left[\frac{\partial (U_{i\alpha} U_{i\beta})}{\partial S_q} \right]_0 \right\} L_{qp} \qquad (4.11)$$

From now on, for conciseness, we drop all zero subscripts. This results in no ambiguities.

In the most simple form of the bond-polarizability theory we assume that the only internal coordinate which changes the internal electronic structure of the bond (hence $\alpha_\perp$ and Δ) is the stretch coordinate associated with that bond. We can now write

$$\left(\frac{\partial \alpha_{i\alpha\beta}}{\partial Q_p} \right)_0 = \left(\alpha_{i\perp}' \delta_{\alpha\beta} + \Delta_i' U_{i\alpha} U_{i\beta} \right) L_{ip}$$

$$+ \Delta_i \sum_q \left[\frac{\partial (U_{i\alpha} U_{i\beta})}{\partial S_q} \right] L_{qp} \qquad (4.12)$$

where $\alpha_{i\perp}'$ and Δ_i' denote the derivatives of the quantities $\alpha_{i\perp}$ and Δ_i with respect to the stretch coordinate of the bond. The stretch coordinate of bond i has the associated L-matrix element L_{ip} for the normal coordinate Q_p . The summation $\sum_q$ is over all internal coordinates. We are now left with the problem of handling the derivatives of the unit vectors. This is done in the following fashion. We can say that

$$\left(\frac{\partial U_{i\alpha}}{\partial S_q} \right) = \left(\frac{\partial U_{i\alpha}}{\partial r_{a\beta}} \right) \left(\frac{\partial r_{a\beta}}{\partial S_q} \right) + \left(\frac{\partial U_{i\alpha}}{\partial r_{b\beta}} \right) \left(\frac{\partial r_{b\beta}}{\partial S_q} \right) \qquad (4.13)$$

where the bond has been defined by the two atoms a and b such that $\underset{\sim}{u}_i = \underset{\sim}{r}_a^\circ - \underset{\sim}{r}_b^\circ \,/\, |\underset{\sim}{r}_a^\circ - \underset{\sim}{r}_b^\circ|$, $\underset{\sim}{r}_a^\circ$ and $\underset{\sim}{r}_b^\circ$ being the equilibrium position vectors of the two atoms. The vectors $\underset{\sim}{r}_a$ and $\underset{\sim}{r}_b$ in (4.13) are the cartesian displacement coordinates of the atoms. It can be shown that for any atom, m , of a molecule, its cartesian displacement coordinate $r_{m\beta}$ may be given by[3]

$$r_{m\beta} = \varepsilon_m \sum_{t,k} S^t_{m\beta} \left(G^{-1}\right)_{tk} S_k \qquad (4.14)$$

where ε_m is the inverse mass of atom m, $S^t_{m\beta}$ represents Wilson's $\underset{\sim}{s}$-vector associated with atom m and internal coordinate S_k and $(G^{-1})_{tk}$ is an element of the inverse of the $\underset{\sim}{G}$-matrix[2] (also see Appendix). The summation $\sum_{t,k}$ is over all the internal coordinates. Using (4.14) we can say that

$$\left(\frac{\partial r_{a\beta}}{\partial S_q}\right) = \varepsilon_a \sum_t S^t_{a\beta} \left(G^{-1}\right)_{tq} \qquad (4.15a)$$

$$\left(\frac{\partial r_{b\beta}}{\partial S_q}\right) = \varepsilon_b \sum_t S^t_{b\beta} \left(G^{-1}\right)_{tq} \qquad (4.15b)$$

If the atomic displacements are very small it is straightforward to show that[4]

$$\left(\frac{\partial u_{i\alpha}}{\partial r_{a\beta}}\right) = -\left(\frac{\partial u_{i\alpha}}{\partial r_{b\beta}}\right) = \sigma_i \left(\delta_{\alpha\beta} - u_{i\alpha} u_{i\beta}\right) \qquad (4.16)$$

where σ_i is the reciprocal of the equilibrium bond length of bond i. Putting (4.15) and (4.16) into (4.13) we get

$$\left(\frac{\partial u_{i\alpha}}{\partial S_q}\right) = \sigma_i \left(\delta_{\alpha\beta} - u_{i\alpha} u_{i\beta}\right) \sum_t \left(\varepsilon_a S^t_{a\beta} - \varepsilon_b S^t_{b\beta}\right)\left(G^{-1}\right)_{tq} \qquad (4.17)$$

From the last term of (4.12) we need

$$\Delta_i \sum_q \left[\frac{\partial (U_{i\alpha} U_{i\beta})}{\partial S_q} \right] L_{qp}$$

$$= \Delta_i \sum_q \left[\left(\frac{\partial U_{i\alpha}}{\partial S_q} \right) U_{i\beta} + U_{i\alpha} \left(\frac{\partial U_{i\beta}}{\partial S_q} \right) \right] L_{qp} \qquad (4.18)$$

Inserting (4.17), (4.18) becomes

$$\Delta_i \sum_q \left[\frac{\partial (U_{i\alpha} U_{i\beta})}{\partial S_q} \right] L_{qp}$$

$$= \sigma_i \Delta_i \left(U_{i\beta} \delta_{\alpha\delta} + U_{i\alpha} \delta_{\beta\delta} - 2 U_{i\alpha} U_{i\beta} U_{i\delta} \right) \times$$

$$\sum_t \left(\varepsilon_a S^+_{a\delta} - \varepsilon_b S^+_{b\delta} \right) \sum_q \left(G^{-1} \right)_{tq} L_{qp}$$

$$= \sigma_i \Delta_i \left(U_{i\beta} \delta_{\alpha\delta} + U_{i\alpha} \delta_{\beta\delta} - 2 U_{i\alpha} U_{i\beta} U_{i\delta} \right) \cdot$$

$$\sum_t \left(\varepsilon_a S^+_{a\delta} - \varepsilon_b S^+_{b\delta} \right) \left(L^{-1} \right)_{tp} \qquad (4.19)$$

---

where we have used the relation[2]

$$\left(L^{-1} \right)_{tp} = \sum_q \left(G^{-1} \right)_{tq} L_{qp} \qquad (4.20)$$

where $(L^{-1})_{tp}$ is the element of the inverse of the vibrational $\underset{\sim}{L}$-matrix associated with internal coordinate t and normal coordinate Q_p.

Future equations are more concisely written if we introduce the following notation. Let

$$\underset{\sim}{d}_i^+ = \varepsilon_a \underset{\sim}{S}_a^+ - \varepsilon_b \underset{\sim}{S}_b^+ \qquad (4.21a)$$

$$A_i^+ = \underset{\sim}{U}_i \cdot \underset{\sim}{d}_i^+ \qquad (4.21b)$$

Introducing (4.21) and putting (4.19) into (4.12) we have finally that

$$\left(\frac{\partial \alpha_{\alpha\beta}}{\partial Q_\rho}\right) = \left(\alpha_i' \delta_{\alpha\beta} + \Delta_i' U_{i\alpha} U_{i\beta}\right) L_{i\rho} + \sigma_i \Delta_i \sum_t \left(U_{i\beta} d^t_{i\alpha} + U_{i\alpha} d^t_{i\beta} - 2 U_{i\alpha} U_{i\beta} A^t_i\right)(L^{-1})_{t\rho} \tag{4.22}$$

Before giving the final form of the Raman optical activity equations we need an expression for $\sum_r \left(\frac{\partial R_{j\gamma}}{\partial S_r}\right) L_{r\rho}$ which occurs in the second product of Equation (4.8). The situation is made more easy if we chose one of the atoms in the bond as the local origin (although we are completely unrestricted in our choice of the position as long as it is on the bond axis). If we choose each bond's atom b (introduced in (4.13)), then we may write, using (4.14) and (4.20)

$$\sum_r \left(\frac{\partial R_{j\gamma}}{\partial S_r}\right) L_{r\rho} = \sum_r \varepsilon_b s^r_{b\gamma} (L^{-1})_{r\rho} \tag{4.23}$$

In the next section, analogous to (4.21), we will use

$$\underset{\sim}{d}^r_b = \varepsilon_b \underset{\sim}{s}^r_b \tag{4.24}$$

as a simplification.

We may now proceed to give the final form of the Rayleigh and Raman optical activity expressions.

4.3.4 The Final Form of the General Bond Polarizability Theory of Raman Optical Activity

Using the results of the preceding section in Equation (4.8) we get that

$$\langle o|\alpha_{\nu\beta}|1_p\rangle\langle 1_p|G'_{\alpha\beta}|o\rangle = \tfrac{1}{3}\omega\langle o|\alpha_{\nu\beta}|1_p\rangle\langle 1_p|\varepsilon_{\alpha\gamma\delta}A_{\gamma\delta\beta}|o\rangle$$

$$-\frac{\hbar\omega}{4\omega_p}\varepsilon_{\beta\gamma\delta}\Bigg\{\sum_{\substack{i,j\\ i<j}} R_{ji\gamma}\Big[\sum_q\Big(\frac{\partial\alpha_{i\alpha\beta}}{\partial s_q}\Big)L_{qp}\Big]\Big[\sum_r\Big(\frac{\partial\alpha_{j\delta\alpha}}{\partial s_r}\Big)L_{rp}\Big]$$

$$+\Big[\sum_i\sum_q\Big(\frac{\partial\alpha_{i\nu\beta}}{\partial s_q}\Big)L_{qp}\Big]\Big[\sum_j\alpha_{j\delta\alpha}\sum_r\Big(\frac{\partial R_{j\gamma}}{\partial s_r}\Big)L_{rp}\Big]\Bigg\}$$

$$=-\frac{\hbar\omega}{4\omega_p}\varepsilon_{\beta\gamma\delta}\Bigg\{\sum_{\substack{i,j\\ i<j}} R_{ji\gamma}\sum_{q,r}\Big[(\alpha'_{i\perp}\delta_{\nu\beta}+v_{i\alpha}v_{i\beta}\Delta'_i)L_{ip}$$

$$+\sigma_i\Delta_i(v_{i\beta}d^q_{i\alpha}+v_{i\alpha}d^q_{i\beta}-2v_{i\alpha}v_{i\beta}A^q_i)(L^{-1})_{qp}\Big]\times$$

$$\Big[(\alpha'_{j\perp}\delta_{\delta\alpha}+v_{j\delta}v_{j\alpha}\Delta'_j)L_{jp}+\sigma_j\Delta_j(v_{j\alpha}d^r_{j\delta}$$

$$+v_{j\delta}d^r_{j\nu}-2v_{j\delta}v_{j\alpha}A^r_j)(L^{-1})_{rp}\Big]+$$

$$\sum_{i,j}\sum_{q,r}\Big[(\alpha'_{i\perp}\delta_{\alpha\beta}+v_{i\alpha}v_{i\beta}\Delta'_i)L_{ip}+$$

$$\sigma_i\Delta_i(v_{i\beta}d^q_{i\alpha}+v_{i\alpha}d^q_{i\beta}-2v_{i\alpha}v_{i\beta}A^q_i)(L^{-1})_{qp}\Big]\times$$

$$\Delta_j v_{j\delta}v_{j\alpha}d^r_{b\gamma}(L^{-1})_{rp}\Bigg\} \qquad (4.25)$$

All the products involving the Kronecker delta are zero so the above simplifies to

$$\langle o|\alpha_{\nu\beta}|1_p\rangle\langle i_p|G'_{\alpha\beta}|o\rangle =$$

$$-\frac{\hbar\omega}{4\omega_p}\varepsilon_{\beta\gamma\delta}\Bigg\{\sum_{\substack{i,j\\ i<j}} R_{ji\gamma}\sum_{q,r}\Big[v_{i\alpha}v_{i\beta}\Delta'_i L_{ip}+$$

$$\sigma_i\Delta_i(v_{i\beta}d^q_{i\alpha}+v_{i\alpha}d^q_{i\beta}-2v_{i\alpha}v_{i\beta}A^q_i)(L^{-1})_{qp}\Big]\times$$

$$\Big[v_{j\delta}v_{j\alpha}\Delta'_j L_{jp}+\sigma_j\Delta_j(v_{j\alpha}d^r_{j\delta}+v_{j\delta}d^r_{j\alpha}-$$

$$2v_{j\delta}v_{j\alpha}A^r_j)(L^{-1})_{rp}\Big]+\sum_{i,j}\sum_{q,r}\Big[v_{i\alpha}v_{i\beta}\Delta'_i L_{ip}+$$

$$+ \sigma_i \Delta_i \left(U_{i\beta} d^q_{i\alpha} + U_{i\alpha} d^q_{i\beta} - 2 U_{i\alpha} U_{i\beta} A^q_i \right) (L^{-1})_{+\rho} \Big] \times$$

$$\Delta_j U_{j\delta} U_{j\alpha} d^r_{b\gamma} (L^{-1})_{r\rho} \Big] \Big\} \qquad (4.26)$$

The required polarizability-polarizability products (4.9a&b) become

$$\langle o | \alpha_{\alpha\beta} | 1_\rho \rangle \langle 1_\rho | \alpha_{\alpha\beta} | o \rangle =$$

$$\frac{\hbar}{2\omega_\rho} \Big[\sum_i \sum_q \left(\frac{\partial \alpha_{i\alpha\beta}}{\partial S_q} \right) L_{q\rho} \Big] \Big[\sum_j \sum_r \left(\frac{\partial \alpha_{j\alpha\beta}}{\partial S_r} \right) L_{r\rho} \Big]$$

$$= \frac{\hbar}{2\omega_\rho} \Big\{ \sum_{i,j} \sum_{q,r} \Big[(\alpha'_{i\perp} \delta_{\alpha\beta} + U_{i\alpha} U_{i\beta} \Delta'_i) L_{i\rho} +$$

$$\sigma_i \Delta_i (U_{i\beta} d^q_{i\alpha} + U_{i\alpha} d^q_{i\beta} - 2 U_{i\alpha} U_{i\beta} A^q_i) \Big] \times$$

$$\Big[(\alpha'_{j\perp} \delta_{\alpha\beta} + U_{j\alpha} U_{j\beta} \Delta'_j) L_{j\rho} +$$

$$\sigma_j \Delta_j (U_{j\beta} d^r_{j\alpha} + U_{j\alpha} d^r_{j\beta} - 2 U_{j\alpha} U_{j\beta} A^r_j) (L^{-1})_{r\rho} \qquad (4.27a)$$

$$\langle o | \alpha_{\alpha\alpha} | 1_\rho \rangle \langle 1_\rho | \alpha_{\beta\beta} | o \rangle =$$

$$\frac{\hbar}{2\omega_\rho} \Big[\sum_i \sum_q \left(\frac{\partial \alpha_{i\alpha\alpha}}{\partial S_q} \right) L_{q\rho} \Big] \Big[\sum_j \sum_r \left(\frac{\partial \alpha_{j\beta\beta}}{\partial S_q} \right) L_{r\rho} \Big]$$

$$= \frac{\hbar}{2\omega_\rho} \Big[\sum_{i,j} (\alpha'_{i\perp} \delta_{\alpha\alpha} + U_{i\alpha} U_{i\alpha} \Delta'_i) L_{i\rho} \times$$

$$(\alpha'_{j\perp} \delta_{\beta\beta} + \Delta'_j U_{j\beta} U_{j\beta}) L_{j\rho} \Big]$$

$$= \frac{\hbar}{2\omega_\rho} \Big[\sum_i (3\alpha'_{i\perp} + \Delta'_i) \Big]^2 \qquad (4.27b)$$

4.4 Discussion

The information necessary to initiate a general two-group calculation falls into two categories. First there is the information from the normal coordinate analysis: the $\underset{\sim}{s}$-vectors which are required to set up the vibrational $\underset{\sim}{G}$ matrix, and the $\underset{\sim}{L}$ and $\underset{\sim}{L}^{-1}$ matrices, all of which may be obtained routinely from normal coordinate analysis programs. If a redundant set of internal coordinates is used (i.e. a number greater than $3N - 6$) the $\underset{\sim}{L}$ matrix will not be square and hence a normal inverse cannot be defined. Nonetheless, it can be shown that a unique $\underset{\sim}{L}$ matrix satisfying (4.20) can be defined and produced without difficulty by a normal coordinate analysis computer package.[5]

The second type of information is the bond polarizability data. For the Raman calculation, in the general case, we need three parameters per bond i, namely $\alpha'_{i\perp}$, Δ_r, Δ'_i. In total, this requires $3(N - 1)$ parameters where N is the number of atoms in the molecule (plus an extra 3 for each ring system).

These parameters are obtained from bond polarizability studies on absolute Raman intensities.[3,6] Since we are using exciting radiation of visible frequency we expect that it will be possible to take information from static polarizability studies for the quantities $\Delta_i \left(= \alpha_{i\parallel} - \alpha_{i\perp} \right)$.[7]

One problem in using bond-polarizability derivatives obtained from Raman studies is that since ordinary Raman intensity depends on polarizability-polarizability products involving the same tensor indices there can be a sign ambiguity associated with the bond-polarizability derivatives. Should the bond polarizability theory

of Raman optical activity prove to be an adequate description of the effect (in certain types of molecules, at least), then an examination of the Raman circular intensity differences could help resolve this sign problem. This is because the two-group model uses polarizability-polarizability products involving different tensor indices. One can envisage a bond-polarizability study for which one chooses a series of similar molecules one or more of which is chiral and shows a measurable circular intensity difference spectrum. The bond-polarizabilities produced would not only have to reproduce the ordinary Raman intensities but also give the correct signs of the circular intensity differences. Two possible series where this type of study could be carried out are illustrated in Figure 4.1.

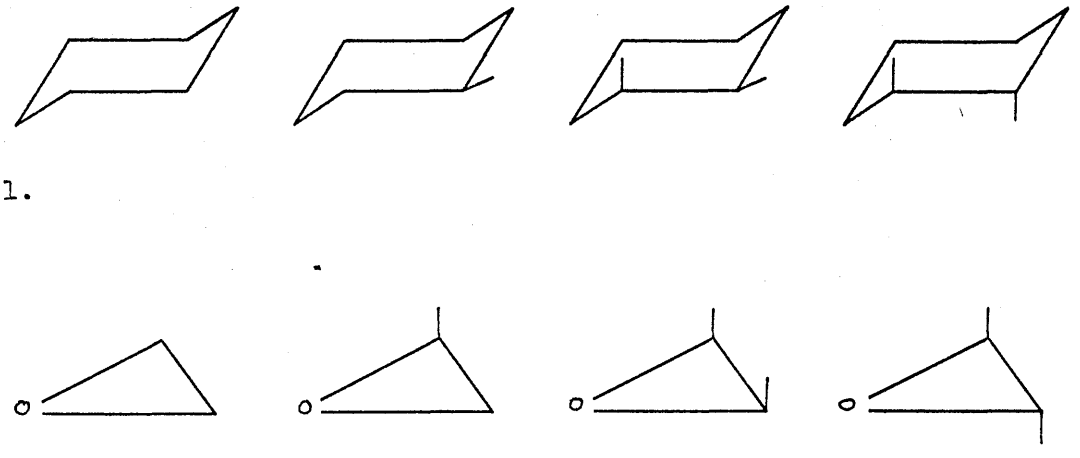

Figure 4.1. Two Series of Related Compounds Suitable for the Bond Polarizability Study Mentioned in Text:
1. Cyclohexane and Various Methylated Derivatives;
2. Ethylene Oxide and Various Methylated Derivatives.

A recent publication [1] used the inertial term to derive expressions for the torsional oscillation of a methyl group. The model molecule this dealt with resulted in all the optical activity coming from the inertial term. However, for almost all molecules this circumstance will not obtain and both the two-group and inertial terms must be considered. It may be simply shown that both the two-group and inertial terms are required to preserve origin invariance of the theory. If we take, for example, a "molecule" consisting of only two bonds, 1 and 2, and assign the molecular origin to be at the local origin of bond 1, we may use Equation (4.8) to produce an expression for $\langle o|\alpha_{\alpha\beta}|1_p\rangle\langle 1_p|G'_{\alpha\beta}|o\rangle$. If we move the local origin on group 2 along the bond axis by a vector $\underset{\sim}{a}$ ($= a\underset{\sim}{u}_2$) then the change in the Raman optical activity expression, from (4.8), is

$$-\frac{\hbar\omega}{4\omega_p}\varepsilon_{\beta\gamma\delta}\left[a_\gamma\left(\frac{\partial\alpha_{1\alpha\beta}}{\partial Q_p}\right)\left(\frac{\partial\alpha_{2\delta\alpha}}{\partial Q_p}\right) + \left(\frac{\partial\alpha_{1\alpha\beta}}{\partial Q_p}\right)\left(\frac{\partial a_\gamma}{\partial Q_p}\right)\alpha_{2\delta\alpha}\right] \qquad (4.28)$$

If we now substitute into the above

$$\alpha_{i\alpha\beta} = \alpha_i(1-\kappa_i)\delta_{\alpha\beta} + 3\alpha_i\kappa_i U_{i\alpha}U_{i\beta} \qquad (3.5)$$

we get the change equal to

$$-a\frac{\hbar\omega}{4\omega_p}\varepsilon_{\beta\gamma\delta}\left\{\left[3\alpha_i\kappa_i\left(\frac{\partial U_{i\alpha}}{\partial Q_p}U_{i\beta}\right) + 3\left(\frac{\partial\alpha_i\kappa_i}{\partial Q_p}\right)U_{i\alpha}U_{i\beta}\right]\times\right.$$

$$\left.\left[3\alpha_j\kappa_j\left(\frac{\partial U_{j\delta}}{\partial Q_p}\right)U_{j\alpha}\right] \quad +\right.$$

$$+ \left[3\alpha_i K_i \left(\frac{\partial U_{i\alpha}}{\partial Q_\rho} U_{i\beta} \right) + 3 \left(\frac{\partial \alpha_i K_i}{\partial Q_\rho} \right) U_{i\alpha} U_{i\beta} \right] \times$$

$$\left[U_{j\delta} U_{j\alpha} \left(\frac{\partial U_{j\gamma}}{\partial Q_\rho} \right) \right]$$

$$= 0 \qquad (4.29)$$

where we have used the general relation, for arbitrary vectors $\underset{\sim}{A}$, $\underset{\sim}{B}$ and $\underset{\sim}{C}$,

$$\varepsilon_{\beta\gamma\delta} A_\beta B_\gamma C_\delta = - \varepsilon_{\beta\gamma\delta} C_\beta B_\gamma A_\delta \qquad (4.30)$$

(this is just the vector triple product rule, $\underset{\sim}{A} . [\underset{\sim}{B} \wedge \underset{\sim}{C}] = - \underset{\sim}{C} . [\underset{\sim}{B} \wedge \underset{\sim}{A}]$ in tensor notation). In (4.29) we see that the latter product, arising from the change in the inertial term, cancels out the former which arises from the change in the two-group term.

In the simple two-group bending calculation in Section (3.4) we avoided using the inertial term by choosing as the local origins the point where the bonds pivot during the vibration so that the $(\partial \underset{\sim}{R}_i / \partial Q)$ are zero. This means that the results of that section only strictly apply when the two atoms chosen as origins are much heavier than the atoms that effectively perform the vibrational motion. It is ideally suited for C-H or O-H deformations but not for, say, a Br-C-C-Br two-group skeleton.

We are of the opinion that most schemes that could be considered to upgrade the theory in this chapter would prove to be unprofitable. One could, for example, go to the next more complicated formulation of the bond-polarizability theory[3] (the "first order" theory as opposed to the "zero order" theory used here). This would involve, in part, letting a bond's electronic structure change as it under-

goes a bending motion. This procedure would bring the number of bond parameters to an unacceptable level. We mention here that although the zero order bond-polarizability theory of ordinary Raman intensity[3,6] is known to have its shortcomings, (it has met with only limited success), this need not prevent us from having high expectations for its usefulness in Raman optical activity. The signs of the larger effects in a molecule's Raman optical activity spectrum would be considered a major success.

Any lowering of the symmetry of the bonds would also bring in more polarizability parameters together with the problem of handling origin-dependent intrinsic $\underset{\sim}{G'}$ and $\underset{\sim}{A}$ tensors whose components, in general, are now non-zero and/or non-antisymmetric.

We have been assuming throughout that there is no static or dynamic coupling[8] between the bonds. It would be a relatively straightforward matter to introduce these effects into our model using the theory given in Reference 8, for example. We are of the opinion, however, that the discrepancies arising from the neglect of static and dynamic coupling are of the same or a lesser magnitude as those arising from the basic failings of the bond-polarizability scheme we have used.

There will, of course, be situations where coupling is important (and hence the bond-polarizability approach of lesser use). These will be where a molecule consists wholly or partly of large groups with polarizable π-electrons; benzene rings, for example. Such a molecule for which this type of analysis might be necessary, α-phenylethylisocyanate, is shown in Figure 4.2.

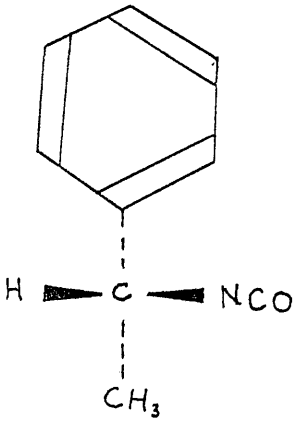

Figure 4.2. (S)-α-Phenylethylisocyanate: Chiral Molecule in which Static and Dynamic Coupling are Expected to be Significant.

The circular intensity difference spectrum of this molecule has been published.[9] It is very likely that there are dominant static and dynamic interactions between the isocyanate group and the benzene ring. This is evidenced by the large Raman optical activity effects in normal modes that are localized on the benzene ring. In general, however, it may be said that coupling models should be of less importance in vibrational optical activity than they have been for electronic optical activity. The situation for the former is more akin to the inherently chiral chromophore model of electronic optical activity since we usually have a chiral vibrational mode embracing extended parts of the molecule.

REFERENCES

1. L.D. Barron and A.D. Buckingham, J. Amer. Chem. Soc., 101, 1979 (1979).

2. E.B. Wilson, J.C. Decius and P.C. Cross, Molecular Vibrations, McGraw-Hill, New York, 1955.

3. L.M. Sverdlov, M.A. Kovner and E.P. Krainov, Vibrational Spectra of Polyatomic Molecules, Wiley (Israel Program for Scientific Translations), 1974.

4. S.M. Ferigle and A. Weber, Canad. J. Phys., 32, 799 (1954).

5. J.H. Schachtschneider, Technical Report, No. 57-65, Shell Development Co., Emeryville, California, 1966.

6. M. Gussoni, S. Abbate and G. Zerbi, J. Raman Spectrosc., 6, 289 (1977).

7. R.J.W. LeFevre, Adv. Phys. Org. Chem., 3, 1 (1965).

8. A.D. Buckingham and P.J. Stiles, Accts. Chem. Res., 7, 258 (1974).

9. L.D. Barron and B.P. Clark, J. Chem. Res. (S), 36 (1979).

CHAPTER 5

THE ATOM-DIPOLE INTERACTION MODEL OF RAYLEIGH AND RAMAN OPTICAL ACTIVITY

5.1 Introduction

The atom-dipole interaction model is the other major method for calculating Rayleigh and Raman optical activity.[1-4] The complete theory is presented in Reference 3, correcting an earlier error in References 1 and 2. The approach is fundamentally different from the two-group model and the two should provide some interesting comparisons. Indeed, the two molecules subjected to a general two-group calculation in this work (Chapters 6 and 7) have already been treated using the atom-dipole theory.[3,5] This chapter provides a brief description of the atom-dipole model, including some criticism of the aspects that we consider unfavourable.

5.2 The Theory of the Atom-Dipole Interaction Model of Rayleigh and Raman Optical Activity

The two-group model is based on a Raman intensity theory which uses bonds as its basic molecular subunit. In contrast, the atom-dipole interaction model is based on atomic rather than bond properties: the atoms in a molecule are each assigned a spherical polarizability which are then allowed to interact via the atomic dipole moments induced by the dynamic electric field of the exciting radiation.[7-11] Using this approach both the polarizability and optical activity tensors (and their derivatives) may be calculated.

If each atom i in an N-atom molecule has associated with

it a spherical (isotropic) polarizability α_i, then the induced electric dipole moment on each atom, μ_i, is given by

$$\mu_{i\alpha} = \alpha_i \delta_{\alpha\beta} \left(E_{i\beta} - \sum_{j \neq i} T^{ij}_{\beta\gamma} \mu_{j\gamma} \right) \qquad i = 1, N \qquad (5.1)$$

where $\underset{\sim}{E}_i$ is the electric field of the light wave at atom i, and $\underset{\sim}{\underset{\sim}{T}}^{ij}$ is the familiar dipole-dipole coupling tensor given by [12]

$$T^{ij}_{\beta\gamma} = \frac{1}{4\pi\epsilon_0} \left(\delta_{\beta\gamma} r_{ij}^2 - 3 r_{i\beta} r_{i\gamma} \right) / r_{ij}^5 \qquad (5.2)$$

in which $\underset{\sim}{r}_{ij}$ is the vector from atom i to atom j, and ϵ_0 is the permittivity of free space. If the assumption is made that the electric field is constant over the dimensions of the molecule we may put $\underset{\sim}{E}_i = \underset{\sim}{\underset{\sim}{E}}$ for all i. Equation (5.1) may then be rearranged to give

$$(\alpha_i)^{-1} \delta_{\alpha\beta} \mu_{i\alpha} + \sum_{j \neq i} T^{ij}_{\alpha\beta} \mu_{j\alpha} = E_\beta \qquad i = 1, N \qquad (5.3)$$

This may be written in matrix form:

$$\begin{bmatrix} (\alpha_1)^{-1}\delta_{\alpha\beta} & T^{12}_{\alpha\beta} & \cdots & T^{1i}_{\alpha\beta} \\ T^{21}_{\alpha\beta} & (\alpha_2)^{-1}\delta_{\alpha\beta} & \cdots & \\ \vdots & & & \vdots \\ T^{i1}_{\alpha\beta} & \cdots & \cdots & (\alpha_i)^{-1}\delta_{\alpha\beta} \end{bmatrix} \begin{bmatrix} \mu_{1\alpha} \\ \mu_{2\alpha} \\ \vdots \\ \mu_{i\alpha} \end{bmatrix} = \begin{bmatrix} E_\beta \\ E_\beta \\ \vdots \\ E_\beta \end{bmatrix} \qquad (5.4)$$

Labelling the coefficients of the first matrix factor on the left of (5.4) by $C^{ij}_{\alpha\beta}$ we have

$$C^{ij}_{\alpha\beta} = (\alpha_i)^{-1} \delta_{\alpha\beta} \qquad \text{if} \quad i = j \qquad (5.5a)$$

$$C^{ij}_{\alpha\beta} = T^{ij}_{\alpha\beta} \qquad \text{if} \quad i \neq j \qquad (5.5b)$$

Equation (5.4) may now be written as

$$\sum_j C^{ij}_{\alpha\beta} \mu_{j\alpha} = E_\beta \qquad i = 1, N \qquad (5.6)$$

If we denote by $B^{ij}_{\alpha\beta}$ the elements of the inverse of the matrix formed by the $C^{ij}_{\alpha\beta}$ we have

$$\mu_{i\alpha} = \sum_j B^{ij}_{\alpha\beta} E_\beta \qquad i = 1,N \tag{5.7}$$

The quantity $\sum_j B^{ij}_{\alpha\beta}$ is then an effective polarizability for each group i. Thus we have that

$$\alpha_{i\alpha\beta} = \sum_j B^{ij}_{\alpha\beta} \qquad i = 1,N \tag{5.8a}$$

$$\alpha_{\alpha\beta} = \sum_{ij} B^{ij}_{\alpha\beta} \tag{5.8b}$$

where $\alpha_{\alpha\beta}$ is the total molecular polarizability. The matrix formed by the $B^{ij}_{\alpha\beta}$ is known as the relay tensor matrix.

As before, the optical activity tensors $\underset{\sim}{G'}$ and $\underset{\sim}{A}$ may be written as a sum over all the intrinsic atom tensors plus their origin-dependent parts.

$$G'_{\alpha\beta} = \sum_i G'_{i\alpha\beta} - \tfrac{1}{2}\omega \sum_i \varepsilon_{\beta\gamma\delta} R_{i\gamma} \alpha_{i\alpha\delta} \tag{5.9}$$

For spherically symmetric groups the intrinsic $\underset{\sim}{G'}$ are identically zero, so

$$G'_{\alpha\beta} = -\tfrac{1}{2}\omega \sum_{ij} \varepsilon_{\beta\gamma\delta} R_{i\gamma} B^{ij}_{\alpha\delta} \tag{5.10}$$

The $\underset{\sim}{A}$ tensor may be handled in a similar fashion. In this case, however, the relation $\alpha_{\alpha\beta} G'_{\alpha\beta} = \tfrac{1}{3}\omega \alpha_{\alpha\beta} \varepsilon_{\alpha\gamma\delta} A_{\gamma\delta\beta}$ cannot be used since this relies on the group polarizabilities being symmetric. In the atom-dipole model the group polarizabilities (the $\sum_j B^{ij}_{\alpha\beta}$) are not, in general, symmetric although the total polarizability $\left(\sum_{ij} B^{ij}_{\alpha\beta}\right)$ is, indeed, symmetric as it must be for molecules with a non-degenerate ground state using exciting radiation of frequency far from any molecular transitions.

Knowing $\underset{\sim}{\alpha}$, $\underset{\sim}{G'}$ and $\underline{A}$, the Rayleigh circular intensity difference may be calculated.

For the Raman case use is made of the following relationship for the derivative with respect to the normal mode Q_ρ

$$\left(\frac{\partial \underset{\sim}{B}^{ij}_{\alpha\beta}}{\partial Q_\rho}\right) = -\sum_{i,j}\sum_{k,l} B^{ik}_{\alpha\delta}\left(\frac{\partial C^{kl}_{\delta\gamma}}{\partial Q_\rho}\right) B^{lj}_{\gamma\beta} \qquad (5.11)$$

The problem of evaluating the polarizability tensor derivatives (and hence the optical activity tensor derivatives) devolves upon calculation of the derivatives of (5.5a&b). In an early version of the theory the spherical polarizability derivatives, $(\partial\alpha_i/\partial Q_\rho)$, were set to zero and the change in the polarizability came about solely through the changes in the $\underset{\sim}{T}^{ij}$. The $(\partial \underset{\sim}{T}^{ij}/\partial Q_\rho)$ are easily calculated using Equation (4.23). However, this produced poor results[10] and it was required to introduce non-zero derivatives of the spherical atom polarizabilities which are then treated as empirical parameters. Presently there are two different ways of doing this.

The first way is to make the atom polarizabilities dependent on the bond stretching internal coordinates in which they are involved:[11]

$$\alpha_i = (\alpha_i)_o + \sum_q \left(\frac{\partial\alpha_i}{\partial S_q}\right)_o \left(\frac{\partial S_q}{\partial Q_\rho}\right)_o Q_\rho + \cdots$$

$$= (\alpha_i)_o + \sum_q \left(\frac{\partial\alpha_i}{\partial S_q}\right)_o L_{q\rho} Q_\rho + \cdots \qquad (5.12)$$

in which the S_q are the bond stretching coordinates only. The value of $(\partial\alpha_i/\partial S_q)_o$ is zero unless atom i is one of the atoms forming S_q . The non-zero $(\partial\alpha_i/\partial S_q)_o$ are adjusted to give the best fit

to the experimental data available and are considered transferable from one atom to another of the same type in a different molecule, so long as the atoms are in similar chemical environments. This method has the obvious drawback in that, for a molecule such as bromochlorofluoromethane, the carbon atom has to be assigned four different polarizability derivatives, one for each bond it forms a part of. In practice, these four derivatives of tetrahedrally substituted atoms have been made equal - not a very satisfying approximation.

The second way of dealing with the spherical polarizability derivatives, and the way in which all the Raman optical activity calculations have been carried out, is to specify the derivatives with respect to cartesian displacement coordinates. Each atom i is assigned a cartesian derivative matrix

$$\begin{bmatrix} \frac{\partial \alpha_i^{xx}}{\partial x_i} & \frac{\partial \alpha_i^{xx}}{\partial y_i} & \frac{\partial \alpha_i^{xx}}{\partial z_i} \\ \frac{\partial \alpha_i^{yy}}{\partial x_i} & \frac{\partial \alpha_i^{yy}}{\partial y_i} & \frac{\partial \alpha_i^{yy}}{\partial z_i} \\ \frac{\partial \alpha_i^{zz}}{\partial x_i} & \frac{\partial \alpha_i^{zz}}{\partial y_i} & \frac{\partial \alpha_i^{zz}}{\partial z_i} \end{bmatrix} \qquad (5.13)$$

where α_i^{xx}, α_i^{yy} and α_i^{zz} are the diagonal polarizability components of atom i, and x_i , y_i , z_i are its cartesian displacement coordinates. To cut down the number of parameters in a calculation the matrix (5.13) is assumed to be symmetric. In terms of this symmetric matrix the derivative of the atomic polarizability of atom i with respect to the normal coordinate may eventually be calculated. In this approach there are seven input parameters per atom - one spherical polarizability and six cartesian derivatives.

In contrast to the first method of dealing with the atomic polarizability derivatives, the second one has the result that an atomic polarizability does not retain its spherical symmetry during the normal mode excursion. In this way, it is claimed, "non-following" electronic effects may be approximated.[14] We have doubts, however, that this second procedure is physically correct. We are of the opinion that if the atom polarizability is spherical in its equilibrium position then it must stay so. If this is the case then there are only three derivative parameters associated with each bond i, $\partial\alpha_i/\partial x_i$, $\partial\alpha_i/\partial y_i$ and $\partial\alpha_i/\partial z_i$. The spherical symmetry is thus preserved. This approach has been considered before but it was dismissed as involving an approximation which was too restrictive.

On a general point about cartesian atomic polarizability derivatives, in whatever form, we find it difficult to consider them transferable between identical atoms in different molecules. For example, changing a molecule by isotopic substitution will change its principal cartesian coordinates while leaving its electronic structure, to a first approximation, unchanged.

It has been stated[3] that the two-group model is inferior to the atom-dipole interaction model due to the former's neglect of intramolecular dynamic coupling. This was substantiated by the fact that when the symmetric and antisymmetric parts of the effective group polarizabilities are considered separately the antisymmetric parts contribute to the Raman optical activity on an equal footing with the symmetric parts. We feel that the conclusions reached by this argument have no real significance. Before dynamic coupling, a molecule in the atom-dipole interaction model is completely iso-

tropic. All the dynamic coupling is required to reproduce the full anisotropy of the "real" molecule. Looking at the Raman optical activity generated solely by the symmetric parts of the effective polarizabilities is equivalent to looking at a version of the "real" molecule which does not have the full (symmetric) anisotropy that the model finally gives it. The full anisotropy only appears when the antisymmetric parts are combined to give the complete molecular polarizability, $\sum_{ij} B^{ij}_{\alpha\beta}$.

REFERENCES

1. P.L. Prasad and D.F. Burow, J. Amer. Chem. Soc., 101, 800 (1979).

2. P.L. Prasad and D.F. Burow, J. Amer. Chem. Soc., 101, 806 (1979).

3. P.L. Prasad and L.A. Nafie, J. Chem. Phys., 70, 5582 (1979).

4. P.L. Prasad, L.A. Nafie and D.F. Burow, J. Raman Spectrosc., 8, 255 (1979).

5. P.L. Prasad and L.A. Nafie, J. Chem. Phys., 73, 1567 (1980).

6. J. Applequist, J.R. Carl and K.-K. Fung, J. Amer. Chem. Soc., 94, 2952 (1972).

7. J. Applequist, J. Chem. Phys., 58, 4251 (1973).

8. J. Applequist, J. Amer. Chem. Soc., 95, 8255 (1973).

9. J. Applequist, J. Amer. Chem. Soc., 95, 8258 (1973).

10. J. Applequist, Accts. Chem. Res., 10, 79 (1977).

11. J. Applequist and C.O. Quicksall, J. Chem. Phys., 66, 3455 (1977).

12. A.D. Buckingham and P.J. Stiles, Accts. Chem. Res., 7, 258 (1974).

13. G. Placzek, in Handbuch der Radiologie, Vol. 6, Part 2, E. Marx, Ed., Akademische Verlagsgesellshaft, Berlin (1934).

14. C.A. Coulson and M.T. Rogers, J. Chem. Phys., 35, 593 (1961).

CHAPTER 6

A GENERAL TWO-GROUP MODEL CALCULATION ON (+)-R-BROMOCHLOROFLUORO-METHANE

6.1 Introduction

We now present a Raman optical activity calculation using the theory of Chapter 4. Bromochlorofluoromethane was chosen for a number of reasons: it is a small molecule and the calculation is relatively straightforward; a reliable force-field had been published[1]; work had been done on the bond polarizability derivatives of various halogenated alkane molecules[2,3] and, finally; a substantial amount of work, mainly theoretical, had been done on the vibrational optical activity of the molecule, both infra-red[4] and Raman[5,6]. The unfortunate point about bromochlorofluoromethane is that, as yet, it has only been partially resolved and no complete Raman optical activity spectrum has been obtained so far.

6.2 Normal Coordinate Analysis

All the information necessary to perform the analysis - the molecular geometry and a simplified general valence force field - are given in Reference 1. We will not duplicate this information here. We do, however, define the internal coordinates used (Table 6.1 and Figure 6.1).

Table 6.2 gives the observed[1] and calculated frequencies of the 9 normal modes of bromochlorofluoromethane. Also given are percentage figures for the potential energy distribution (see Appendix) of the internal coordinates which make the major contribution to each normal mode. Thus, internal coordinate 1 (see Table 6.1) makes a

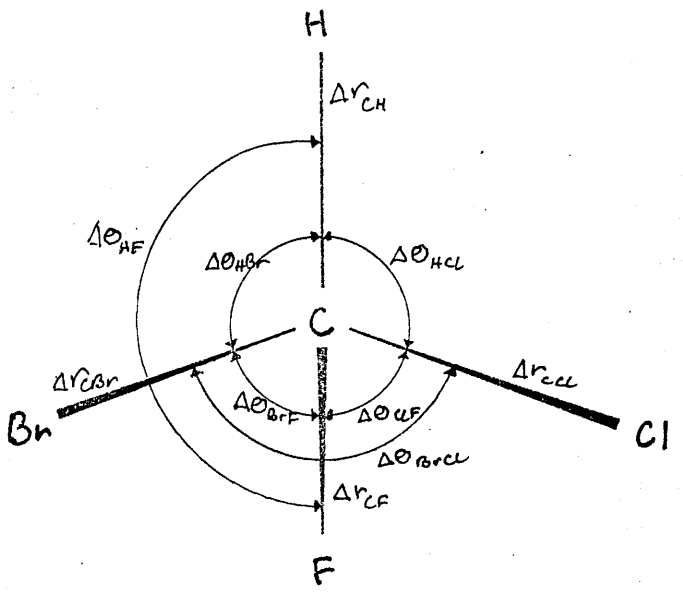

Figure 6.1. The Internal Coordinates of Bromochlorofluoromethane.

Table 6.1. Internal Coordinate Definitions for Bromochlorofluoromethane (see Figure 6.1)

Number of Coordinate	Definition
1	Δr_{CH}
2	Δr_{CBr}
3	Δr_{CCl}
4	Δr_{CF}
5	$\Delta\theta_{HF}$
6	$\Delta\theta_{HCl}$
7	$\Delta\theta_{HBr}$
8	$\Delta\theta_{ClF}$
9	$\Delta\theta_{BrF}$
10	$\Delta\theta_{BrCl}$

Table 6.2. The Observed and Calculated Normal Modes of Bromochlorofluoromethane

Mode	Wavenumber		Percentage
	Observed	Calculated	P.E.D. Contributions
1	3026	3039	1(99)
2	1311	1302	6(26), 7(68)
3	1205	1203	5(50), 7(45)
4	1078	1074	4(95)
5	788	794	3(82), 8(22)
6	664	670	2(56), 9(21), 10(17)
7	427	425	8(50)
8	315	310	2(42), 9(50)
9	226	224	3(11), 8(21), 10(65)

99% contribution to the potential energy distribution of the first normal mode.

6.3 The Raman Optical Activity Calculation

6.3.1 The Bond Polarizability Data

The 12 bond polarizability parameters used in the calculation are given in Table 6.3. The information per bond is given in the form of the anisotropy, Δ , the derived anisotropy, Δ' , and the derived mean polarizability, α' . The use of Δ' and α' is entirely equivalent to that of Δ' and $\alpha_\perp'$, the derived transverse polarizability, which the theory in Chapter 4 uses. Since $\alpha' = (\alpha_\parallel' + 2\alpha_\perp')/3$ we have that $\alpha_\perp' = (3\alpha' - \Delta')/3$. We give α' here since this is the quantity usually reported in bond polarizability studies.

The polarizability anisotropy for the C-Br, C-Cl and C-F bonds were taken from Reference 8, a review of molecular refractivity and polarizability. The anisotropy for the C-H bond is quoted in this article as zero. But this was for C-H bonds in aliphatic hydrocarbons, so we use what we think to be a more realistic value taken from a bond polarizability study on some halogenated methane derivatives.[9] We also took the derived bond anisotropies for the C-H, C-Cl and C-Br bonds from the same source. Values for derivatives of the mean bond polarizabilities for all four bonds have been worked out in a bond polarizability study of the totally symmetric vibrations of the series of trihalogenomethanes CX_3H where X = Cl,F,Br.[2] This now leaves only a value for the derived anisotropy of the C-F bond. By an educated guess we ascribed to this the value of $2.0 \times 10^{-2}\,nm^2$. Adjusting this value by $\pm\ 1.0 \times 10^{-2}\,nm^2$ did not alter any of the

Table 6.3. Bond Polarizability Data for Bromochlorofluoromethane

Bond	α' $\times 10^2$ nm^2	Δ $\times 10^3$ nm^3	Δ^r $\times 10^2$ nm^2
C-H	1.08	0.20	2.13
C-Br	2.07	3.40	2.40
C-Cl	2.00	2.10	2.14
C-F	1.00	0.80	2.00

signs predicted by the calculation.

6.3.2 The Calculated Circular Intensity Differences of (+)-R-Bromo chlorofluoromethane

Table 6.4 presents the calculated polarized and depolarized circular intensity differences of all the normal modes of (+)-R-bromochlorofluoromethane.

Since all pairs of bonds in the molecule have a plane of symmetry the predicted Rayleigh optical activity is zero. In fact, dynamic coupling is required to produce differential Rayleigh scattering using a two-group approach.

The results show effects of the correct order of magnitude. On the whole, though, the circular intensity differences are smaller than those predicted for the other molecule studied, 3-methylcyclohexanone. This is because bromochlorofluoromethane is a relatively small molecule. Inspection of the simple two-group equations shows that Raman optical activity, according to this model, increases with increasing separation of the bonds involved.

The C-H stretching vibration at 3039 cm^{-1} produces a very small calculated effect. This is consistent with the general observation with present instrumentation that no Raman optical activity has been observed for any normal modes above 2500 cm^{-1}.

There is not much else one can say about these results, having no experimental data with which to compare them. Still, the incentive is now that little bit greater to resolve the molecule.

In Table 6.5 we compare the results of this calculation with those of the atom-dipole interaction model calculation.[5,6] As can be seen, the results are quite different and if this state of affairs

Table 6.4. The Calculated Polarized and Depolarized Circular Intensity Differentials of (+)-(R)-Bromochlorofluoromethane.

Normal Mode Wavenumber	Polarized CID $\times 10^4$	Depolarized CID $\times 10^4$
3039	0.00	0.00
1302	0.83	0.54
1203	0.15	0.13
1074	-0.65	-0.42
794	0.10	0.11
670	0.13	0.22
425	-0.86	-0.77
310	0.77	0.64
224	0.37	0.28

Table 6.5. Comparison of the Circular Intensity Differences of (+)-(R)-Bromochlorofluoromethane Calculated by the General Two-Group (GTG) Model and the Atom-Dipole Interaction (ADI) Model[a]

Normal Mode Wavenumber	Polarized CID $\times 10^4$		Depolarized CID $\times 10^4$	
	GTG	ADI	GTG	ADI
3039	0.00	-0.08	0.00	0.46
1302	0.83	-5.16	0.54	-8.16
1203	0.15	3.01	0.13	5.77
1074	-0.65	0.35	-0.42	0.88
794	0.10	-2.01	0.11	-1.41
670	0.13	-1.90	0.22	-2.25
425	-0.86	-7.67	-0.77	-10.9
310	0.77	7.64	0.64	34.3
224	0.37	-6.16	0.28	-4.74

a. Reference 6.

is general then it should make it easier to decide which model provides a better description of the effect.

REFERENCES

1. M. Diem and D.F. Burow, J. Chem. Phys., 64, 5179 (1976).

2. W. Holzer, J. Mol. Spectrosc., 27, 522 (1968).

3. L.M. Sverdlov, M.A. Kovner and E.P. Krainov, Vibrational Spectra of Polyatomic Molecules, Chapter 7, Wiley (Israel Program for Scientific Translations), New York, 1974.

4. C. Marcott, T.R. Faulkner, A. Moscowitz and J. Overend, J. Amer. Chem. Soc., 99, 8169 (1977).

5. M. Diem, Ph.D. Thesis, Toledo (1976).

6. P.L. Prasad and L.A. Nafie, J. Chem. Phys., 70, 5582 (1979).

7. M. Diem, M.J. Diem, B.A. Hudgens, J.L. Fry and D.F. Burow, 31st Symposium on Molecular Spectroscopy, The Ohio State University, Columbus, Ohio, 1976.

8. R.J.W. LeFevre, Adv. Phys. Org. Chem., 3, 1 (1965).

9. A. Weber and S.M. Ferigle, J. Chem. Phys., 23, 2207 (1955).

CHAPTER 7

A GENERAL TWO-GROUP MODEL CALCULATION ON (+)-(3R)-METHYLCYCLOHEXANONE

7.1 Introduction

After the bromochlorofluoromethane calculation, chosen for its simplicity, it was decided to study 3-methylcyclohexanone. This molecule's Raman optical activity spectrum has been measured[1] and is very rich in effects (Figure 7.1). The molecule contains a carbonyl and a methyl group - both very interesting from the viewpoint of Raman optical activity.[1-3] Although no directly applicable force field was at hand, a thorough normal coordinate analysis of cyclohexanone itself was available,[4] whose force field could be adapted for the methylated molecule. This adaptation, unfortunately, was not very successful. Nevertheless, the path has been paved for the future when a good, reliable force field has been developed.

7.2 The Normal Coordinate Analysis of 3-Methylcyclohexanone

7.2.1 Molecular Geometry.

The molecule 3-methylcyclohexanone in solution is known to exist predominantly in the equatorial conformation.[5] Hence the calculation was restricted to this conformation (Figure 7.2).

As a slightly better alternative to obtaining the molecular geometry by taking measurements from a model, the molecule (in the equatorial conformation) was subjected to a molecular mechanics calculation.[6] The results of this calculation, in the form of cartesian coordinates referred to principal inertial axes, are given in Table 7.1. The numbering used is shown in Figure 7.3.

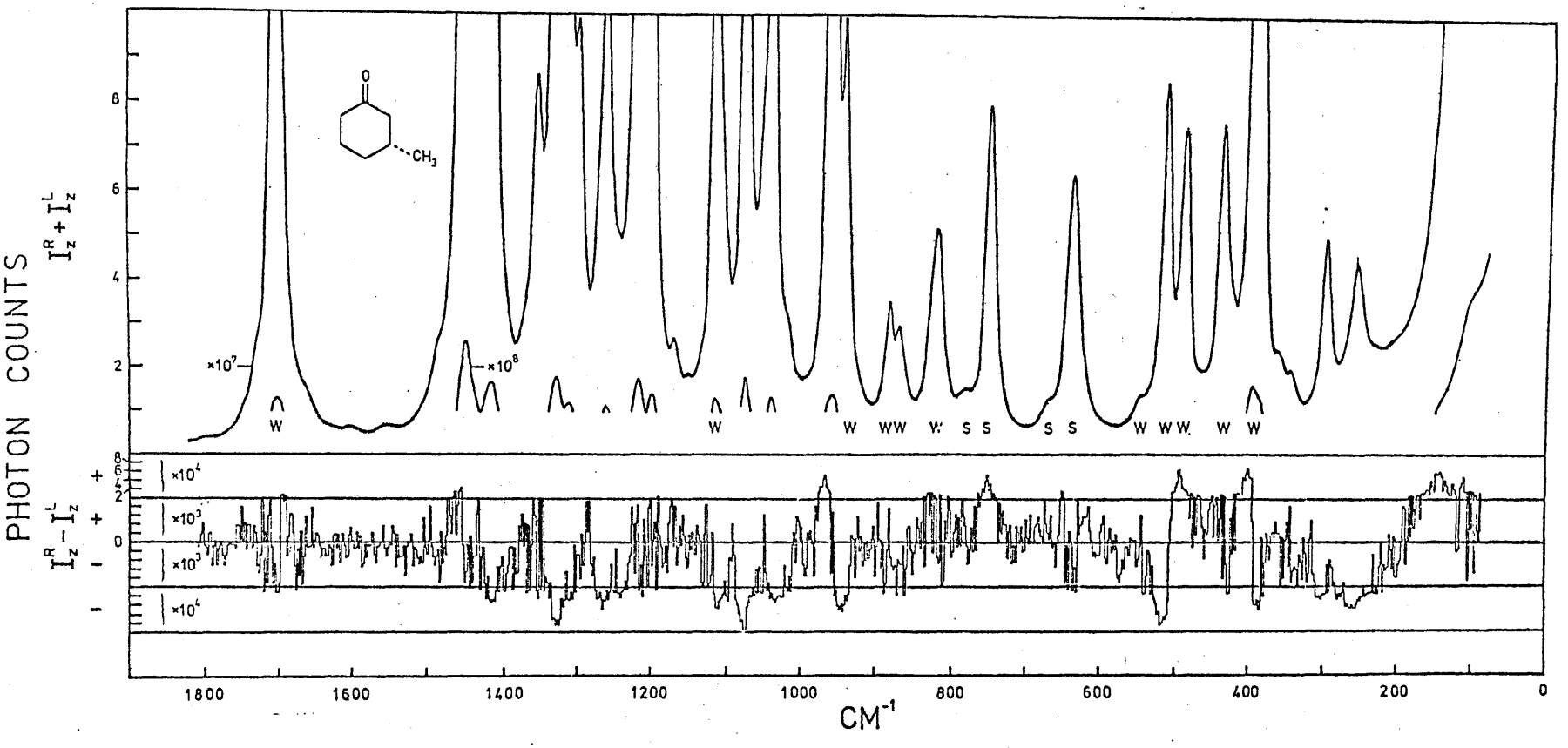

FIGURE 7.1. THE DEPOLARIZED CIRCULAR INTENSITY SUM AND DIFFERENCE SPECTRA OF NEAT (1)-(3R)-METHYLCYCLOHEXANONE

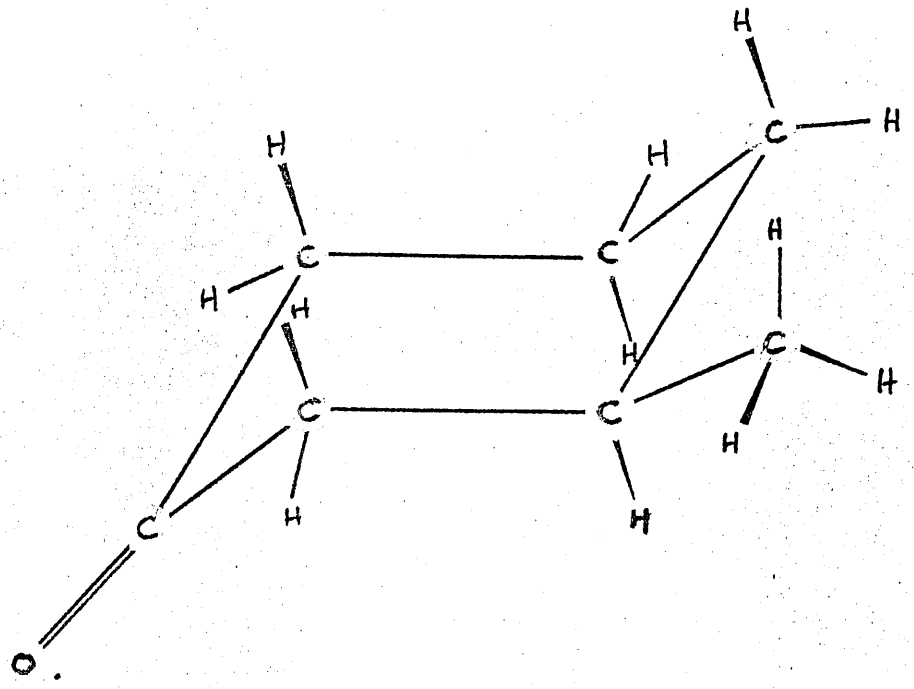

Figure 7.2. The Equatorial Conformation of (+)-(3R)-Methylcyclohexanone.

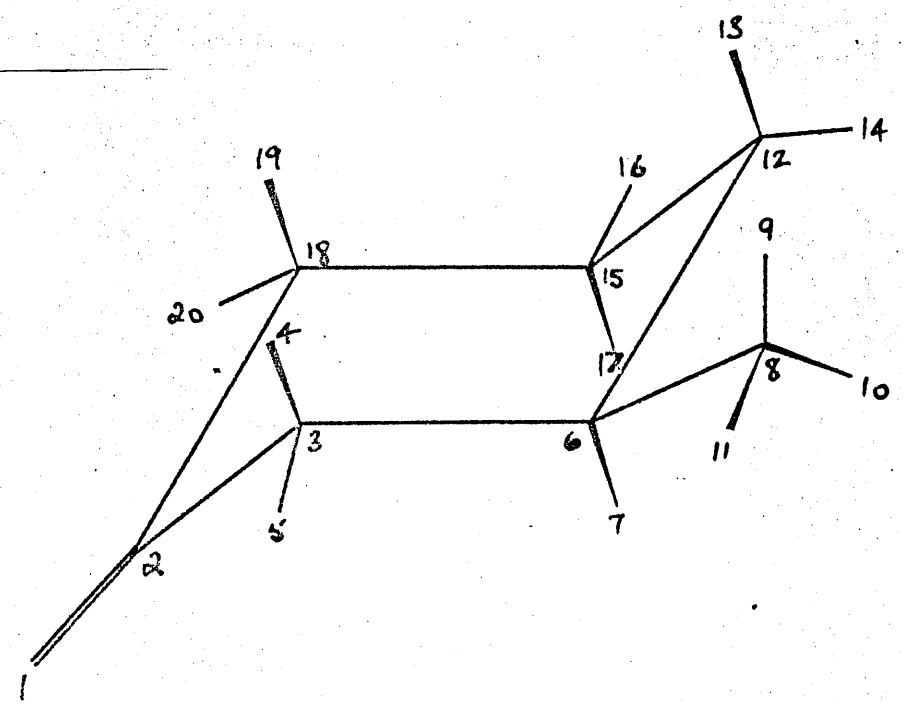

Figure 7.3. The Atom Numbering System for 3-Methylcyclohexanone.

Table 7.1. The Principal Cartesian Coordinates of (+)-(3R)-Methylcyclohexanone

Atom No.	X nm	Y nm	Z nm
1	-0.02589	0.11697	0.22327
2	0.01024	0.04783	0.12676
3	0.03253	0.10906	-0.00968
4	0.14037	0.11615	-0.02665
5	-0.00798	0.21068	-0.01042
6	-0.03191	0.02769	-0.12345
7	-0.14056	0.02845	-0.10909
8	-0.00152	0.08795	-0.26188
9	-0.03778	0.19113	-0.26434
10	0.10660	0.08581	-0.27843
11	-0.05228	0.02871	-0.33857
12	0.01767	-0.11784	-0.11291
13	0.12695	-0.12079	-0.11913
14	-0.02244	-0.17656	-0.19618
15	-0.02899	-0.17921	0.02028
16	0.00141	-0.28424	0.02612
17	-0.13836	-0.17593	0.02449
18	0.02864	-0.10155	0.14001
19	0.13595	-0.12146	0.14754
20	-0.01856	-0.13631	0.23250

7.2.2 Internal Coordinates

The definitions of the internal coordinates and the nomenclature of the resulting force constants not involving the carbonyl group follow Reference 7 closely. Those involving the carbonyl group are the same as given in Reference 4. The 67 internal coordinates chosen are illustrated in Figure 7.4. The set comprises 20 bond stretch coordinates (r, d, s, R, v), 39 valence angle bend coordinates (δ, α, γ, β, η, ω, $\varkappa$, ϵ, ϕ), 1 out-of-plane bend coordinate (ρ), and 7 torsion coordinates (τ). The torsions were defined as the sum of all the possible torsion coordinates about the centre bond involved.

7.2.3 The Molecular Force Field

All the non-zero force constants are shown in Table 7.2. The major part of the force field was obtained from that of cyclohexanone given in Reference 4. The remainder, involving new coordinates brought about by the presence of the methyl group, was obtained from a general valence force field for hydrocarbons given in Reference 7.

7.2.4 Results of the Normal Coordinate Analysis

The normal mode frequencies predicted by the normal coordinate analysis are shown in Table 7.3 along with the potential energy distribution coefficients[8] (see Appendix) of the major contributors in each mode.

Table 7.4 shows the measured Raman and infrared band frequencies. The laser spectrometer used for the Raman frequencies has been described in the literature.[9] An internal calibration procedure was carried out by illuminating the spectrometer with a neon lamp. The atomic transition frequencies of neon are known exactly and these were used

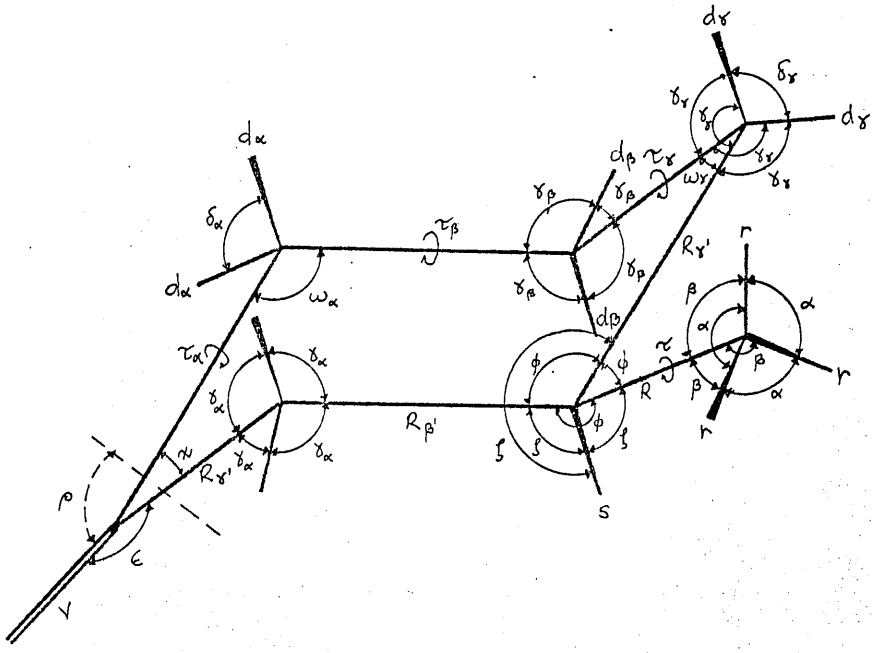

a.

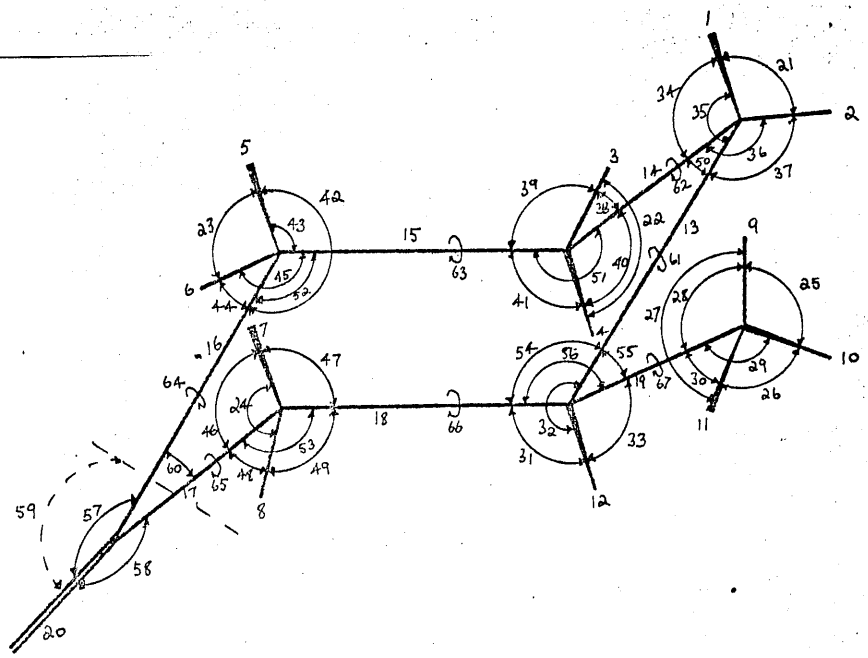

b.

Figure 7.4. The Internal Coordinates of 3-Methylcyclohexanone.
a. Coordinate Type
b. Coordinate Number

Table 7.2. Values of the Force Constants for 3-Methyl-Cyclohexanone

Type	Value mDA°$^{-1}$	Type	Value mDA°$^{-1}$
Diagonal		$H_{\tau(\alpha)}$	0.008
Stretch		$H_{\tau(\beta)}$	0.093
$K_{d(\alpha)}$	4.685	$H_{\tau(\gamma)}$	0.093
$K_{d(\beta)}$	4.610	H_{ζ}	0.657 *
$K_{d(\gamma)}$	4.533	H_{λ}	0.540 *
K_{γ}	9.723	H_{β}	0.645 *
$K_{R(\alpha)}$	4.564	H_{ϕ}	1.084 *
$K_{R(\beta)}$	4.186	H_{τ}	0.024 *
$K_{R(\gamma)}$	4.136	Interaction	
$K_{R(\beta')}$	4.337 *	Stretch-Stretch	
$K_{R(\gamma')}$	4.337 *	F_{ϕ}	0.006
K_{ζ}	4.588 *	F_{R}	0.101
K_{R}	4.387 *	F_{r}	0.043 *
K_{r}	4.699 *	Stretch-Bend	
Bend		$F_{R\omega}$	0.417
$H_{\zeta(\alpha)}$	0.554	$F_{R\gamma}$	0.328
$H_{\zeta(\beta)}$	0.567	$F_{R'\gamma}$	0.079
$H_{\zeta(\gamma)}$	0.579	$F_{R\epsilon}$	0.417
$H_{\gamma(\alpha)}$	0.628	$F_{R\chi}$	0.417
$H_{\gamma(\beta)}$	0.679	Bend-Bend	
$H_{\omega(\alpha)}$	1.068	$F_{\gamma\gamma}$	-0.021
$H_{\omega(\beta)}$	1.024	$F_{\gamma\gamma'}$	0.012
$H_{\omega(\gamma)}$	1.024	$F^{t}_{\gamma\gamma}$	0.127
H_{χ}	1.111	$F^{g}_{\gamma\gamma}$	-0.005
H_{ϵ}	0.919	$F_{\gamma\omega}$	-0.031
H_{ρ}	0.534	$F^{+}_{\gamma\omega}$	0.049

Table 7.2. (cont.)

Type	Value mDA^{-1}
$F^{g}_{\gamma\omega}$	-0.052
$F_{\beta\beta}$	-0.012 *
$F_{\xi\xi'}$	0.012 *
$F_{\phi\phi}$	-0.041 *
$F^{t}_{\gamma\gamma''}$	-0.014 *
$F^{g}_{\gamma\gamma''}$	-0.025 *
$F^{t}_{\xi\gamma}$	0.002 *
$F^{g}_{\xi\gamma}$	0.009 *
$F^{'t}_{\gamma\gamma'}$	0.002 *
$F^{'g}_{\gamma\gamma'}$	0.009 *
$F^{t}_{\gamma\phi}$	0.049 *
$F^{g}_{\gamma\phi}$	-0.052 *

* Denotes force constant taken from Reference 7.
The rest are from Reference 4.

Table 7.3. Calculated Vibrational Frequencies and Potential Energy Distribution of 3-Methylcyclohexanone

Mode No.	Wavenumber	Potential Energy Distribution
1	2967	5(29), 6(30), 7(19), 8(20)
2	2965	5(19), 6(19), 7(29), 8(30)
3	2963	9(52), 10(47)
4	2963	9(15), 10(18), 11(67)
5	2943	3(49), 4(48)
6	2920	1(47), 2(46)
7	2905	12(80)
8	2900	5(33), 6(31), 7(15), 8(12)
9	2899	5(18), 6(17), 7(30), 8(28)
10	2881	9(32), 10(33), 11(32)
11	2877	3(49), 4(50)
12	2853	1(50), 2(49)
13	1711	20(75)
14	1497	21(64), 22(12)
15	1468	22(13), 25(19), 26(45)
16	1465	25(37), 27(52)
17	1463	21(11), 22(54), 26(13)
18	1436	23(41), 24(35)
19	1434	23(40), 24(41)
20	1402	13(11), 33(12), 34(15), 35(13)
21	1380	18(12), 31(19)
22	1360	25(15), 26(13), 27(17), 28(15), 29(24), 30(17)
23	1343	38(12), 40(13), 41(16)
24	1319	38(14), 39(19)
25	1303	36(10), 37(13)
26	1272	35(10), 46(13), 47(15)

Table 7.3. (cont.)

Mode No.	Wavenumber	Potential Energy Distribution
27	1257	33(12), 48(20), 49(25)
28	1236	16(19), 17(26), 53(14)
29	1224	42(11), 43(12)
30	1207	16(11), 38(13), 45(12)
31	1142	13(14), 18(17)
32	1108	31(18), 32(13), 46(13)
33	1107	41(11)
34	1091	19(43)
35	1045	14(33), 15(16), 19(15)
36	979	13(13), 15(13), 30(18)
37	964	28(21), 29(14)
38	920	18(19)
39	877	14(22), 15(27)
40	848	47(16)
41	830	14(11), 43(11), 45(11)
42	819	13(20), 16(17), 17(19)
43	743	13(14), 16(17)
44	632	59(33)
45	511	56(11), 57(23), 58(16)
46	495	51(14), 58(15), 59(13)
47	445	50(10), 60(24)
48	425	54(16)
49	382	54(27)
50	315	55(34), 56(31)
51	243	50(13), 51(16), 56(13), 63(15)
52	147	53(14), 66(20)
53	133	64(14), 65(14), 67(17)
54	110	67(82)

Table 7.4. The Measured Raman and Infrared Spectra of 3-Methylcyclohexanone

Raman		Infrared	
Wavenumber	Strength	Wavenumber	Strength
2957	s	2954	s
2929	s	2927	s
		2914	m(sh)
2897	s		
		2882	w
2869	s	2870	m
2850	s(sh)	2850	w
2826	s(sh)	2828	w
2737	w		
2730	w		
2711	w		
2647	w		
2628	w		
2602	w		
2541	w		
2497	w		
1739	w		
1716	s(sh)	1717	m
1707	s	1711	m
1677	w		
1666	w		
1638	w		
1610	w		
1459	s	1456	m
1451	m(sh)	1447	m
1428	m	1427	m
1421	m	1420	m
1381	w	1377	w
1361	m	1360	w
		1345	w
1335	m	1334	w
1317	m	1317	w
1304	m	1303	w
1279	w(sh)	1275	m
1268	m		
1252	w	1251	w
1225	m	1225	m
1206	m	1206	w
1187	w		
1177	w		
1123	s	1119	m
		1115	m
		1108	m
1092	w(sh)		
1081	m	1080	m
1056	m	1056	m
1044	m	1045	m
1023	w	1023	w
969	m	970	m
961	m	960	m

Table 7.4. (cont.)

Raman		Infrared	
Wavenumber	Strength	Wavenumber	Strength
946	m	946	m
		913	w
886	m	886	m
873	w		
867	w	866	m
824	m		
		818	m
804	w(sh)		
782	w	782	w
752	m	751	m
745	m(sh)	745	m(sh)
672	m	672	w
641	m	641	m
547	w	546	w
514	m	514	m
490	m	490	m
		462	w
439	w	439	m
427	w	427	w
398	m		
388	m	386	m
		369	w
362	w	363	w
344	w	345	w
298	w	299	w
258	w	259	w
142	w		

(sh) denotes shoulder

to calculate reliable Raman frequencies. Frequencies measured below about 500 cm^{-1} are slightly more inaccurate than those above due to the paucity of good calibration marks in this region. Overall, the Raman frequencies are probably accurate to about ± 1 cm^{-1}, perhaps slightly greater than this for the lower frequencies. The infrared spectrum was measured (by the infrared service at this department) on a Perkin-Elmer 580 spectrometer. The results are of similar accuracy to those in the Raman case.

Table 7.5 compares the observed and calculated frequencies. The more obvious combination/overtone bands have been omitted but some undoubtedly remain and thus complicate the comparison. As this table shows, the agreement between observed and calculated frequencies is not startling. There is, however, a region from about 400-1700 cm^{-1} in which the agreement is passable and it is only for this range that we will compare observed and calculated circular intensity differences. This is not too restrictive since Raman optical activity is not observed with carbon-hydrogen stretching vibrations. Even in the truncated range several rogue calculated bands are evident - noticeably those at 1497 and 1402 cm^{-1}.

7.3 The Rayleigh and Raman Optical Activity Calculations

7.3.1 The Bond Polarizability Data

Figure 7.5 shows the numbering used for the 20 bonds of the molecule. The bond polarizability data are given in Table 7.6. These data were taken from several sources: bond polarizability studies of acetone[10] (for bonds 5-8,16,17,20); cyclohexane[11] (for bonds 1-4,12-15, 18); and ethane[12] (for bonds 9-11,19). The isotropic bond polarizabilities

Table 7.5. Comparison of Observed (Raman) and Calculated Vibrational Frequencies of 3-Methylcyclohexanone

Calc.	Obs.	Calc.	Obs.	Calc.	Obs.
		Wavenumbers			
2967	2957	1272	1268		672
2965		1257	1252	632	641
2963		1236			547
2963		1224	1225	511	514
2943		1207	1206	495	490
2920	2929		1187	445	438
2905		1142	1176	425	426
2900		1108	1123		397
2899	2897	1107		382	387
2881		1091	1092		361
2877	2869		1081	315	343
1711	1707		1055		297
1497		1045	1044	243	258
1468			1023	147	142
1465	1459	979	967	133	
1463	1451	964	961	110	
1436	1428	920	946		
1434	1421		886		
1402		877	872		
1380	1381	848	867		
1360	1361	830	824		
1343	1335	819	804		
1319	1317		782		
1303	1304		752		
	1279	743	745		

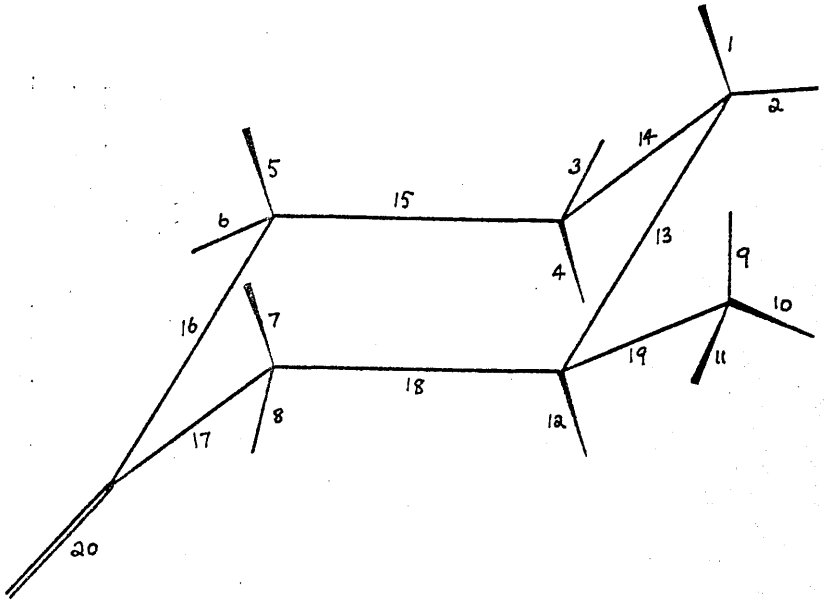

Figure 7.5. The Bond Numbering System for 3-Methyl-cyclohexanone.

Table 7.6. Bond Polarizability Data for 3-Methylcyclohexanone

Bond	α $\times 10^3$ nm^3	α' $\times 10^2$ nm^2	Δ $\times 10^3$ nm^3	Δ' $\times 10^2$ nm^2
1	0.64	1.30	0.32	2.20
2	0.64	1.30	0.32	2.20
3	0.64	1.30	0.32	2.20
4	0.64	1.30	0.32	2.20
5	0.64	1.13	0.11	1.25
6	0.64	1.13	0.11	1.25
7	0.64	1.13	0.11	1.25
8	0.64	1.13	0.11	1.25
9	0.64	1.13	0.11	2.04
10	0.64	1.13	0.11	2.04
11	0.64	1.13	0.11	2.04
12	0.64	1.30	0.32	2.20
13	0.51	0.92	0.05	1.46
14	0.51	0.92	0.05	1.46
15	0.51	0.92	0.05	1.46
16	0.51	0.99	0.18	2.78
17	0.51	0.99	0.18	2.78
18	0.51	0.92	0.05	1.46
19	0.51	0.99	0.18	2.78
20	1.39	1.83	1.20	2.80

for the Rayleigh case and the polarizability anisotropies are from Reference 13. At the moment, this scavenging procedure is the only means available for a molecule as large as this one.

The carbonyl group poses a problem. It is obvious that the assumption of a cylindrical bond in this case is very poor. The acetone study, from which the carbonyl data was taken, used the next order bond polarizability approach so that each bond was completely anisotropic giving two values for the anisotropy, $(\alpha_{\parallel} - \alpha_{\perp})$ and $(\alpha_{\parallel} - \alpha_{\perp'})$, corresponding to the two transverse polarizability elements $\alpha_{\perp}$ and $\alpha_{\perp'}$. It turns out that the use of either value of $(\alpha_{\parallel} - \alpha_{\perp})$ or $(\alpha_{\parallel} - \alpha_{\perp'})$ in the calculation does not affect the sign of any of the predicted circular intensity differences and so the arbitrary choice of the larger value was made. Fortunately, the values given in Reference 10 for the two derived anisotropies are equal.

7.3.2 The Calculated Circular Intensity Differences of (+)-(3R)-Methylcyclohexanone

Table 7.7 displays the calculated polarized and depolarized circular intensity differences for all the normal modes of the molecule. The observed depolarized circular intensity difference spectrum (Figure 7.1) is expressed in tabular form in Table 7.8. The dimensionless magnitude of each effect is quoted along with the Raman band or bands producing it. These former quantities were obtained by simply measuring peak heights (in terms of photon counts, Figure 7.1) of respective bands in the depolarized sum and difference spectra and taking their quotient. The information in Tables 7.7 and 7.8 is synthesised in Table 7.9 to give a comparison of observed and calculated results for the region 400-1700 cm^{-1}.

Useful criticism of the results is made difficult by the

Table 7.7. The Calculated Polarized and Depolarized Circular Intensity Differences of (+)-(3R)-Methylcyclohexanone

Normal Mode Wavenumber	Polarized CID $\times 10^4$	Depolarized CID $\times 10^4$
2967	0.02	0.01
2965	0.40	0.24
2963	-0.81	-0.48
2963	0.13	0.07
2943	1.38	0.82
2920	-1.54	-0.95
2905	-0.06	-0.26
2900	0.30	4.10
2899	-0.11	-0.07
2881	0.00	0.00
2877	0.01	0.07
2852	-0.02	-0.07
1711	-0.15	-0.15
1497	-3.75	-2.68
1468	8.01	4.83
1465	2.84	1.66
1463	-1.10	-0.66
1436	-0.44	-0.28
1434	-1.28	-1.37
1402	-1.42	-0.92
1379	0.37	0.24
1360	0.19	0.20
1343	-0.13	-0.07
1319	5.92	3.46
1303	-0.86	-0.53

Table 7.7. (continued)

Normal Mode Wavenumber	Polarized CID $\times 10^4$	Depolarized CID $\times 10^4$
1272	-8.89	-7.34
1257	-1.26	-0.77
1236	0.60	0.35
1224	-1.46	-2.29
1207	-1.13	-0.67
1142	-8.23	-4.84
1108	0.64	0.47
1107	-1.12	-1.21
1091	2.10	1.40
1045	-13.5	-20.9
979	-0.48	-0.29
964	-3.28	-3.06
920	-3.25	-4.29
877	5.34	8.77
848	-0.34	-0.52
830	-0.95	-3.36
819	8.21	5.44
743	-0.50	-1.65
632	-0.20	-0.54
511	-1.26	-1.39
494	-2.51	-1.68
445	0.33	0.25
425	4.81	5.28
382	6.14	5.47
315	4.49	2.69
243	0.63	0.37

Table 7.7. (continued)

Normal Mode Wavenumber	Polarized CID $\times 10^4$	Depolarized CID $\times 10^4$
147	3.59	2.09
133	-0.30	-0.17
110	2.61	1.52

Table 7.8. Observed Depolarized Circular Intensity Differences of (+)-(3R)-Methylcyclohexanone

Observed CID Wavenumber	Associated Raman Band(s) Wavenumber	CID $\times 10^3$
1459	1459	0.21
1425	1427	-0.31
1327	1334	-0.73
1311	1317 1304	-0.28
1265	1268	-0.30
1240	1252	-0.50
1112	1110	-0.59
1094	1092	-1.50
1076	1081	-0.95
1059	1056 1045	-0.40
1029	1023	-0.34
968	969 961	0.56
942	946	-0.58
825	824 818	0.38
752	752	0.77
648	640	0.83
630	620	-0.18
539	547	-2.29
513	514	-1.11
491	490	0.93
465	461	1.00
433	439	0.14
423	427	-0.53
412	sh on band at 398	0.30
400	398	0.63

Table 7.8. (continued)

Observed CID Wavenumber	Associated Raman Band(s) Wavenumber	CID $\times 10^{3}$
385	388	-0.47
300	298	-0.66
276	sh on band at 258	-2.00
262	258	-2.29
238		-2.00
224	sh on band at 258	-2.00
145	142	+ve
112	obscured by Rayleigh wing	+ve
100		+ve

Table 7.9. Comparison of Observed and Calculated Depolarized Circular Intensity Differences (400-1700 cm^{-1}) of (+)-(3R)-Methylcyclohexanone

Observed CID Wavenumber	Associated Observed Raman Band(s) Wavenumber	Calculated Raman Wavenumber	Observed CID $\times 10^4$	Calculated CID $\times 10^4$
1459	1459	1465	2.1	1.7
		1463		-0.7
1425	1427	1436	-3.1	-0.3
		1434		-1.4
1327	1334	1343	-7.3	-0.1
1311	1317	1318	-2.8	3.5
	1304	1303		-0.5
1265	1268	1272	-3.5	-7.3
1240	1252	1257	-5.0	-0.8
1112	1110	1108	-5.9	0.5
		1107		-1.2
1094	1092	1091	-15.0	1.4
1076	1081		-9.5	
1059	1056		-4.0	
	1045	1045		-13.5
1029	1023		-3.4	
968	969	979	5.6	-0.3
	961	964		-3.1
942	946	920	-5.8	-4.3
825	824	830	3.8	-3.4
	818	819		5.4
752	752	743	7.7	-1.7
648	640		8.3	
630	620	632	-1.8	-0.5
539	547		-22.9	
513	514	511	-11.1	-1.4
491	490	494	9.3	-1.7
465	461		10.0	
433	439	445	1.4	0.3
423	427	425	-5.3	5.3
412	412		3.0	
400	398	382	6.3	5.5

unreliability of the vibrational analysis. Overall, the agreement between observed and calculated effects leaves a lot to be desired. One significant point, though, is that the success of the calculation becomes poorer as we move to lower frequencies. Above 1200 cm^{-1}, 5 out of 6 effects are predicted with the correct sign. Below 1200 cm^{-1}, however, the statistic is a miserable 7 out of 14 correct. One might expect poor results at lower frequencies for two reasons. First and foremost is that at lower frequencies the normal modes become much more complicated and the unreliability of the normal mode calculation is more likely to be significant. The second reason is that at lower wavenumbers the contribution to normal modes of internal coordinates which involve the carbonyl group becomes greater. The completely anisotropic polarizability of the carbonyl group produces effects not accounted for in the theory, as mentioned before. Nonetheless, there are significant failures: notably the prediction of two negative effects for the couplet observed at 950 cm^{-1}. The measured Raman spectrum indicates that the couplet is associated with 3 bands. The normal coordinate analysis, however, predicts only 2 bands in this vicinity so it is not surprising that no success is registered here. We must also note the failure to predict the massive effects at 1334 and 1070 cm^{-1}. Again, we can point to the shortcomings of the normal coordinate analysis.

On the whole, it must be said that the results are inconclusive. We take heart at the relative success at higher wavenumbers and must await a thorough, full-blooded normal coordinate study of this very important molecule.

The polarized and depolarized Rayleigh circular intensity differences of (+)-(3R)-methylcyclohexanone are 0.25×10^{-6} and

0.11×10^{-3} , respectively. At the present time it is not possible to measure Rayleigh optical activity due to the presence of the high background intensity of the Rayleigh wing. There seems to be no obvious connection between the calculated Rayleigh and Raman optical activity.

REFERENCES

1. L.D. Barron, J. Chem. Soc. Perkin 2, 1074 (1977).

2. L.D. Barron, Nature, 255, 458 (1975).

3. L.D. Barron, J. Chem. Soc. Perkin 2, 1790 (1977).

4. H. Fuhrer, V.B. Kartha, P.J. Krueger, H.H. Mantsch and R.N. Jones, Chem. Rev., 72, 439 (1972).

5. D.A. Lightner and B.V. Crist, Appl. Spectrosc., 33, 307 (1979).

6. C. Morrow, Ph.D. Thesis, University of Glasgow, (1979). The calculation was run overnight on a PDP-11 computer using a standard force field.

7. R.G. Snyder and J.H. Schachtschneider, Spectrochim. Acta, 21, 169 (1965).

8. S. Califano, Vibrational States, Wiley, 1976.

9. L.D. Barron and A.D. Buckingham, Ann. Rev. Phys. Chem., 26, 381 (1975).

10. V.I. Vakhlyueva, S.M. Kats and L.M. Sverdlov, 23, 287 (1967).

11. M. Gussoni, S. Abbate and G. Zerbi, J. Raman Spectrosc., 6, 289 (1977).

12. L.M. Sverdlov, M.A. Kovner and E.P. Krainov, Vibrational Spectra of Polyatomic Molecules, Wiley (Israel Program for Scientific Translations), 1974.

13. R.J.W. LeFevre, Adv. Phys. Org. Chem., 3, 1 (1965).

CHAPTER 8

RAMAN OPTICAL ACTIVITY SPECTRA OF RELATED MOLECULES

In addition to the main body of research involving the two-group model some work was carried out in which the spectra of some similar molecules were analysed to establish stereochemical correlations. The results obtained have been published[1,2] and this chapter consists of copies of these papers.

Raman Optical Activity of Menthol and Related Molecules

By **Laurence D. Barron** * and **Brian P. Clark**, Chemistry Department, The University, Glasgow G12 8QQ

Raman circular intensity difference spectra between 80 and 2 000 cm^{-1} of (−)-menthol, (−)-menthylamine, (−)-menthyl chloride, (−)-isopulegol, (−)-menthone, (−)-3,3-dimethylcyclohexanol, (+)-pulegone, (−)-limonene, and (+)-carvone are presented. Several stereochemical correlations are pointed out involving, in particular, bands characteristic of the isopropyl and *gem*-dimethyl groups, methyl torsions, and out-of-plane olefinic hydrogen deformations.

A SMALL difference in the intensity of Raman scattering from chiral molecules in right and left circularly polarized incident light provides a measure of vibrational optical activity.[1-11] At this early stage in the development of the subject it is of interest to compare the Raman optical activity spectra of series of related compounds to see what common features emerge. Here the spectra of menthol and some related molecules are presented. This article is a continuation of the series started by refs. 7 and 8, where a more detailed introduction to Raman optical activity can be found.

EXPERIMENTAL

The instrument used has been described previously.[2,7] The samples were studied as near saturated solutions or neat liquids. The instrumental conditions were as follows: laser wavelength 488.8 nm, laser power 3 W, slit width 10 cm^{-1}, scan speed 1 cm^{-1} min^{-1}. As before,[2,7] only the depolarized Raman circular intensity sum ($I_z^R + I_z^L$) and difference ($I_z^R - I_z^L$) spectra between 100 and 2 000 cm^{-1} were recorded, the difference spectra being presented on a scale that is linear within each decade range but logarithmic between decade ranges. S and W indicate strongly and weakly polarized bands; all other bands are effectively depolarized.

DISCUSSION

Figures 1—9 show the depolarized Raman circular intensity sum and difference spectra of, respectively, (—)-menthol, (—)-menthylamine, (—)-menthyl chloride, (—)-isopulegol, (—)-menthone, (—)-3,3-dimethylcyclohexanol, (+)-pulegone, (—)-limonene, and (+)-carvone.

The first three Raman circular intensity difference (c.i.d.) spectra in the region 1 100—1 400 cm^{-1} are very similar: neglecting an extra positive c.i.d. at 1 210 cm^{-1} in Figure 3, the positions and signs of the c.i.d.s are the same although relative intensities are variable. This correlation is gratifying because (—)-menthol, (—)-menthylamine, and (—)-menthyl chloride have the same basic skeletons with the same absolute configurations and are expected to have similar conformations. Definite band assignments in this spectral region are difficult due to the large number of CH and CH_2 deformation and C–C stretching vibrations which contribute here. However, the isopropyl group, which is present in all three molecules, gives rise to group frequencies in this region: two bands, at *ca.* 1 170 and 1 140 cm^{-1}, arise from an interaction between the rocking modes of the two isopropyl methyl groups together with C–C stretches.[12] These bands are seen most clearly in

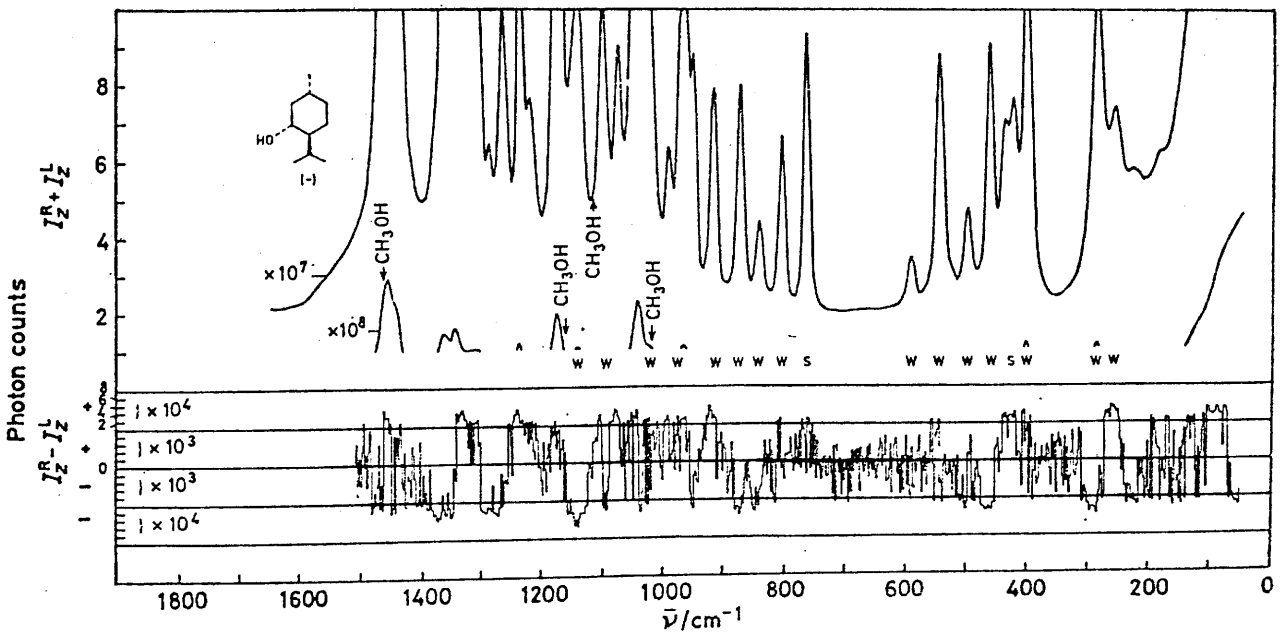

FIGURE 1 The depolarized Raman circular intensity sum and difference spectra of (−)-menthol in methanol

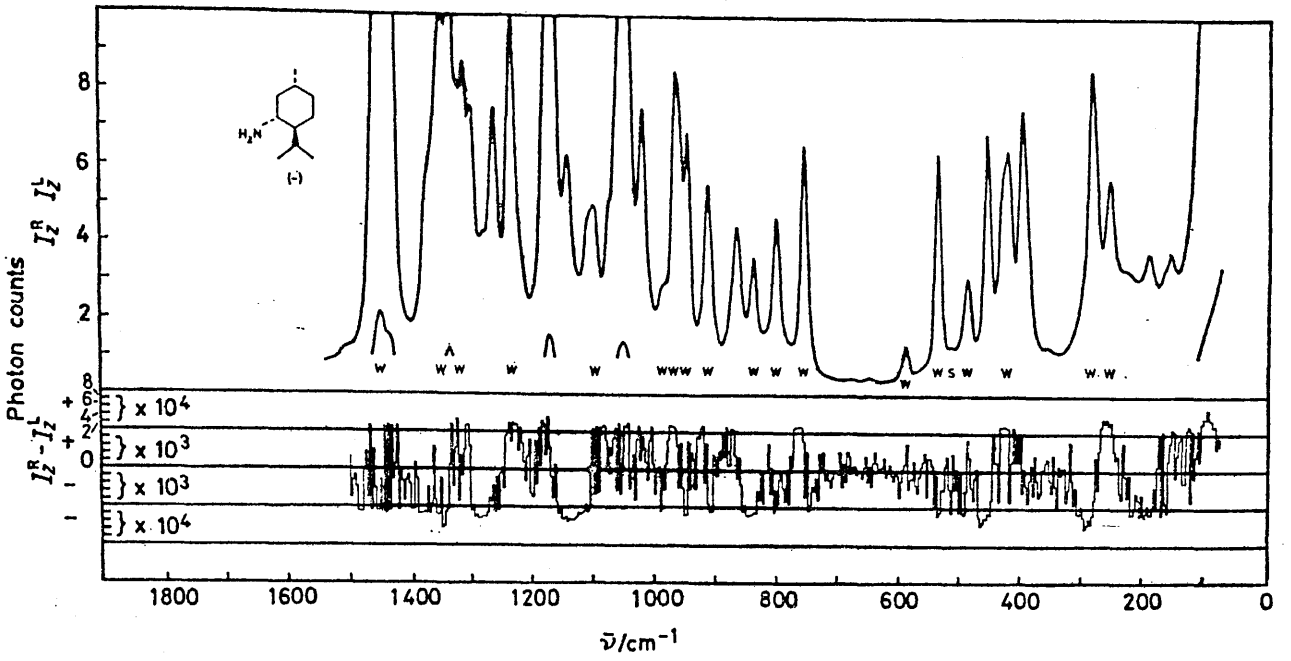

FIGURE 2 The depolarized Raman circular intensity sum and difference spectra of neat (−)-menthylamine

(−)-menthyl chloride (Figure 3) at 1 175 and 1 145 cm^{-1}, and are associated with a c.i.d. couplet. This couplet, with the same sign, is also present in (−)-menthylamine (Figure 2) and in (−)-menthol (Figure 1), although in the last case the higher frequency component has all but disappeared. The appearance of a couplet may be due to a mechanism, described elsewhere,[3,7,8] which involves the coupling of two local group vibrational modes (in this case the methyl rocking deformations) by a chiral perturbation. Lending strength to this assignment is the absence of any such couplet in the c.i.d. spectrum of (−)-isopulegol (Figure 4) in which the isopropyl group has been replaced by an isopropenyl group. Features appearing in the same region in the Raman c.i.d. spectrum of (−)-menthone (Figure 5) also probably originate in the isopropyl methyl rocking vibrations, but now the stereochemical environment of the isopropyl group is rather different on account of the adjacent sp^2-

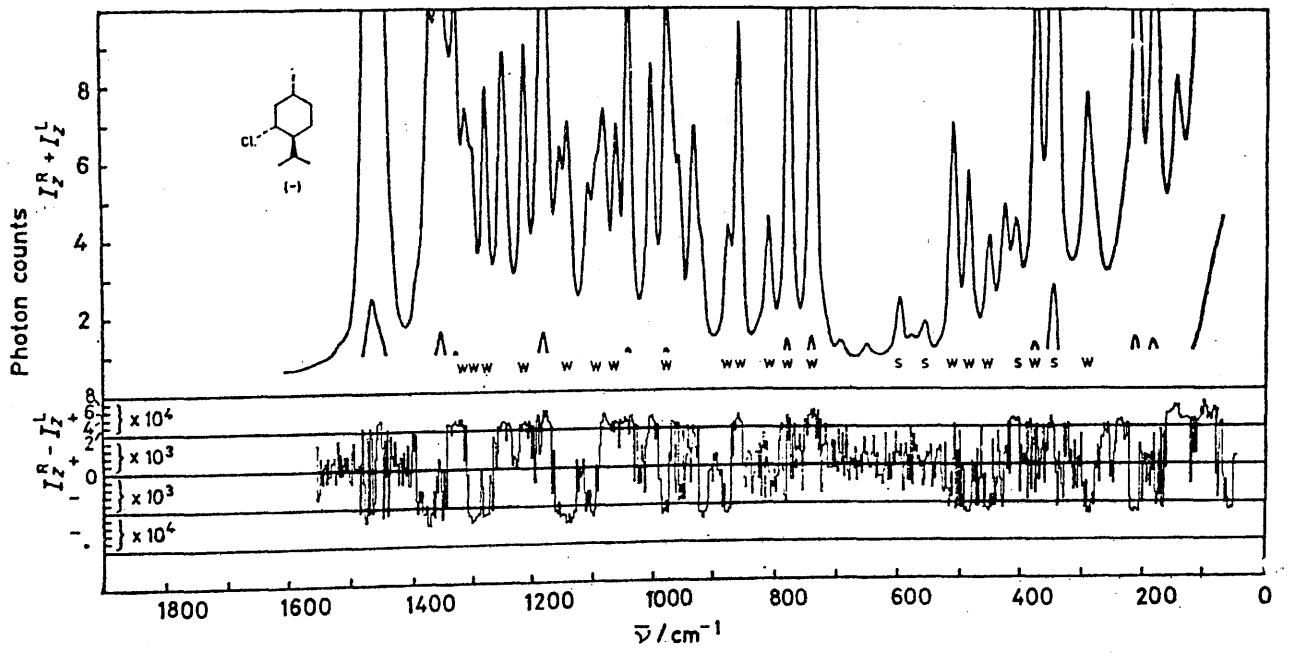

FIGURE 3 The depolarized Raman circular intensity sum and difference spectra of neat (−)-menthyl chloride

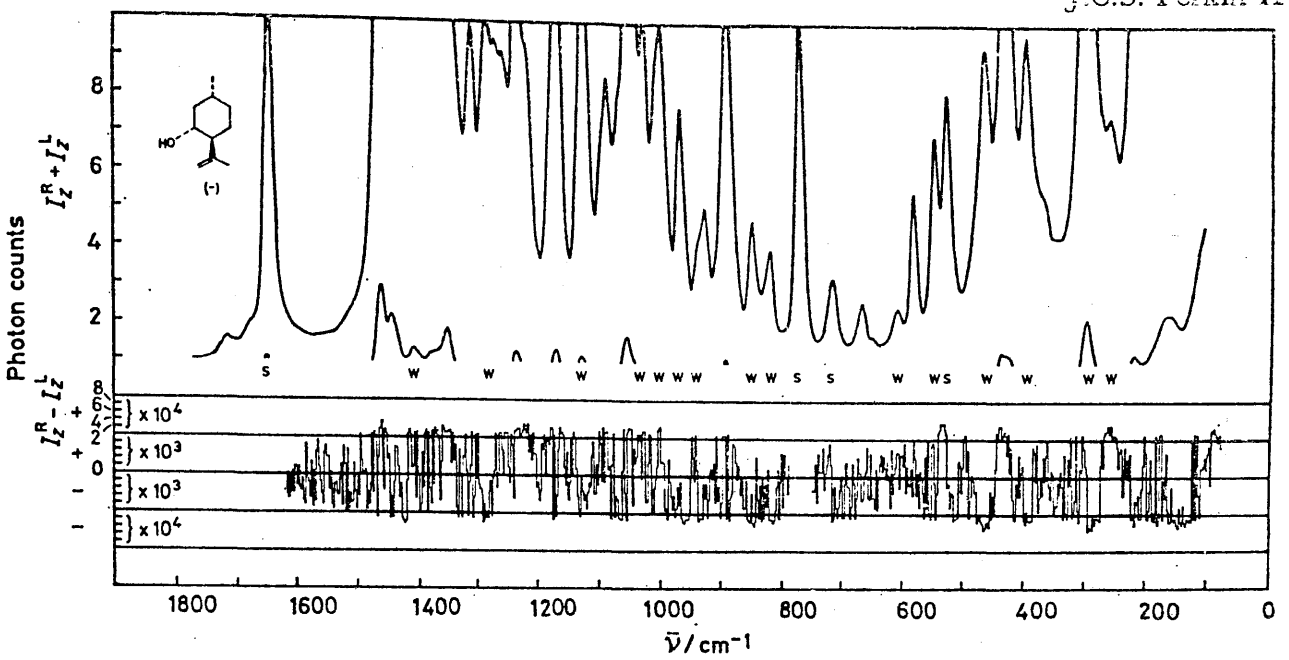

FIGURE 4 The depolarized Raman circular intensity sum and difference spectra of neat (−)-isopulegol

hybridized carbon atom in the ring, so no direct correlations with the first three examples can be made.

The *gem*-dimethyl group also gives rise to two characteristic bands at slightly higher frequencies than the isopropyl group.[12] The Raman optical activity spectra indicate that the situation is more complex than the isopropyl case with both bands sometimes producing c.i.d.s of the same sign. This is probably due to the increased participation of C–C stretching in the *gem*-dimethyl modes which are centred around a quaternary carbon atom. In (−)-3,3-dimethylcyclohexanol (Figure 6), for example, the two *gem*-dimethyl bands are probably those at just under 1 200 cm^{-1} and at 1 175 cm^{-1}: both show a positive Raman optical activity. This is balanced by a negative effect associated with a Raman band at 1 240 cm^{-1} which could originate in stretching of the C–C bonds around the quaternary carbon atom. Previously published Raman c.i.d. spectra

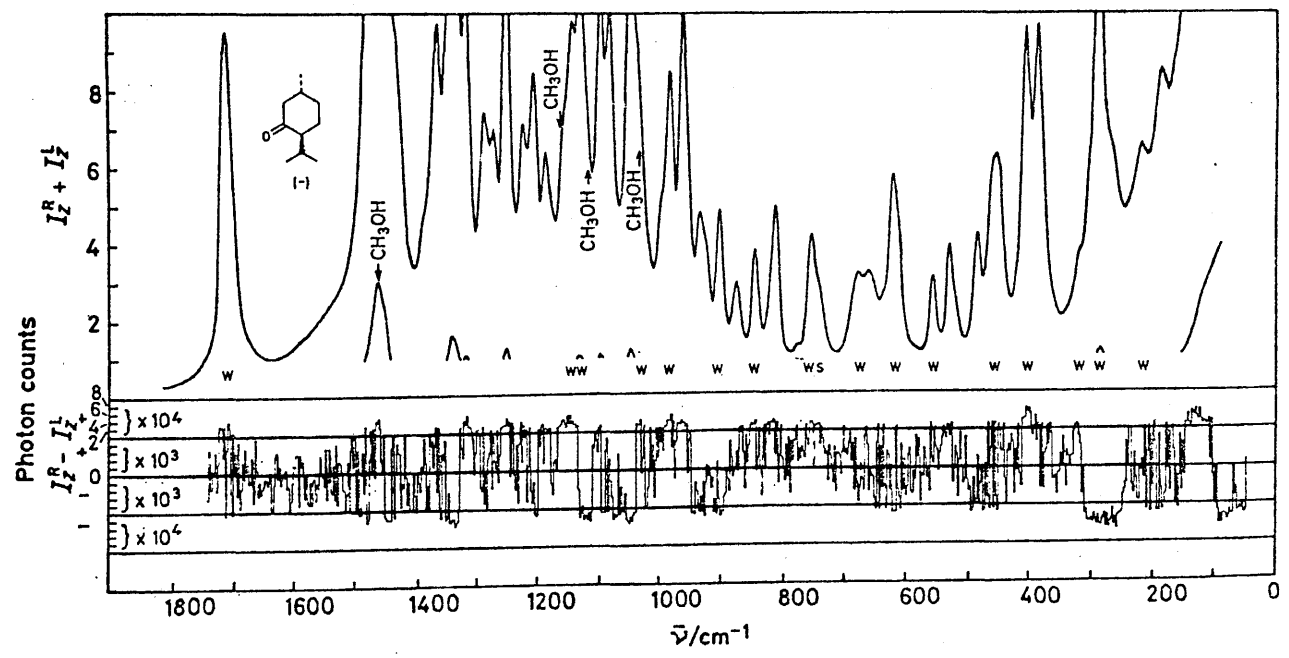

FIGURE 5 The depolarized Raman circular intensity sum and difference spectra of (−)-menthone in methanol

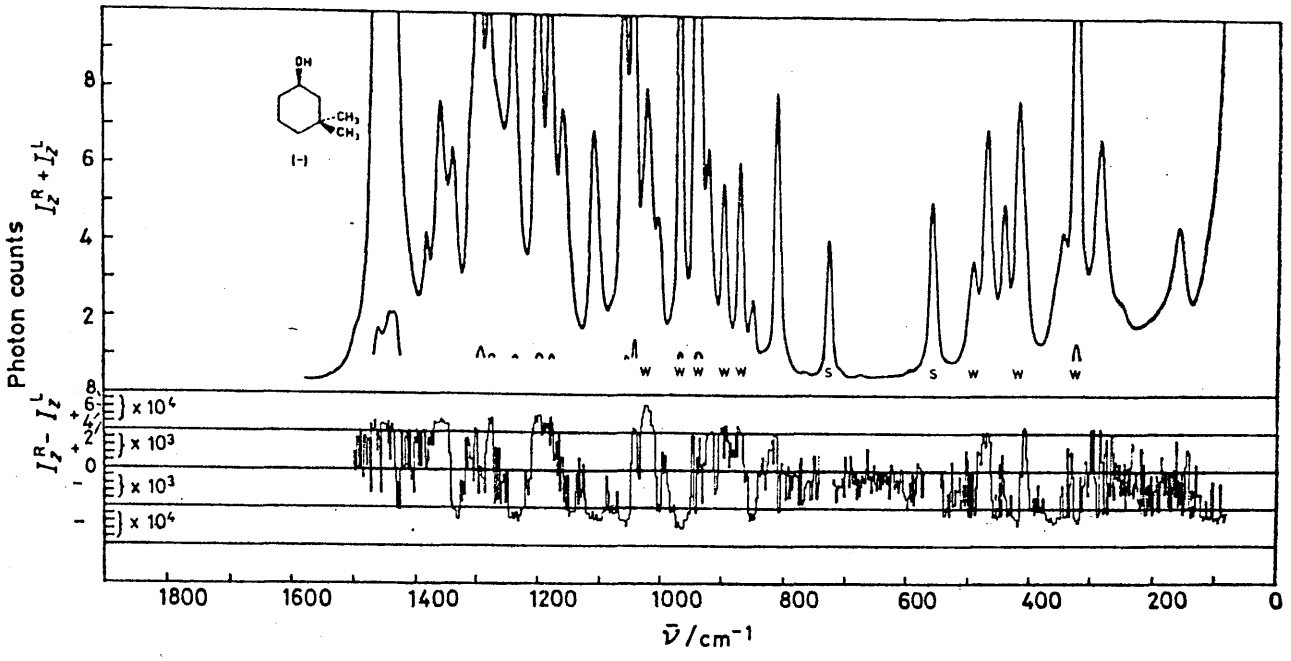

FIGURE 6 The depolarized Raman circular intensity sum and difference spectra of neat (−)-3,3-dimethylcyclohexanol

of camphor and related molecules [7] contain additional examples, although these were not pointed out at the time: camphor itself, for instance, shows a c.i.d. couplet associated with the Raman bands at 1 190 and 1 175 cm^{-1} which were assigned in an earlier i.r. study of camphor to the *gem*-dimethyl group.[13]

Several of the Raman c.i.d. spectra presented here show large effects in the 1 300—1 400 cm^{-1} region. Some of these features almost certainly originate in CH deformations at tertiary carbon atoms.[12] The large negative c.i.d. at 1 345 cm^{-1} in (+)-pulegone (Figure 7) might be an example: this molecule contains only one R_3C–H group. It is worth noting that a large negative c.i.d. occurs at 1 340 cm^{-1} in (+)-3-methylcyclohexanone (Figure 7 of ref. 7) which might have a similar origin.

The Raman c.i.d. spectrum of (−)-3,3-dimethylcyclo-

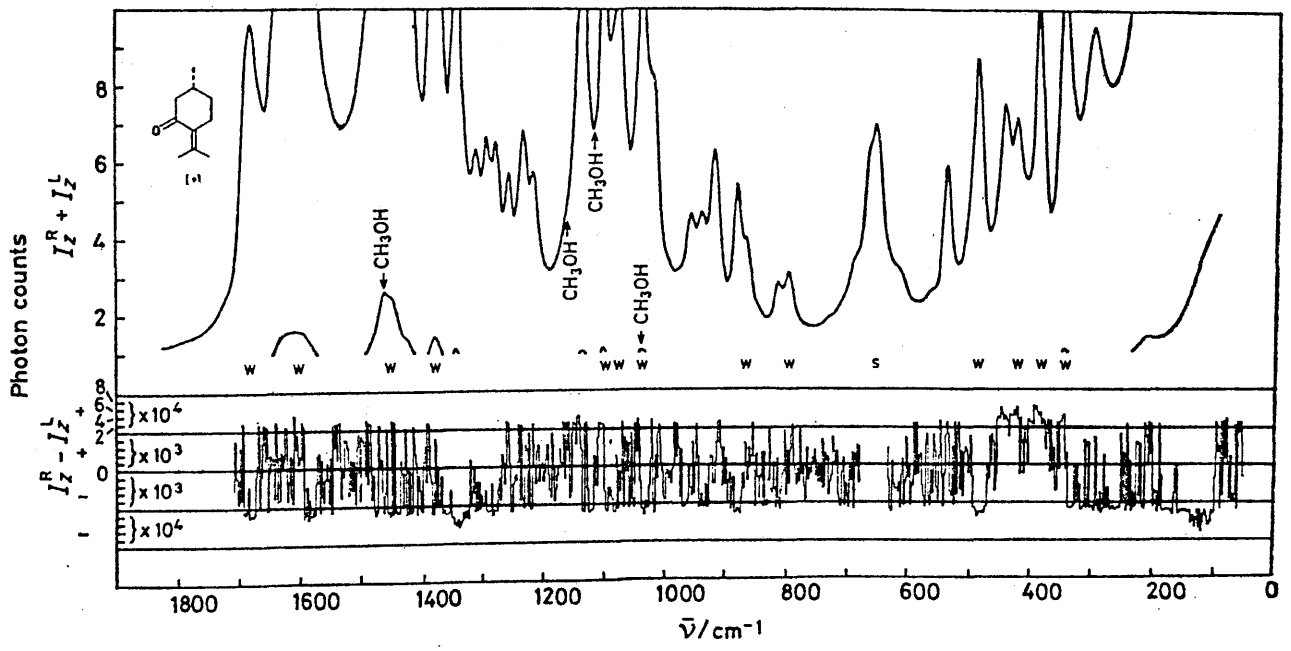

FIGURE 7 The depolarized Raman circular intensity sum and difference spectra of (+)-pulegone in methanol

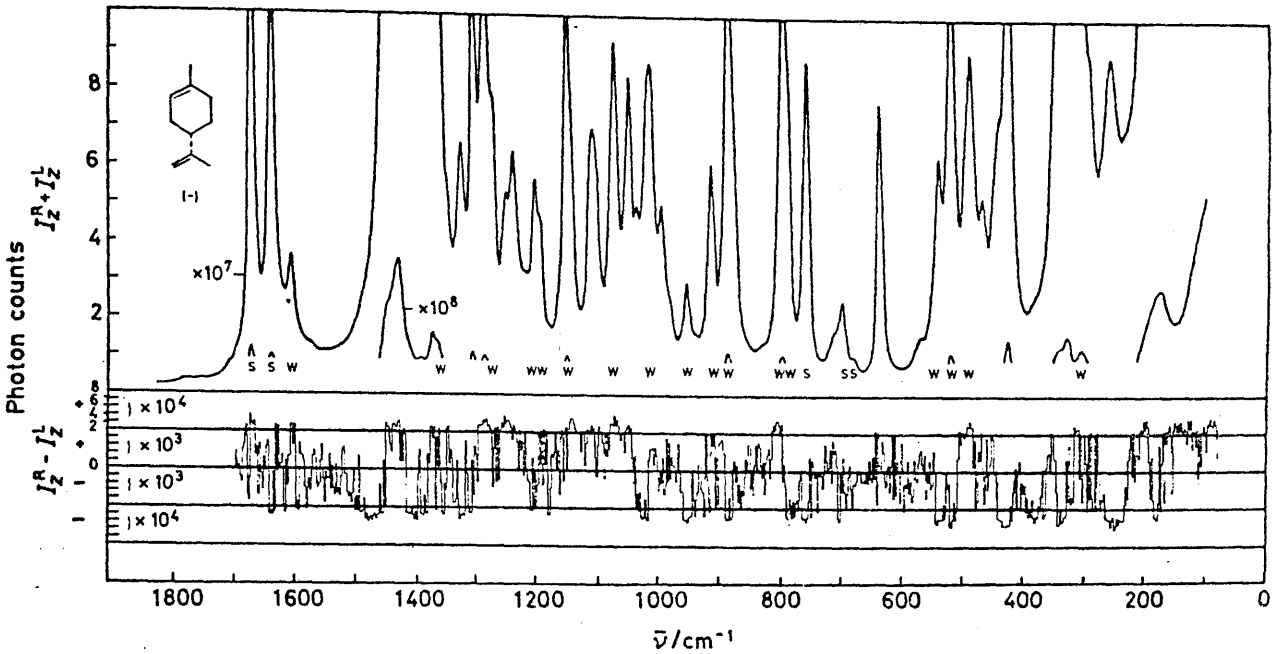

FIGURE 8 The depolarized Raman circular intensity sum and difference spectra of neat (−)-limonene

hexanol (Figure 6) shows a number of strong features above *ca.* 800 cm^{-1}. Some of these effects, together with the effects in the other molecules which we have not assigned, are likely to be due to CH_2 wagging, twisting, and rocking modes. These vibrations are variable in frequency due to the ease with which they couple with other modes (CH_2 wagging and twisting are generally to be found in the region 1 150—1 350 cm^{-1} and CH_2 rocking at 700—1 100 cm^{-1} [14]).

Chiral organic molecules containing methyl groups often show large optical activity in broad, weak, depolarized Raman bands below *ca.* 300 cm^{-1} that originate in methyl torsion vibrations.[15] The frequencies of methyl torsion modes can be very variable so band assignment can be difficult. However, the assignment of torsion modes of methyl groups attached to saturated ring systems is reasonably certain. In methylcyclohexane, the methyl torsion occurs at *ca.* 237 cm^{-1},[16] so the broad, weak, depolarized band at *ca.* 260 cm^{-1} in the Raman spectrum of (+)-3-methylcyclohexanone (Figure 7 of ref. 7), which shows a large negative c.i.d., almost certainly originates in the methyl torsion. The environ-

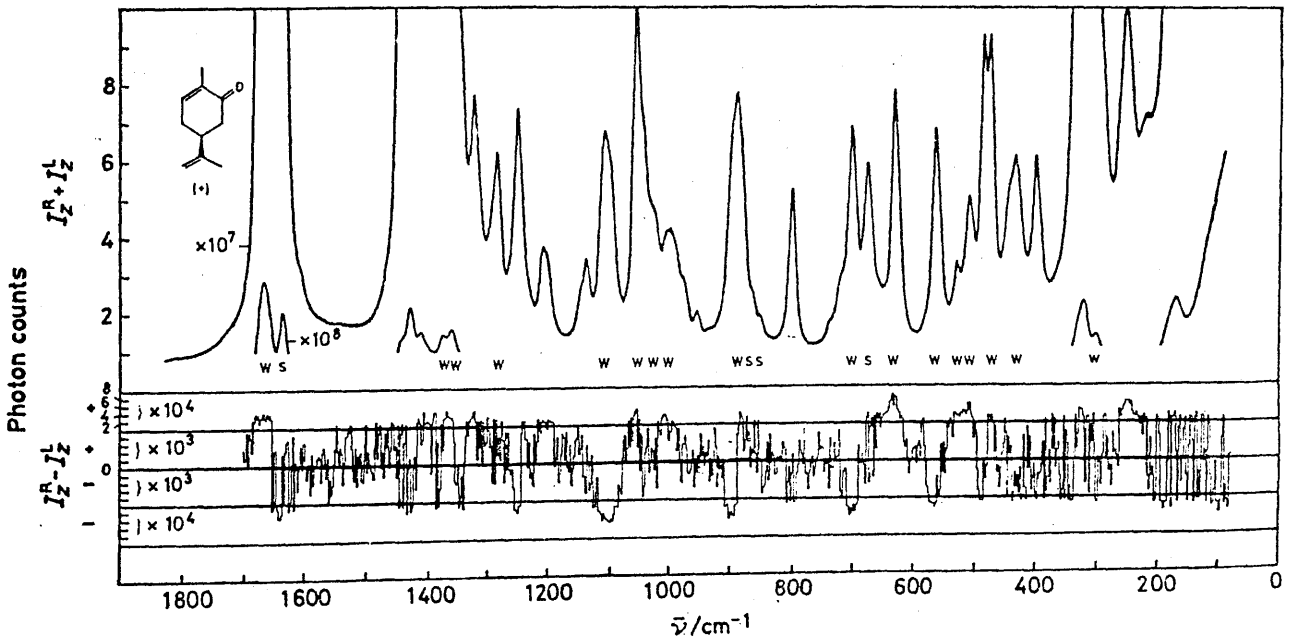

FIGURE 9 The depolarized Raman circular intensity sum and difference spectra of neat (+)-carvone

ment of the methyl group attached to the ring in (−)-menthone (Figure 5) should be very similar to that in (+)-3-methylcyclohexanone. The large negative c.i.d. in a weak Raman band in (−)-menthone at *ca.* 260 cm^{-1} (which merges with a large negative effect in a much stronger Raman band at slightly higher frequency) correlates with the negative effect in (+)-3-methylcyclohexanone since the two molecules have the same absolute configuration in the region of the ring methyl group. The weak, depolarized Raman bands at *ca.* 260 cm^{-1} showing large positive c.i.d.s in (−)-menthol (Figure 1) and (−)-menthylamine (Figure 2) might also originate in torsions of the ring methyl group. The Raman band shoulders at *ca.* 260 and 230 cm^{-1} showing small positive c.i.d.s in (−)-menthyl chloride (Figure 3) might have similar origins. The corresponding methyl torsion Raman band in (−)-isopulegol (Figure 4) might be that at *ca.* 260 cm^{-1}, which again shows a positive c.i.d. The Raman optical activity spectrum of (−)-limonene (Figure 8) shows a large negative effect associated with a broad, weak, Raman band at *ca.* 250 cm^{-1}; that of (+)-carvone (Figure 9) shows a large positive effect associated with a Raman band of similar shape at the same frequency. These effects might originate in torsions of the isopropenyl methyl groups since the opposite signs correlate with the opposite absolute configurations of the structural features common to both molecules,[15] and might be generated through an ' inertial ' mechanism discussed elsewhere.[17] As mentioned above, the Raman band with a positive c.i.d. at 260 cm^{-1} in (−)-isopulegol (Figure 4) is assigned to the torsion of the ring methyl group rather than to the isopropenyl methyl group. If this assignment is correct, the absence of correlatable optical activity in the torsion of the isopropenyl methyl group in (−)-isopulegol might be attributed to intramolecular hydrogen bonding (between the OH group and the π-electrons) holding the isopropenyl group in a very different conformation to that in limonene and carvone. Although this is speculative, it is worth noting that the i.r. spectrum of isopulegol in the OH stretching region indicates that intramolecular hydrogen bonding exists in a large proportion of the molecules.

It was mentioned above that CH deformations at tertiary carbon atoms, and also CH_2 deformations, can show large optical activity, although the complexity of the Raman and Raman c.i.d. features in the appropriate spectral region can make it difficult to extract useful stereochemical information. On the other hand, olefinic CH and CH_2 deformations give rise to bands that are sufficiently well defined to be of diagnostic value in conventional i.r. and Raman spectroscopy,[12,13] and we have found a number of examples of c.i.d.s in the corresponding Raman bands. Most of these are presented elsewhere,[18] but examples occur in two of the spectra presented here, (−)-limonene (Figure 8) and (+)-carvone (Figure 9). The vinylidene CH_2 out-of-plane, in-phase vibration in (−)-limonene is assigned to the strong, weakly polarized, Raman band at 888 cm^{-1} (following an earlier assignment of an i.r. band at this frequency in limonene [13]), which shows a small negative c.i.d. And at 885 cm^{-1} in the Raman spectrum of (+)-carvone a strong, weakly polarized, Raman band generates a small positive c.i.d. which correlates with the corresponding negative effect in (−)-limonene because in the two molecules the vinylidene CH_2 groups are in equivalent stereochemical environments but with opposite absolute configurations. The out-of-plane olefinic CH deformation of a trisubstituted double bond occurs in the region 790—840 cm^{-1}.[12] There are several clear examples elsewhere of Raman c.i.d.s associated with this mode.[18] This band occurs at 802 cm^{-1} in limonene; [13] it is present in Figure 8 as a shoulder on a Raman band at slightly lower frequency, and is associated with a positive c.i.d. There is a hint of a small negative effect at the same frequency in (+)-carvone (Figure 9), although a direct correlation between limonene and carvone is not expected on account of the adjacent carbonyl group in the latter.

Although we will not speculate on their origins, other definite Raman optical activity correlations can be seen in the spectra of (−)-limonene and (+)-carvone. Note particularly the region at *ca.* 510 cm^{-1} where three Raman bands at almost identical frequencies in the two molecules produce the same c.i.d. pattern but with opposite signs: from the lower frequency end the relative signs in (−)-limonene are positive–negative–negative. The additional Raman c.i.d. structure shown by (+)-carvone between *ca.* 550 and 720 cm^{-1} could originate in carbonyl deformation vibrations.[3,7] Also worth mentioning are the effects at *ca.* 1 010, 1 250, and 1 325 cm^{-1}, all of which have opposite signs in the two molecules.

With the exception of (−)-isopulegol and (−)-3,3-dimethylcyclohexanol, all of the absolute configurations shown were taken from ref. 19. That of (−)-3,3-dimethylcyclohexanol was provided by Professor H. S. Mosher, and that of (−)-isopulegol was deduced by assuming that the positive Raman optical activity in the band at *ca.* 260 cm^{-1} in both (−)-menthol and (−)-isopulegol originates in the torsion of the ring methyl group (other features at low frequency also correlate). Because of an error, the absolute configuration of (−)-menthyl chloride shown in Figure 3 is incorrectly assigned to the (+)-isomer in ref. 19. This was noticed because it is clear from the correlation of many Raman optical activity features in Figures 1 and 3 that (−)-menthol and (−)-menthyl chloride must have the same absolute configuration. This indicates that correlations of absolute configuration from Raman optical activity data are reliable.

We are grateful to Professor H. S. Mosher for the sample of (−)-3,3-dimethylcyclohexanol, and to the S.R.C. for an equipment grant and a Research Studentship to B. P. C.

[8/972 *Received*, 24*th May*, 1978]

REFERENCES

[1] L.D. Barron, M. P. Bogaard, and A. D. Buckingham, *J. Amer. Chem. Soc.*, 1973, **95**, 603.

[2] L. D. Barron and A. D. Buckingham, *Ann. Rev. Phys. Chem.*, 1975, **26**, 381.
[3] L. D. Barron, 'Advances in Infrared and Raman Spectroscopy,' eds. R. J. H. Clark and R. E. Hester, Heyden, London, vol. 4, p. 271.
[4] W. Hug, S. Kint, G. F. Bailey, and J. R. Scherer, *J. Amer. Chem. Soc.*, 1975, **97**, 5589.
[5] M. Diem, M. J. Diem, B. A. Hudgens, J. L. Fry, and D. F. Burow, *J.C.S. Chem. Comm.*, 1976, 1028.
[6] L. D. Barron, *J.C.S. Chem. Comm.*, 1977, 305.
[7] L. D. Barron, *J.C.S. Perkin II*, 1977, 1074.
[8] L. D. Barron, *J.C.S. Perkin II*, 1977, 1790.
[9] H. Boucher, T. R. Brocki, M. Moskovits, and B. Bosnich, *J. Amer. Chem. Soc.*, 1977, **99**, 6870.
[10] L. D. Barron, H. Numan, and H. Wynberg, *J.C.S. Chem. Comm.*, 1978, 259.
[11] L. D. Barron, *Tetrahedron*, 1978, **34**, 607.
[12] N. B. Colthup, L. H. Daly, and S. F. Wiberley, 'Introduction to Infrared and Raman Spectroscopy,' Academic Press, New York, 1975.
[13] K. Nakanishi, 'Infrared Absorption Spectroscopy—Practical,' Holden-Day, San Francisco, 1962.
[14] N. Sheppard and D. M. Simpson, *Quart. Rev.*, 1953, **7**, 19.
[15] L. D. Barron, *Nature*, 1975, **255**, 458.
[16] M. M. Sushchinskii, 'Raman Spectra of Molecules and Crystals,' Israel Program for Scientific Translations, Jerusalem, 1972, p. 207.
[17] L. D. Barron and A. D. Buckingham, *J. Amer. Chem. Soc.* 1979, **101**, 1979.
[18] L. D. Barron and B. P. Clark, following paper.
[19] W. Klyne and J. Buckingham, 'Atlas of Stereochemistry,' Chapman and Hall, London, 1974.

Raman Optical Activity of Pinenes, Carenes, and Related Molecules

By **Laurence D. Barron,*** and **Brian P. Clark**, Chemistry Department, The University, Glasgow G12 8QQ

Raman circular intensity difference spectra between 80 and 2 000 cm^{-1} of (+)- and (−)-α-pinene, (−)-β-pinene, (−)-cedrene, (+)-car-3-ene, (+)-car-2-ene, (−)-caryophyllene, and (−)-β-bourbonene are presented. A stereochemical correlation in bands originating in skeletal modes of the two pinenes is pointed out. Other features noted include effects in bands characteristic of the *gem*-dimethyl group and out-of-plane olefinic hydrogen deformations.

VIBRATIONAL optical activity spectra, obtained using the Raman circular intensity difference (c.i.d.) technique, of some pinenes, carenes, and related molecules are presented and compared to see what common features emerge. The basic references, together with the experimental details, are given in the preceding paper.[1]

DISCUSSION

Figures 1—7 show the depolarized Raman circular intensity sum and difference spectra of, respectively, (+)- and (−)-α-pinene, (−)-β-pinene, (−)-cedrene, (+)-car-3-cne, (+)-car-2-ene, (−)-caryophyllene, and (−)-β-bourbonene. The complete Raman c.i.d. spectrum of (−)-α-pinene has been published previously by Hug *et al.*,[2] and is virtually identical with that shown here.

By examining the Raman spectra of 13 molecules which all have pinane-type skeletons, Freeman and Mayo have discovered seven common bands between 1 100 and 375 cm^{-1} which they attribute to skeletal vibrations.[3] The frequencies of these bands are given in the Table. The spectra of two molecules in this series, α- and β-pinene, are presented here (Figures 1 and 2) and it is interesting to compare the Raman optical

Seven pinane-type skeletal frequencies (cm^{-1}) identified by Freeman and Mayo [3]

1 082 ± 3
852 ± 13
822 ± 4
758 ± 17
656 ± 26
472 ± 12
387 ± 12

activity of corresponding skeletal modes. Of the seven Raman bands in the correlation only two, at 1 082 and 656 cm^{-1}, do not show significant c.i.d.s in both α- and β-pinene. The statistically significant parts of the c.i.d.s in the remaining five bands have been shaded black. Comparing the spectrum of the (−)-enantiomer of α-pinene with that of (−)-β-pinene, both molecules

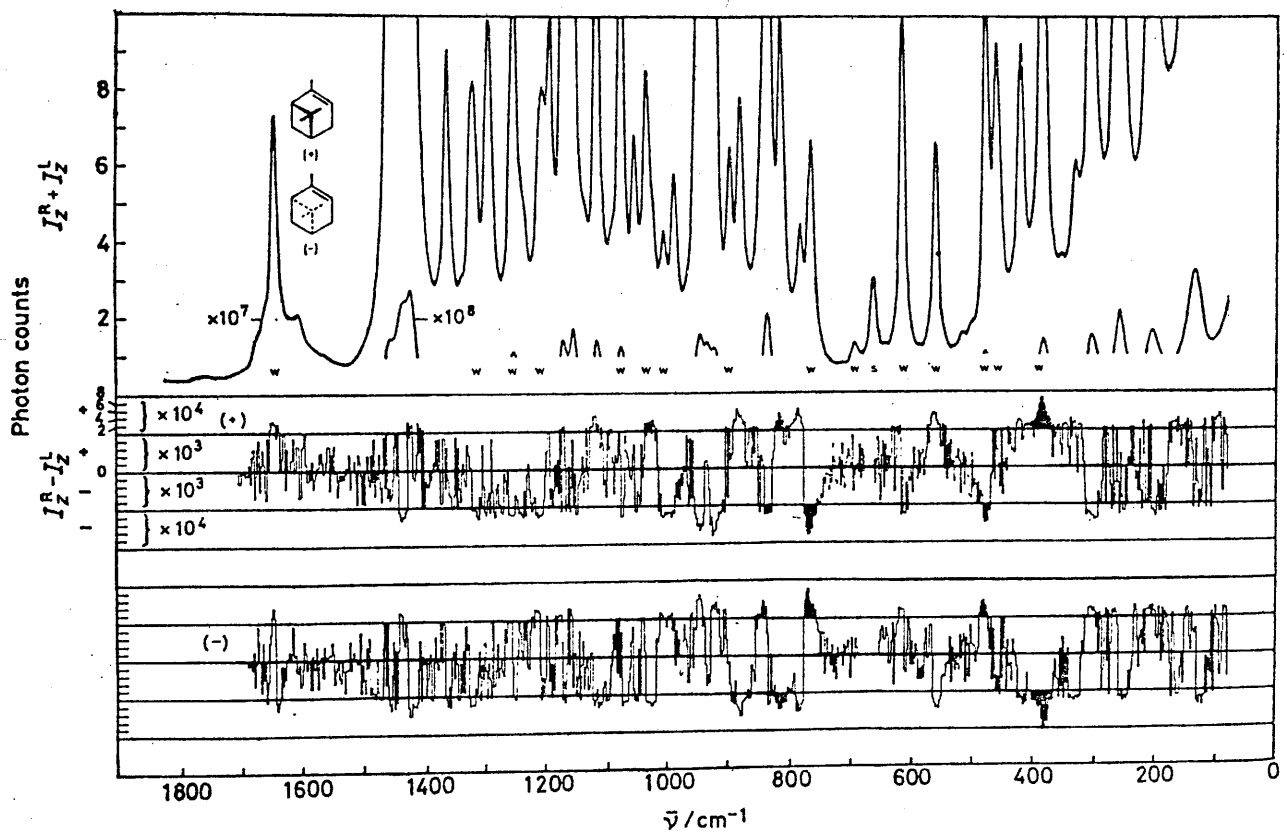

FIGURE 1 The depolarized Raman circular intensity sum and difference spectra of neat (+)- and (−)-α-pinene

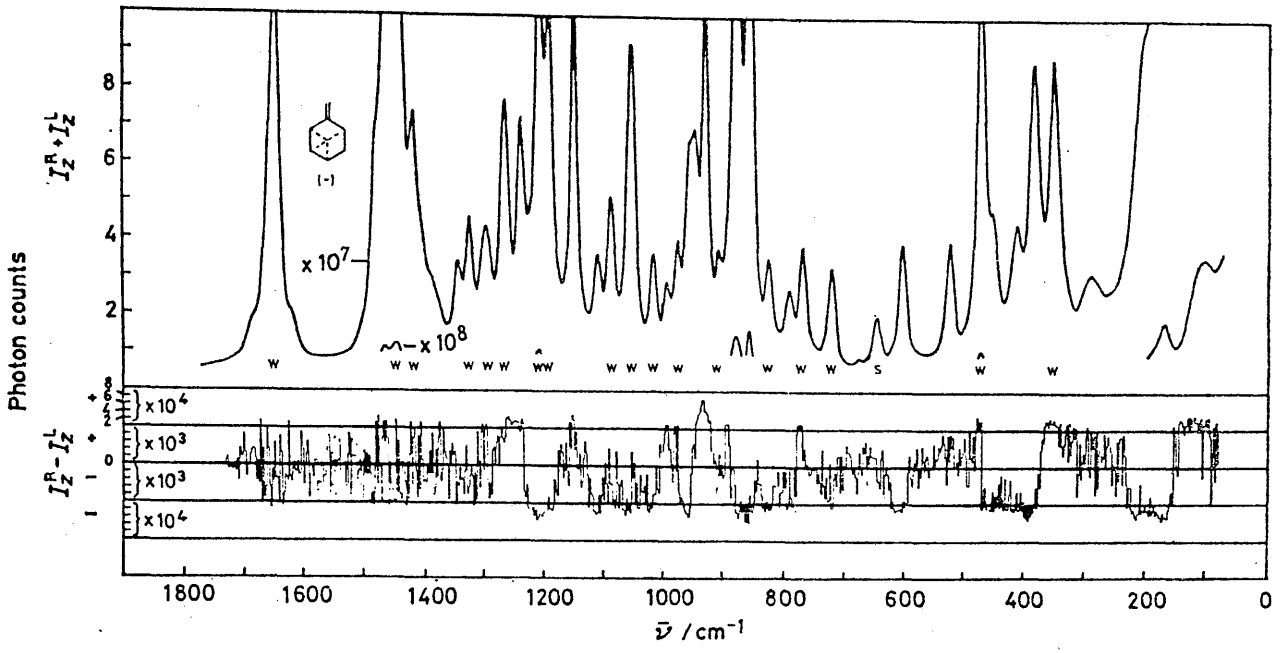

FIGURE 2 The depolarized Raman circular intensity sum and difference spectra of neat (—)-β-pinene

having ' analogous ' absolute configurations, we see that four of the five Raman c.i.d.s, at 387, 472, 758, and 822 cm^{-1}, have the same sign in the corresponding bands while the remaining one, at 852 cm^{-1}, changes sign. It would be interesting to examine the Raman optical activity of spectra of other pinane-type molecules to discover if the correlations persist.

Mayo and Freeman have also published a five-band correlation for the Raman spectra of cedrane-type molecules.[4] Unfortunately, in the spectrum of (—)-cedrene (Figure 3), only one skeletal mode, at 780 cm^{-1}, which is strongly polarized and hence particularly sensitive to artifacts,[5] shows any significant Raman optical activity. It is worth noting that, due to the considerable size of molecules with the cedrane skeleton and the resulting complexity of their Raman spectra, in order to compile the list of skeletal vibrations an intensity constraint had to be imposed in which the empirical selection was limited to the seven most intense bands in the spectrum.[4] It may be that the Raman optical activity spectra of a series of related molecules could be used to identify bands of similar origin, should this type of study be undertaken in the future.

All the molecules presented here are unsaturated, and

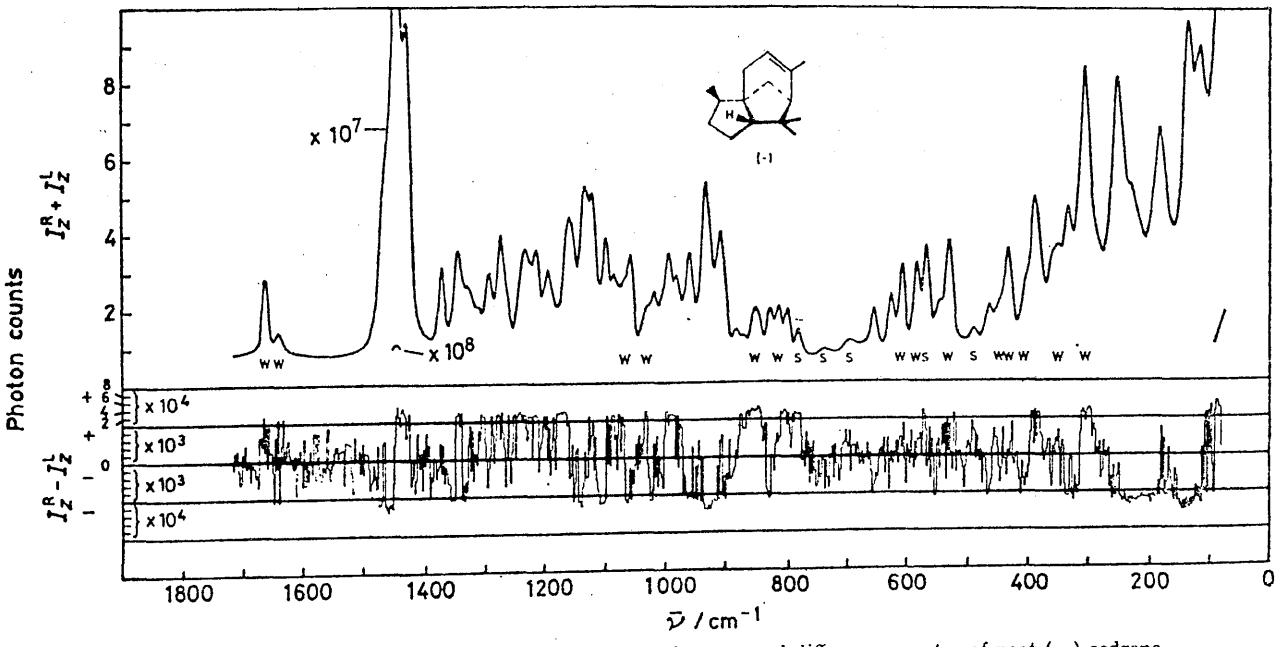

FIGURE 3 The depolarized Raman circular intensity sum and difference spectra of neat (—)-cedrene

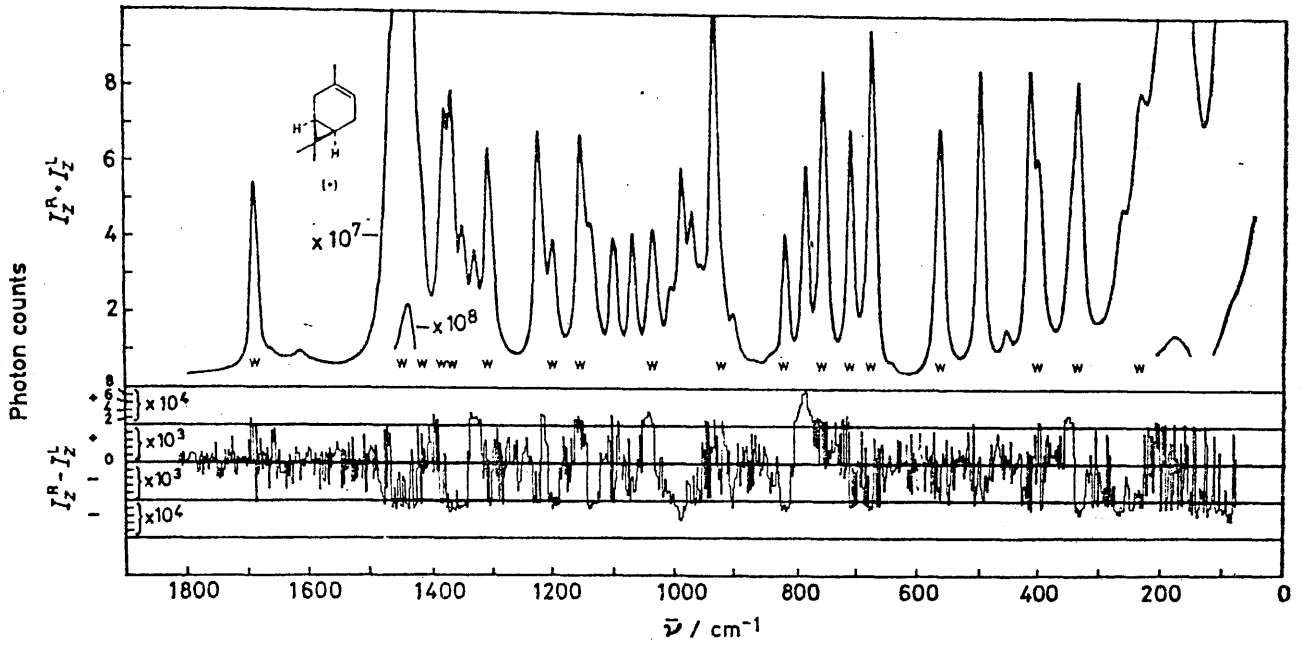

FIGURE 4 The depolarized Raman circular intensity sum and difference spectra of neat (+)-car-3-ene

we have found that vibrations involving out-of-plane deformations of olefinic hydrogen atoms are consistently producing Raman optical activity effects. A tri-substituted double bond gives rise to an out-of-plane CH deformation in the region 790—840 cm^{-1}.[6] This band is seen clearly at 820 cm^{-1} in the Raman spectrum of (+)-car-3-ene (Figure 4) and generates a negative c.i.d. The corresponding Raman band in (+)-car-2-ene (Figure 5) occurs at 830 cm^{-1} and, although quite strongly polarized, its attendant positive c.i.d. is probably genuine. The opposite signs of the corresponding c.i.d.s in (+)-car-3-ene and (+)-car-2-ene indicate that the intramolecular environments of the olefinic hydrogen atoms in the two molecules are such as to induce enantiomeric chirality in the two deformations. In larger molecules it is difficult to pick out these out-of-plane olefinic CH deformation bands. In the case of α-pinene (Figure 1), Freeman and Mayo eliminate two bands at 820 and 845 cm^{-1} as being skeletal modes,[3] leaving only the Raman band at just under 790 cm^{-1} as the candidate for the deformation. This shows a large Raman c.i.d., negative in the (−)-enantiomer. However, there is also a Raman band at 790 cm^{-1} in the spectrum of (−)-β-pinene which shows a hint of a negative c.i.d. If

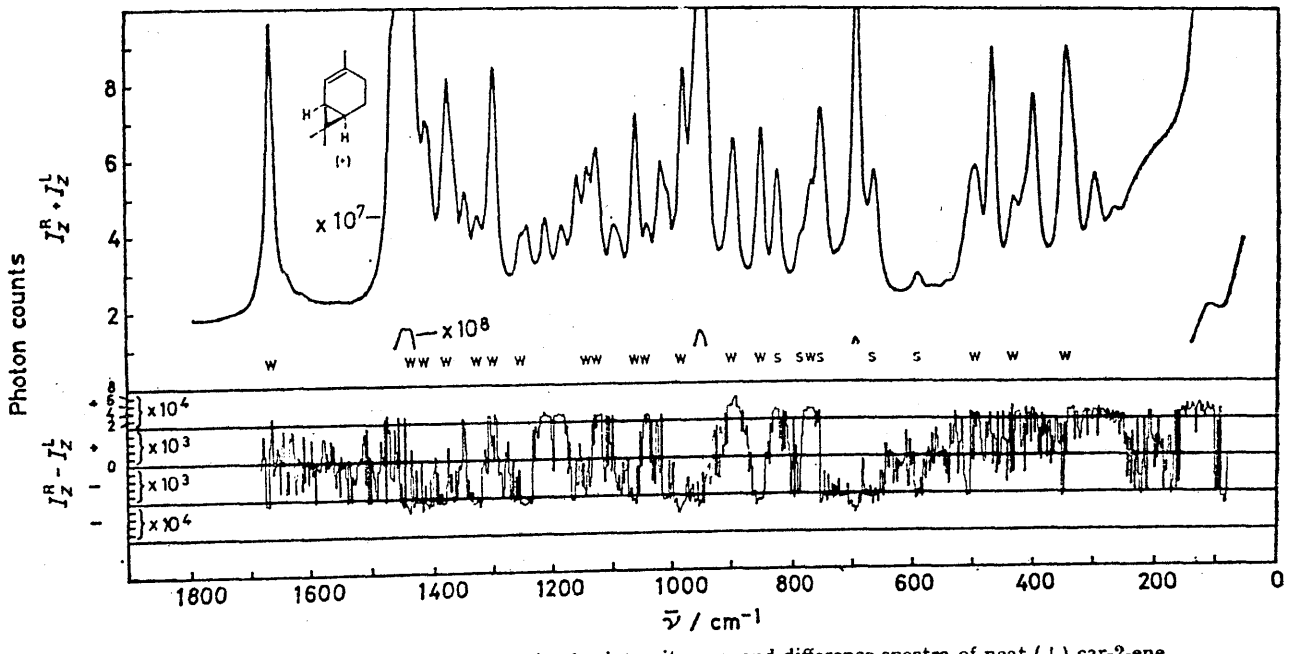

FIGURE 5 The depolarized Raman circular intensity sum and difference spectra of neat (+)-car-2-ene

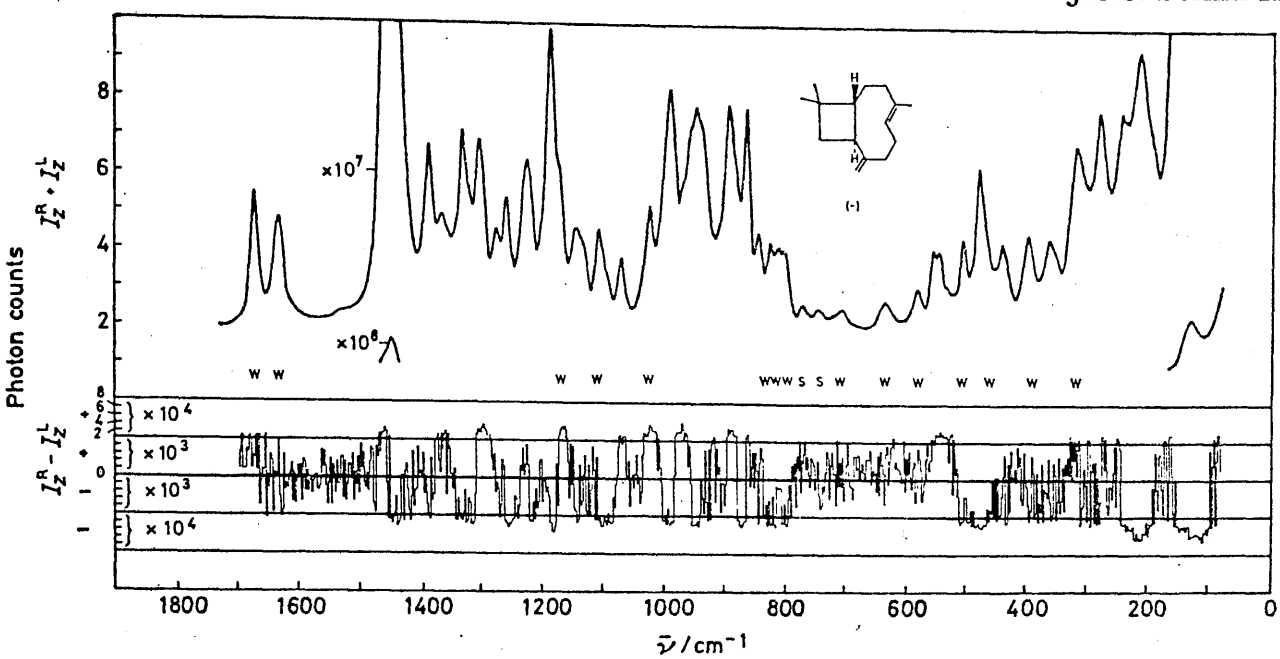

FIGURE 6 The depolarized Raman circular intensity sum and difference spectra of neat (−)-caryophyllene

these two bands are of similar origin, it could be that the Raman band at 845 cm^{-1} is not, in fact, a skeletal mode but the CH deformation and that the skeletal mode actually occurs at 875 cm^{-1}, although this is outwith the range quoted by Freeman and Mayo. This band at 875 cm^{-1} shows a negative c.i.d. in (−)-α-pinene and if it is the skeletal mode then all five of the Raman c.i.d.s associated with corresponding skeletal modes in (−)-α- and (−)-β-pinene have the same sign. Cedrene and caryophyllene, which both contain a trisubstituted olefinic group, have complicated Raman spectra (Figures 3 and 6). (−)-Cedrene shows three Raman bands in the appropriate region: one of them, at 820 cm^{-1}, is a skeletal mode [4] and shows no c.i.d.; the remaining two at 805 and 835 cm^{-1} both show c.i.d.s, positive and negative respectively. There are also three candidates in (−)-caryophyllene: at 825, 815, and 800 cm^{-1}, the first and third of which generate negative Raman c.i.d.s. The out-of-plane, in-phase, vinylidene CH_2 deformation occurs within the fairly small spectral range 885—895 cm^{-1}.[6] This narrower range helps to identify the band. The three molecules in this series with a vinylidene group give corresponding Raman c.i.d.s. This band occurs at 885 cm^{-1} in (−)-β-pinene (Figure 2) as the

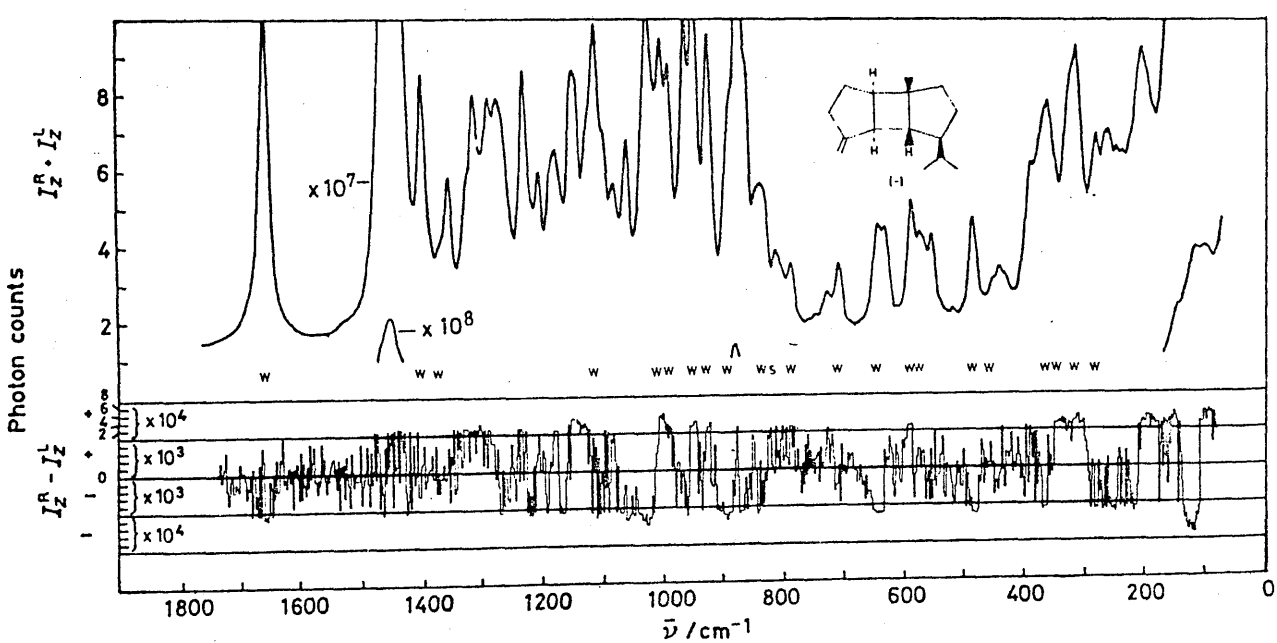

FIGURE 7 The depolarized Raman circular intensity sum and difference spectra of neat (−)-β-bourbonene

shoulder of a lower frequency skeletal band and exhibits a small positive c.i.d. The Raman band at 890 cm^{-1} in (−)-caryophyllene (Figure 6) shows a positive c.i.d. and that at 890 cm^{-1} in (−)-β-bourbonene (Figure 7) shows a negative one. All that may be done here is to point out these effects; the molecules are too complex for any stereochemical correlations to be made at present. Other examples of Raman c.i.d.s in these olefinic CH and CH_2 deformations are given in the preceding paper.[1]

The isopropyl group produces two Raman bands at *ca.* 1 140 and 1 170 cm^{-1} arising from an interaction of the two methyl rocking modes together with C–C stretching.[6] Raman c.i.d.s have been observed previously in these modes.[1] The couplet present in the optical activity spectrum of (−)-β-bourbonene (Figure 7) associated with Raman bands at 1 145 and 1 170 cm^{-1} could be due to the isopropyl group.

The *gem*-dimethyl group gives rise to two bands of similar origin at slightly higher frequencies.[6] The Raman c.i.d.s in these bands indicate that the situation is more complicated than in the isopropyl group, presumably due to increased participation of C–C stretching. Take the cases of (+)-car-3-ene and (+)-car-2-ene (Figures 4 and 5). In the former there are two relatively isolated bands at 1 195 and 1 220 cm^{-1} which we assign to the *gem*-dimethyl group. These generate a Raman c.i.d. couplet. In (+)-car-3-ene, however, two new bands occur in the region of 1 250 cm^{-1} and one new one appears just above 1 200 cm^{-1}. The result is that the couplet observed in car-2-ene is replaced by two positive effects. Coupling to the higher frequency bands at 1 250 cm^{-1} could be indicated by them showing negative c.i.d.s. With two molecules as similar as α- and β-pinene one might expect the Raman optical effects due to their *gem*-dimethyl groups to be similar also. However, the complexity of the Raman spectra in the region of 1 200 cm^{-1} in these molecules precludes any meaningful comparison. A c.i.d. couplet in (−)-β-pinene (Figure 2) centred at 1 240 cm^{-1} encompasses six Raman bands altogether. Perplexingly, the Raman optical activity in the same region in (−)-α-pinene (Figure 1) is limited to a small positive feature at *ca.* 1 220 cm^{-1}. The couplet centred at 1 170 cm^{-1} in the Raman optical activity spectrum of (−)-caryophyllene (Figure 6) could originate in the *gem*-dimethyl group. Cedrene (Figure 3) also contains a *gem*-dimethyl group but the complexity of the Raman spectrum and the presence of three other methyl groups in the molecule make band assignments almost impossible in this region.

The two (+)-carenes (Figures 4 and 5) reveal several Raman c.i.d. effects of uncertain origin which correlate in sign. Best examples are the positive effects common to both molecules at *ca.* 1 050 cm^{-1}, the negative effects at *ca.* 990 cm^{-1}, and the large positive effects at *ca.* 780 cm^{-1}.

Finally, we should mention that chiral organic molecules containing methyl groups often show large optical activity in broad, weak, depolarized Raman bands below *ca.* 300 cm^{-1} that originate in methyl torsion vibrations,[7,8] and this could be the origin of some of the large c.i.d.s at low frequency in several of the spectra shown here.

We are grateful to Dr. D. H. Grayson for the samples of (+)-car-2-ene and (+)-car-3-ene, to Dr. A. L. Porte for the sample of (−)-caryophyllene, and to the S.R.C. for an equipment grant and a Research Studentship to B. P. C.

[8/973 *Received*, 24*th May*, 1978]

REFERENCES

[1] L. D. Barron and B. P. Clark, preceding paper.
[2] W. Hug, S. Kint, G. F. Bailey, and J. R. Scherer, *J. Amer. Chem. Soc.*, 1975, **97**, 5589.
[3] S. K. Freeman and D. W. Mayo, *Appl. Spectroscopy*, 1970, **24**, 595.
[4] D. W. Mayo and S. K. Freeman, *Appl. Spectroscopy*, 1970, **24**, 591.
[5] L. D. Barron and A. D. Buckingham, *Ann. Rev. Phys. Chem.*, 1975, **26**, 381.
[6] N. B. Colthup, L. H. Daly, and S. F. Wiberley, 'Introduction to Infrared and Raman Spectroscopy,' Academic Press, New York, 1975.
[7] L. D. Barron, *Nature*, 1975, **255**, 458.
[8] L. D. Barron and A. D. Buckingham, *J. Amer. Chem. Soc.*, 1979, **101**, 1979.

REFERENCES

1. L.D. Barron and B.P. Clark, J. Chem. Soc. Perkin 2, 1164 (1979).

2. L.D. Barron and B.P. Clark, J. Chem. Soc. Perkin 2, 1171 (1979).

APPENDIX

NORMAL COORDINATE ANALYSIS

The theory of normal coordinate analysis is well established[1,2] and calculations have been made routine by the availability of comprehensive computer packages[3,4]. The series of programs used here were written by Snyder and Schachtsneider[3] and are in popular use.

We now present the principal equations in the theory these programs use. The general approach is known as Wilson's F-G method.[1] This produces a description of a molecule's normal modes in terms of its bond stretch and angle bend internal coordinates. For a general, N-atom molecule, the internal coordinates are written as a linear combination of the 3N cartesian displacement coordinates of the atoms

$$\underset{\sim}{S} = \underset{\sim}{B}\,\underset{\sim}{x} \qquad \text{(A.1)}$$

where $\underset{\sim}{S}$ is a row vector of the internal coordinates, $\underset{\sim}{x}$ is a column vector of the cartesian displacement coordinates and $\underset{\sim}{B}$ is the transformation matrix (Wilson's $\underset{\sim}{B}$ matrix), the elements of which appear in the bond polarizability theory.

The normal coordinates and the internal coordinates are related by the $\underset{\sim}{L}$ matrix

$$\underset{\sim}{S} = \underset{\sim}{L}\,\underset{\sim}{Q} \qquad \text{(A.2)}$$

where $\underset{\sim}{Q}$ is a column vector of the normal coordinates. $\underset{\sim}{L}^{-1}$, the inverse of $\underset{\sim}{L}$, defines the reverse relation

$$\underset{\sim}{Q} = \underset{\sim}{L}^{-1}\,\underset{\sim}{S} \qquad \text{(A.3)}$$

To set up the vibrational secular equations the matrices $\underset{\sim}{F}$ and $\underset{\sim}{G}$ are introduced[1] such that

$$2T = \tilde{\dot{S}}\,\underset{\sim}{G}^{-1}\,\dot{S} \qquad \text{(A.4a)}$$

$$2V = \tilde{S}\,\underset{\sim}{F}\,S \qquad \text{(A.4b)}$$

where T and V are the total vibrational kinetic and potential energies. $\underset{\sim}{G}$, the inverse kinetic energy matrix, is given by

$$\underset{\sim}{G} = \underset{\sim}{B}\,\underset{\sim}{M}^{-1}\,\underset{\sim}{\tilde{B}} \qquad (A.5)$$

where $\underset{\sim}{M}$ is a diagonal matrix whose elements are the atomic masses. Program GMAT in the Snyder/Schachtsneider package produces $\underset{\sim}{B}$ and $\underset{\sim}{G}$ using the molecular geometry and the atomic masses as input. $\underset{\sim}{F}$ is the matrix of force constants. These are empirical parameters chosen to give the closest fit of calculated to observed vibrational frequencies.

The utility of introducing $\underset{\sim}{F}$ and $\underset{\sim}{G}$ is revealed by the fact that the eigenvectors of the product matrix $\underset{\sim}{GF}$ together form the transformation matrix $\underset{\sim}{L}$ between the internal and normal coordinates. That is, the vibrational secular equation is given by

$$\underset{\sim}{G}\,\underset{\sim}{F}\,\underset{\sim}{L} = \underset{\sim}{L}\,\underset{\sim}{\Delta} \qquad (A.6)$$

where $\underset{\sim}{\Delta}$ is the diagonal matrix of eigenvalues. Moreover, these eigenvalues are related by a numerical factor to the vibrational frequencies of the normal modes.

The vibrational problem has thus become that of solving the following determinant equation

$$|\underset{\sim}{G}\,\underset{\sim}{F} - \underset{\sim}{E}\,\lambda| = 0 \qquad (A.7)$$

where λ represents the eigenvalues and $\underset{\sim}{E}$ is the unit matrix. Program VIBSEC solves the secular equation and produces the vibrational frequencies, $\underset{\sim}{L}$ and $\underset{\sim}{L}^{-1}$.

One last item that VIBSEC produces is the potential energy distribution[2] in the diagonal force constants. This is a measure of the contribution of each diagonal force constant F_{jj} to the normal modes. It is given (here as a percentage) by

$$L_{ji}^2\, F_{jj} / \lambda_i \times 100 \qquad (A.8)$$

This gives the value for the potential energy distribution for the diagonal force constant F_{ii} in the normal mode with eigenvalue λ_i. The potential energy distribution is a better guide to the constitution of a normal mode than the elements of $\underset{\sim}{L}$ since these latter have different units depending on whether the internal coordinate associated with the diagonal force constant is a bond stretch or an angle bend.

REFERENCES

1. E.B. Wilson, J.C. Decius and P.C. Cross, Molecular Vibrations, McGraw-Hill, New York, 1955.

2. S. Califano, Vibrational States, Wiley, London, 1976.

3. J.H. Schachtschneider, Technical Report, No. 57-65, Shell Development Co., Emeryville, California, 1966.

4. T. Shimanouchi, Computer Programs for Normal Coordinate Treatment of Polyatomic Molecules, Department of Chemistry, Faculty of Science, University of Tokyo, 1968.